The Applicability of
Robot-guided Laser Osteotomy
in a Clinical Environment
and the Interaction of
Laser Light and Bone Tissue

Inauguraldissertation

Zur Erlangung der Würde eines

Dr. sc. med.

vorgelegt der Medizinischen Fakultät der Universität Basel

von

Kyung-won Baek

aus Gunten

Basel, 2017

Genehmigt von der Medizinischen Fakultät auf Antrag von

Prof. Dr. Dr. Philipp Jürgens, Basel
Dissertationsbetreuer

Prof. Dr. Philippe C. Cattin, Basel
Koreferenten

Prof. Dr. Kurt Alexander Schicho, Wien
Prof. Dr. Michael Schmidt, Erlangen
Externe Gutachter

Basel, den

Prof. Dr. med. Thomas Gasser, Basel
Dekan

외할머니께

Mim liebä Grosi
Magdalena, Sung-ja Huh
(1924–2016)

Acknowledgements

Summary

Laser is an integral part of diagnostics and therapy in modern medicine. However, removing hard tissue with laser became successful only recently. The advantages of laser osteotomy are high precision and complete freedom in designing the cutting geometry. Nevertheless, these can be fully realized only when the laser system is guided by a robot. The most important challenges here are the miniaturization and the ergonomic design of the entire system.

In this dissertation, I presented our first experience with a computer-assisted, integrated and miniaturized laser system, which is driven by a surgical robot. An Er:YAG laser source was integrated into a housing with an optical system and attached to the surgical robot arm. Pre-operatively generated planning data was imported and used to execute the osteotomies. Intraoperatively, a navigation system performed the positioning. In the actual operation room environment, the laser osteotome was used to produce different defect geometries in the mandibular bones of six minipigs. On the contralateral side of the mandible, surgeons used a PZE osteotome to create the same defects for comparison. The performance of the laser osteotome was analyzed in terms of the workflow, ergonomics, bone healing, user-friendliness, and safety. We were able to demonstrate that the laser osteotome could be ergonomically integrated into the operation room environment. It showed a high precision and the complex cutting geometries were transferred as planned. We expect that the computer-assisted and robot-guided laser osteotome will routinely used in the future, whenever special incision and high precision are required in osteotomies.

Zusammenfassung

Der Laser ist aus der Diagnostik und der Therapie in der modernen Medizin nicht mehr wegzudenken. Das Abtragen von Hartgeweben konnte allerdings erst vor einigen Jahren erfolgreich realisiert werden. Die Vorteile der Laserosteotomie sind die sehr hohe Präzision und erhöhte Freiheit bei der Gestaltung der Schnittgeometrien. Damit man diese Eigenschaften auch vollständig ausschöpfen kann, braucht man ein geeignetes Trägermedium für das Laserosteotom, wie etwa ein Roboter. Die grösste Herausforderung stellt dabei die ergonomische Gestaltung des Gesamtsystems dar.

In dieser Dissertation präsentiere ich erste Erfahrungen mit einem computerassistierten Lasersystem, das von einem chirurgischen Roboter geführt wird. Eine Er:YAG Laserquelle mit der dazugehörigen Optik wurden in ein Gehäuse gebaut, das am Kopf eines Roboters montiert wurde. Zur Durchführung der Osteotomien wurden präoperative Planungsdaten importiert. Intraoperativ erfolgte eine Positionskontrolle über ein Navigationssystem. Im OP Umfeld wurde das Laserosteotom dann genutzt, um unterschiedliche Schnittgeometrien in den Unterkieferknochen von sechs Minischweinen zu erzeugen. Die Leistungsfähigkeit des Laserosteotoms wurde hinsichtlich Workflow, Ergonomie, Knochenheilung, Benutzerfreundlichkeit und Sicherheit analysiert. Wir konnten zeigen, dass das Laserosteotom ergonomisch sinnvoll in das OP Umfeld integriert werden kann. Es zeigte eine hohe Genauigkeit und komplizierten Schnittgeometrien liessen sich nach Plan übertragen. Wir erwarten, dass das computerassistierte und robotergeführte Laserosteotom in der Zukunft immer dann sinnvoll eingesetzt werden kann, wenn Osteotomien einer besonderen Schnittführung und hoher Präzision bedürfen.

Contents

Nomenclature

Abbreviations

CMF surgery	cranio-maxillo-facial surgery
CO_2 laser	carbon dioxide laser
CT	computed tomography
cw	continuous-wave
Er,Cr:YSGG laser	erbium, chromium-doped yttrium scandium gallium garnet laser
Er:YAG laser	erbium-doped yttrium aluminium garnet laser
Holmium:YSGG laser	holmium-doped yttrium scandium gallium garnet laser
Nd:YAG laser	neodymium-doped yttrium aluminium garnet laser
OR	operation room
post-op	postoperative
pre-op	preoperative
PZE osteotome	piezoelectric osteotome
SEM	scanning electron microscope

Chapter 1

Introduction

Medicine was one of the first fields where laser was applied, since its first realization in 1960. Medical laser is now an integral part of routine in various clinical practices, including dentistry. But in this thesis we have applied laser to a rather new field, laser bone cutting. The biggest differentiation of laser from conventional osteotomy tools lies in its contact-free ablation. This results in several advantages which come from the absence of a cutting tip. Neither the material characteristic of the bone nor the mechanical property of the tip affects the cut, hence we have absolute freedom over the cutting geometry. With the thin cutting width of 200 µm (up to 500 µm *in vivo*), laser enables us to achieve the highest precision in bone surgery. Cut bone is free from the friction, heat, and the debris from the tip (and from the bone itself). Therefore, better healing of the bone is expected.

However, there are many challenges as well to realize laser osteotomy in a clinical environment. This thesis includes those challenges and shares possible solutions from our experience. Through this experience, we did not only make new findings but also learn old school lessons again—which became major contributions of this thesis.

Laser Bone Cutting

We built a computer-assisted and robot-guided laser system dedicated to bone cutting in Cranio-maxillo-facial (CMF) surgery. Er:YAG (Erbium-doped Yttrium Aluminium Garnet) laser was the photoablation source. Clinical application was

clearly aimed from the early stage. Soon we were confronted with the question how we could consistently reflect this aim to the rapidly evolving system design. Our first publication tried to answer this question, with the *in vitro* simulations and the *in vivo* preclinical study. It explained how we realized laser bone cutting, from building up the prototype to applying the computer-laser-robot system to the mandibles of adult Göttingen minipigs in an actual CMF Operation Room (OR) setting.

Analyses of Bone Healing

The preclinical study was designed as a comparative surgery on the mandibles of the Göttingen minipigs, with a piezoelectric (PZE) osteotome and our computer-laser-robot system. From the second surgical phase of the preclinical study, bone blocks were taken out of the mandible defects. These blocks were assessed with Scanning Electron Microscope (SEM) to analyze the cut surface. SEM images revealed smooth surface characteristics from the bone cut by the PZE osteotome. On the contrary, the cut surface from laser osteotomy showed different surface characteristics, which were similar to those of natural bone. Where did this difference come from, and how would it affect the bone healing? Answers to these questions were included in our second and third publications. After 4 and 8 weeks, the minipigs were sacrificed and the bone healing was compared with histology. We could confirm unproblematic healing from both osteotomies, but there was a tendency to better healing on the laser osteotomy side. Trying to explain this tendency, laser scanning microscope analysis was added for further assessments. Combining intraoperative, immediate postoperative (post-op), and post-op histologic findings, the third publication became convergent analyses of bone healing after laser osteotomy.

Chapter 2

Background

"Let there be light," and there was light (Genesis 1:3).

Light is said to be the start of world creation, and has been the start of fundamental questions of theology, philosophy, art, and science.
It was also the starting point of our research.

Laser in Medicine

Laser is the acronym of Light Amplification by Stimulated Emission of Radiation, which was first suggested by Albert Einstein in 1917 [1]. Today laser is widely used in science, engineering, industry (from IT to weapon), and our everyday life (from the barcode scanner to the speedometer). Also in medicine, laser became indispensable for diagnosis and treatment in various practices. The first realization of laser was done by Maiman in 1960 [2]. The following year, the first laser application in medicine was published by Zaret et al. in Opthalmology [3]. Two years later Goldman, Blaney, Kindel, Richfield, & Franke published the effect of the laser beam on the skin [4]. Opthalmology and Dermatology are still the leading fields of medical laser use, along with Otolaryngology and Gastroenterology (often combined with endoscopes in these practices). But apparently laser applications have been extended to other medical and research fields as well.

In dentistry, Goldman et al. first published the impact of the laser on dental caries in 1964. But it was Taylor, Shklar, & Roeber's publication in 1965 which applied laser to diverse important tissues dealt in dentistry *in vivo* [5]. Using
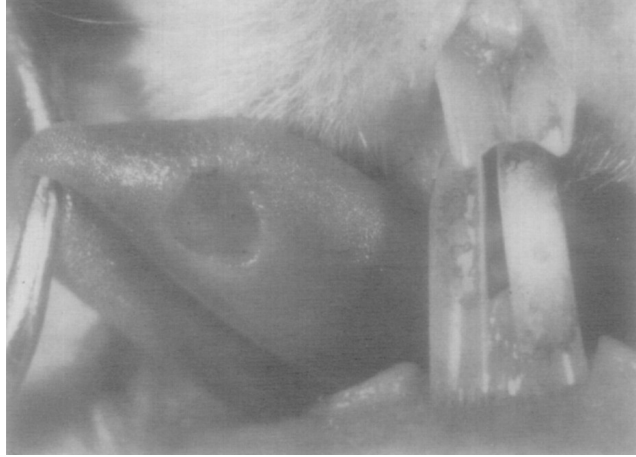
Figure 2.1: A clinical picture from the experiment of Taylor et al. Tissues of a hamster 3 days following 35 J radiation of ruby laser to the left mandibular incisor and the left lateral border of the tongue. (Reprinted with permission from Reference [5] R. Taylor et al., Copyright 1965 Elsevier Inc.)

Syrian hamsters, they applied a solid state ruby laser to the mandibular incisor, surrounding gingiva, and the lateral border of the tongue. With a 35 joule and 55 joule radiation from ruby laser, teeth, pulp, tongue, and gingival tissue showed inflammation and degeneration after 3 and 7 days of healing time (Figure 2.1). They concluded that the possible use of laser energy presented many problems and severe degenerative changes. Indeed it took several decades from the study of Taylor et al. until the laser became a part of dental practice [6]. Even when the laser was finally brought into the dental clinics, its use had been limited to soft tissue for a long time [7]. The problem was that the low water content of hard tissue made it difficult to photoablate. Often the laser beam overheated and denaturated the surfaces of bones and teeth. As a result, carbonized layer covered the cut surface, caused inflammation, and inhibited proper healing.

From late 1970s, Horch published several attempts to ablate the bone with continuous-wave (cw) carbon dioxide (CO_2) lasers and concluded that laser osteotomy was not feasible [8] [9]. Even with the cooling, ablated bones showed severe carbonization and serious complications (Figure 2.2). Until the laser technology was advanced and effective cooling system got established, laser bone cutting had been considered to be impossible.
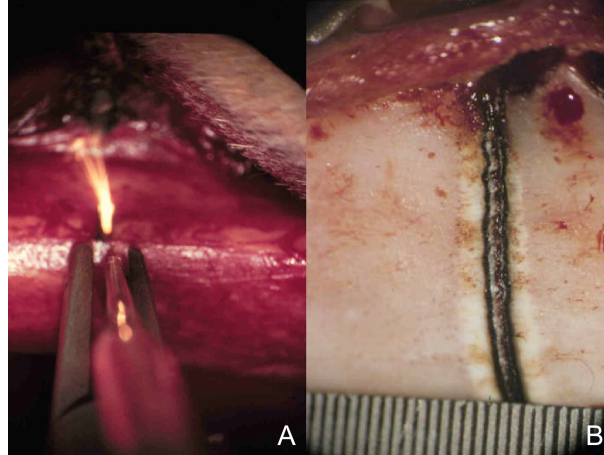
Figure 2.2: A clinical picture from the experiment of Horch HH. Carbonized bone surface by cw CO_2 laser ablation with wavelength $\lambda = 10.6\,\mu m$ and power $34\,W$. (Reprinted with permission from Prof. Hans-Florian Zeilhofer)

Er:YAG Laser in Bone Surgery and Dentistry

From the late 1980s several research groups applied laser to hard tissue cutting. They found pulsed lasers could solve the problem of carbonization that occurred with continuous-wave lasers. In 1988, Nuss, Fabian, Sarkar, & Puliafito tested various lasers—cw Neodymium-doped Yttrium Aluminium Garnet (Nd:YAG, $\lambda = 1.064\,\mu m$), cw CO_2 ($\lambda = 10.6\,\mu m$), Q-switched Nd:YAG ($\lambda = 1.064\,\mu m$), pulsed Holmium-doped Yttrium Scandium Gallium Garnet (Holmium:YSGG, $\lambda = 2.10\,\mu m$), and pulsed Er:YAG ($\lambda = 2.94\,\mu m$) laser—to the skull calvaria from the guinea pig *in vitro* and concluded that Er:YAG laser was the most appropriate system for bone cutting [10]. Their conclusion was based on high cutting efficacy and minimal thermal tissue damage measured with histology. (Here we should note that they purposely dried the bone sample for Er:YAG lasing, to remove unbound water and study the ablation effect without it. Nowadays the study condition is not modified like this.) In 1989, Keller & Hibst applied Er:YAG laser on 30 extracted human teeth and compared its effect to that of CO_2 laser [11]. Detailed ablation mechanism of Er:YAG laser was still unexplored. However, reporting minimal heating of the adjacent tissues—"no-melt, no-fused zones and no cracks"—and only little damage of the dental pulp, they suspected the mi-
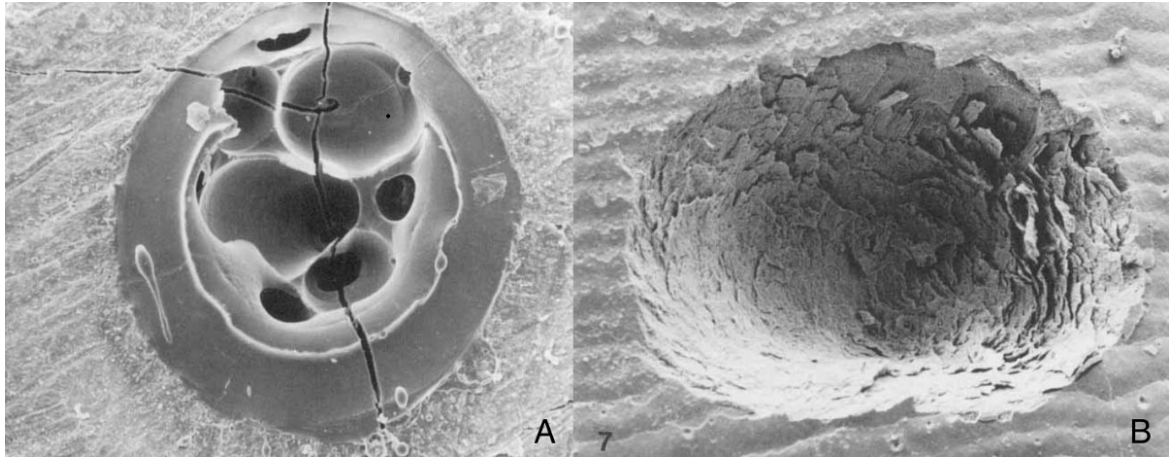
Figure 2.3: Results from the study of Keller & Hibst. SEM view of the enamel surface after (A) CO_2 laser treatment of one pulse with $2\,W$, $500\,ms$ and (B) Er:YAG laser treatment of ten pulses with $200\,mJ$ each pulse. (Reprinted with permission from [11] U. Keller et al., Copyright 1989 Alan R. Liss, Inc.)

croexplosion theory could explain their favorable result of Er:YAG laser ablation (Figure 2.3).

Many studies followed, using Er:YAG laser in dental handpiece setting. It was easy to use for the clinicians and convenient to compare with conventional tools. Following studies were focused on the evaluation of how tissue reacted to laser. Sasaki, Aoki, Ichinose, & Ishikawa analyzed the ultrastructure of the rat parietal bone irradiated by Er:YAG laser and CO_2 laser, and cut by bur drilling [12]. Using light microscope, transmission electron microscopy, and electron diffraction analysis & energy dispersive X-ray spectroscopy, they showed the laser-altered layer from Er:YAG irradiation was approximately five times thinner than that from CO_2 laser. Compared to the even cut surface from bur drilling, the surface of the Er:YAG laser cut showed irregular borders. From the minimal change of the irradiated surface and the lack of the smear layer, they anticipated favorable start of the healing process with Er:YAG laser cutting. In 1999, Friesen, Cobb, Rapley, Forgas-Brockman, & Spencer raised questions with Nd:YAG laser and CO_2 laser used in periodontal treatment. Those two lasers had long been used for gingivitis and periodontitis, but when the disease involved more bone tissue, they left a charred layer on the bone surface and delayed the healing [13]. That
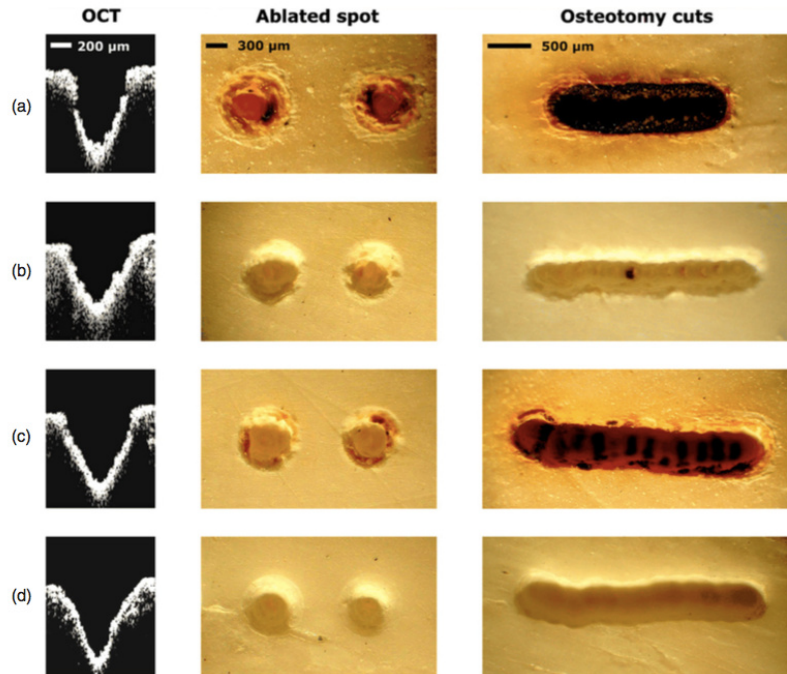
Figure 2.4: Results of the Kang et al.'s investigation. Cross-sectional OCT, top view onto ablated spots by Er,Cr:YSGG laser, and top view onto ablated line with sequence of 5 pulses of Er,Cr:YSGG laser; under (a) dry, (b) water layer, (c) perfluorocarbon layer, and (d) water spray ablation. (Reprinted with permission from Reference [15] H. Kang et al., Copyright 2008 Institute of Physics and Engineering in Medicine. Reprinted with permission of IOP Publishing.)

was how Er:YAG laser (in dental handpiece setting) was introduced as a periodontal treatment tool. In 2003, Schwarz et al. published their 2-year clinical follow-up data, which concluded Er:YAG laser might represent an alternative to conventional scaling and root planing treatment [14].

Another direction of research was focused on the ablation environment and the systematic setup to enhance the efficacy of laser bone cutting. In 2008, Kang, Oh, & Welch investigated the liquid environment of the laser hard tissue ablation [15]. The idea was to compare energy loss, ablation performance, and thermal side effects with the attenuation of the laser beam by liquid layer. Using a conventional Erbium, Chromium-doped Yttrium Scandium Gallium Garnet (Er,Cr:YSGG) laser system ($\lambda = 2.79\,\mu m$) on the fresh bovine tibia in dry and

different wet environments, they concluded that liquid-assisted ablation could provide significant beneficial effects—such as augmented material removal, liquid cooling, and abrasive cleaning effects during laser bone treatments (Figure 2.4). Er,Cr:YSGG laser is one of the most commonly used lasers in dentistry together with Er:YAG laser. Similar in their basic design and characteristics, those two lasers are often misunderstood and confused in the dental laser market. Diaci & Gaspirc clarified their subtle differences and suggested optimal applications for each laser [16]. In 2012, Zhang, Zhan, Liu, & Xie moved forward from Kang et al. and studied the critical water layer thickness to prevent carbonization and smear layer formation with pulsed CO_2 laser [17]. They concluded that there was a critical thickness of water layer for a given radiant exposure, which was $0.4\,\mathrm{mm}$ with pulsed CO_2 laser at $50\,\mathrm{J/cm^2}$. They also confirmed that the water layer actually mediated the interaction of laser with tissue and took an important role in micro-structure changes.

Wolff et al. applied a navigation control and an automatic power control to a hand-held Er:YAG laser in an experimental setting [18]. With the target phantom fixed on the table, the relative position and the orientation of the laser handpiece was calculated. The laser was set to be automatically switched off if the end of the laser beam didn't hit the preoperative planned area. Their work aimed to improve the accuracy of the hand-held laser system, but at the same time, it clearly illustrated the problem of this combination—lack of tactile feedback cancels the advantage of the hand-held instrument and manual guidance kills laser's high precision. They could not reach the required accuracy, even with several fabrications for the experimental setting. However, soon came the time of the real-time navigation achieving corresponding accuracy to the laser, especially with the robot-guidance system.

Robot-guided Laser Osteotomy
State of the Art

Until now most of the medical lasers for hard tissue cutting (*e.g.* dental lasers from growing market or experimental laser osteotomes from increasing publica-

tions) have similar appearances to conventional tools in terms of their usage: be it handpiece or endoscope, the cutting tip/working end of a conventional tool is replaced with the laser head and driven by the surgeon's manipulation. However, in order to maximize the advantages of laser osteotomy, the laser should be guided by a robot through a real-time navigation system. Otherwise the benefits of laser cutting are canceled out, for (one and not the only) example, as the surgeon's hand easily decompensates $200\,\mu m$ of precision.

Robotic laser systems are commonly used in industry but still rare in medicine, except in Opthalmology. One problem of the robot guided laser system is that, due to the bulky size of the robot and the laser, it can easily end up with an unergonomic setup. We could see the situation clearly from the experimental setup in preceding papers [19] [20] [21]. A good illustration from Burgner, Müller,
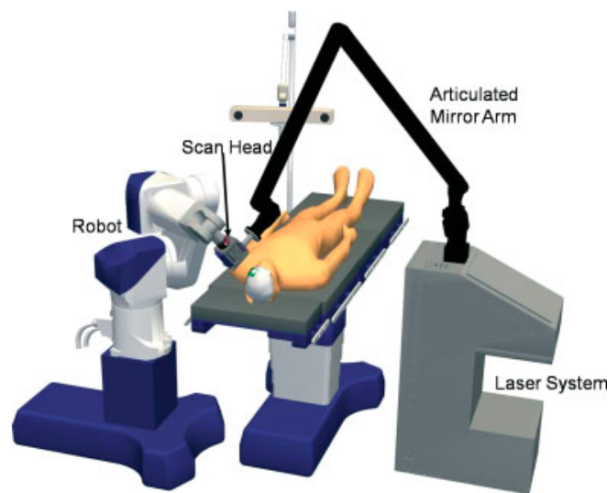
Figure 2.5: Diagram from the experiment of Burgner et al. Setup for robot assisted laser bone ablation. (Reprinted with permission from Reference [20] J. Burgner et al., Copyright 2010 John Wiley & Sons, Ltd.)

Raczkowsky, & Wörn's "*Ex vivo* accuracy evaluation for robot assisted laser bone ablation" shows a system setup with a prototype pulsed CO_2 laser (Figure 2.5) [20]. They analyzed the bone cutting and the workflow of their system, and proved high accuracy of the robot assisted laser bone surgery. Henn et al. analyzed plasma spectra from the ablation by robot-guided pulsed CO_2 laser to identify the ablated tissue (Figure 2.6) [21]. They proved an instant spectral
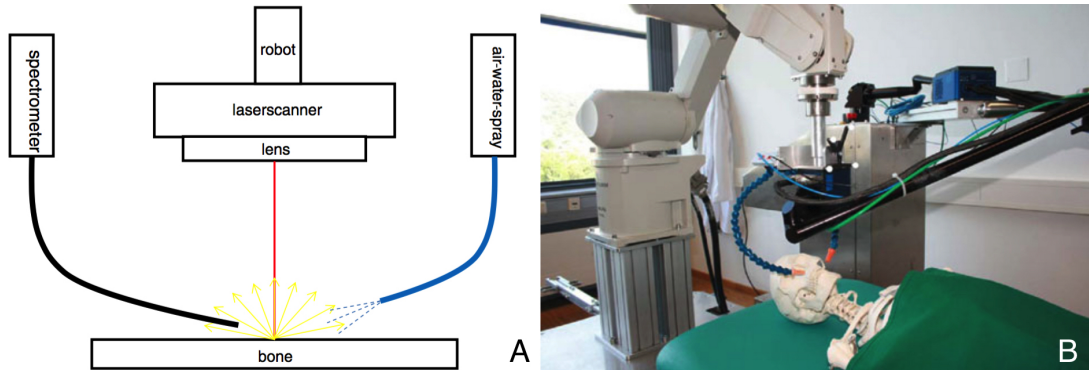
Figure 2.6: Diagram from the experiment of Henn et al. Experimental setup to monitor the cut processing during a robot-assisted laser osteotomy surgery. (Reprinted with permission from Reference [21] K. Henn et al., Copyright 2012 Springer-Verlag London Ltd.)

change when cutting progressed into a different tissue. By combining automatic control, they hoped their finding could enhance the safety of laser bone ablation. Apart from the achievement with the robot-guided laser bone cutting, in those papers we could see that the considerable space around the operation table is occupied by the laser and its control system. Especially in CMF surgery, the surgical approach is limited and complicated, accordingly often the operation field is already crowded with surgeons and assistants. Miniaturization of the whole system is critical. Otherwise even irreplaceable equipment like the surgical microscope would be only very selectively (and reluctantly) used, since it would require a whole rearrangement around the operation table during the surgery. Including preparation and cleaning up, it would take up the operation time and the patient anesthesia time.

In addition, we should remark that many of preceding studies with robot-guided laser were *ex vivo* applications. Moreover, the target object was fully exposed and often fixed to the operation table. A good example would be the study of Sotsuka et al. where they combined cw ytterbium-doped fiber laser (λ = 1.07 μm) with a computer-aided design (CAD)/computer-aided manufacturing (CAM) robotic system [22]. Their *in vivo* osteotomy of the rabbit radial bone showed acceptable healing after 3 weeks compared to saw osteotomy, and *ex vivo* osteotomy on the cow femur achieved good precision (Figure 2.7). However, we
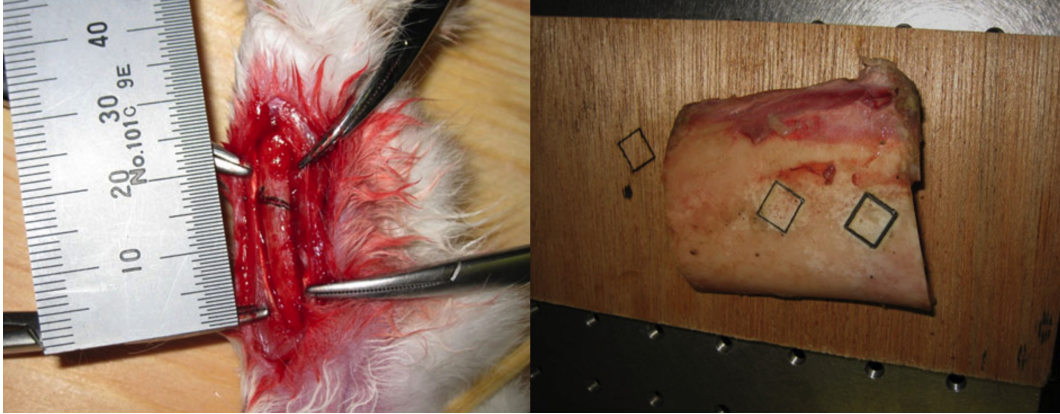
Figure 2.7: Diagram from the experiment of Sotsuka et al. Gross photograph of (A) acute *in vivo* laser osteotomy on the rabbit radial bone and (B) fresh *ex vivo* laser osteotomy on the cow femur. (Reprinted with permission from Reference [22] Y. Sotsuka et al., Copyright 2013 Springer-Verlag London.)

can see their experimental setup is still distant from the actual clinical environment. As they titled, "the dawn of computer-assisted robotic osteotomy with laser" might have broken, but still more time was needed till the day of robotic laser systems actually came to the clinic.

Chapter 3

Motivation and Questions

We developed a miniaturized computer-assisted and robot-guided laser osteotome. Our biggest motivation was to deliver our system into clinical environment—starting from, but not confined to, CMF surgery. Our system consists of;

- integrated miniaturized Er:YAG laser system

- surgical light-weight robotic arm

- computer-assisted pre-operative planning

- intra-operative real-time navigation system

To achieve the goals mentioned above, we had to answer several questions:

1. What are the optimal laser parameters and cooling conditions for bone cutting?

2. How do we deliver the pre-op planning to the intraoperative environment and guide the laser to the operation field in a compact way?

3. How shall we integrate the whole system so that it allows simultaneous work of the surgeon and the laser?

4. How will the bone tissue react to laser?

5. Will laser osteotomy lead to acceptable bone healing?

Chapter 4

System Integration of the Computer-assisted and Robot-guided Laser Osteotome

We built up our laser osteotome in the clinical environment. Serial *in vitro* studies drove the computer-laser-robot system from bench to operation-bedside. Our first publication summarized the system development and integration.

Clinical Applicability of Robot-guided Contact-free Laser Osteotomy in Cranio-maxillo-facial Surgery: in-vitro Simulation and in-vivo Surgery in Minipig Mandibles

In the process of serial studies, intermediate results were presented in several conferences. Graphical test was presented in a poster at the 9th *Bernd-Spiessl Symposium (BSS)*, June 2013 in Basel. The experience of the preclinical study was presented at the 21st *International Conference on Oral and Maxillofacial Surgery (ICOMS)*, October 2013 in Barcelona. Immediate post-op analysis was presented at the 28th *Annual Reunion of Swiss Society of Oral and Maxillo-Facial Surgery (SGMKG)*, November 2013 in Basel.

This paper was published in the *British Journal of Oral and Maxillofacial Surgery*, in December 2015[1].

---

[1] The article is available online at http://www.sciencedirect.com/science/article/pii/S0266435615002788 (last accessed on November 19, 2017).

Clinical applicability of robot-guided contact-free laser osteotomy in cranio-maxillo-facial surgery: in-vitro simulation and in-vivo surgery in minipig mandibles

K.-W. Baek [a,b], W. Deibel [c,d], D. Marinov [d], M. Griessen [c,d], A. Bruno [d], H.-F. Zeilhofer [a,b], Ph. Cattin [c,1], Ph. Juergens [a,b,*,1]

[a] *Department of Cranio-Maxillofacial Surgery, University Hospital Basel, Spitalstrasse 21, 4031 Basel, Switzerland*
[b] *Hightech Research Centre of Cranio-Maxillofacial Surgery, University of Basel, Gewerbestrasse 14, 4123 Allschwil, Switzerland*
[c] *Medical Image Analysis Center, Department of Biomedical Engineering, University of Basel, Gewerbestrasse 14, 4123 Allschwil, Switzerland*
[d] *Advanced Osteotomy Tools AG, Gewerbestrasse 14, 4123 Allschwil, Switzerland*

Abstract

Laser was being used in medicine soon after its invention. However, it has been possible to excise hard tissue with lasers only recently, and the Er:YAG laser is now established in the treatment of damaged teeth. Recently experimental studies have investigated its use in bone surgery, where its major advantages are freedom of cutting geometry and precision. However, these advantages become apparent only when the system is used with robotic guidance. The main challenge is ergonomic integration of the laser and the robot, otherwise the surgeon's space in the operating theatre is obstructed during the procedure. Here we present our first experiences with an integrated, miniaturised laser system guided by a surgical robot. An Er:YAG laser source and the corresponding optical system were integrated into a composite casing that was mounted on a surgical robotic arm. The robot-guided laser system was connected to a computer-assisted preoperative planning and intraoperative navigation system, and the laser osteotome was used in an operating theatre to create defects of different shapes in the mandibles of 6 minipigs. Similar defects were created on the opposite side with a piezoelectric (PZE) osteotome and a conventional drill guided by a surgeon. The performance was analysed from the points of view of the workflow, ergonomics, ease of use, and safety features. The integrated robot-guided laser osteotome can be ergonomically used in the operating theatre. The computer-assisted and robot-guided laser osteotome is likely to be suitable for clinical use for ostectomies that require considerable accuracy and individual shape.
© 2015 The British Association of Oral and Maxillofacial Surgeons. Published by Elsevier Ltd. All rights reserved.

Keywords: Er:YAG laser; Bone; Laser osteotomy; Ergonomic; Computer assisted surgery; Robot guided surgery

* Corresponding author at: Cranio-Maxillofacial Surgery, University Hospital Basel, Spitalstrasse 21, 4031 Basel, Switzerland. Tel.: +41 61 2652525; fax: +41 61 2657298.

E-mail addresses: kyung-won.baek@unibas.ch (K.-W. Baek), waldemar.deibel@unibas.ch (W. Deibel), d.marinov@aot-swiss.ch (D. Marinov), mathias.griessen@aot-swiss.ch (M. Griessen), abruno@aot-swiss.ch (A. Bruno), hans-florian.zeilhofer@usb.ch (H.-F. Zeilhofer), philippe.cattin@unibas.ch (Ph. Cattin), Philipp.Juergens@usb.ch (Ph. Juergens).

Introduction

Laser-photoablation has been used in medicine since the development of laser in 1960, and its first medical use was reported in 1961 in ophthalmology.[1] Three years later, the effects of laser radiation on teeth, pulp, and oral mucosa

[1] Both authors equally contributed to this paper.

were reported,[2] but because of the low water content of bone and teeth, it was difficult to photoablate them. However, the use of lasers in dentistry is now common, and Er:YAG lasers have been used to treat dental problems. The first lasers used to cut bone tissue were carbon dioxide (CO_2) gas lasers, which cut well but initially bone healing was impaired by carbonisation.[3–5] This problem was solved with improvements in laser technology together with more effective cooling systems. The development of Q-switched CO_2 lasers that could deliver sub-microsecond pulses finally achieved char-free cutting of bone.[6] However, it was with the advent of solid-state Er:YAG lasers that photoablation of bone improved considerably. Er:YAG lasers had a more efficient photoablation rate than conventional lasers, and left almost no charred layer under experimental conditions.[7–9] Despite all these advances, the use of lasers in osteotomy is still in the developmental stage. We know of only a few reports of experimental animal studies, and the clinical application is limited to oral surgery.[10–12]

Cutting, drilling, and healing of bone are fundamental issues in oral and craniomaxillofacial surgery, and many treatments are based on disuniting, repositioning, and refixing of bony structures in the facial skeleton. Because of the complex 3-dimensional anatomy and close proximity of vulnerable structures, the interventions demand precision and accuracy. The approach is challenging, as the oral cavity is one of the most common access routes in the specialty. To make laser osteotomy clinically applicable, considerable downsizing of the whole laser-robot system will be required.

Miniaturised, computer-assisted, and robot-guided laser osteotomy would be ideal in craniomaxillofacial surgery. The fact that laser osteotomy is contact-free minimises mechanical and thermal damage to the bone and preserves vulnerable tissues nearby. The most challenging aspect is to provide an appropriate operative system and to find a way to implement such an integrated system into the operating theatre. Various technologies have been introduced in medicine, but not all are used clinically. Even when the surgeon needs them, they often hinder his routine by obstructing both space and view, as is the case with the 3-dimensional navigation systems or laser osteotomy systems that are currently available.[13]

Here we have analysed our first experience with a new computer-assisted, robot-guided laser osteotome and illustrated its advantages for cutting bone, compared with a manually operated piezoelectric (PZE) osteotome and conventional drills.

An Er:YAG laser was erected in a miniaturised setting and mounted on a surgical lightweight robotic arm. Preoperative imaging enabled accurate surgical planning. Intraoperative navigation and robotic guidance ensured its correct execution. The system was initially erected in a dummy operating theatre to simulate a series of craniomaxillofacial operations. It was then used in an actual operating theatre for an in vivo study to create different shapes of defects in one side of the mandibles of 6 minipigs. Similar defects were created on the opposite side with a PZE osteotome and conventional drills, and performance was analysed in terms of workflow, ergonomics, and safety.

Material and Methods

Laser head

We used the prototype laser head. The laser source is an Er:YAG laser (wavelength 2940 nm) that is integrated with an optical system in a compact casing and mounted on a surgical robot. The Er:YAG laser provides a cutting width of 500 μm. The tissue being photoablated is permanently cooled and hydrated by a nozzle system to create a fine sterile aqueous vapour of sterile sodium chloride.

Surgical robot

A KUKA light-weight-robot (LWR4+, KUKA Robotics, Augsberg, Germany) was used to position the laser head. This robot features 7 degrees of freedom and provides a range of movement up to 170° or 120°. The robot is extremely sensitive because of its integrated sensors, which make it ideal for force-controlled tasks, and provide increased safety.

System control

The entire robot-guided laser system is integrated with a computer-assisted preoperative planning and intraoperative navigation system. A software package developed in house uses preoperative imaging to define sites and designs of osteotomies. The navigation system is a key safety feature: it monitors the position of the laser's casing with respect to the target, and converts the preoperative digital data into a real osteotomy by driving the robot. Referencing was done through fixed markers and anatomical landmarks with a passive marker system (Fig. 1).

In vitro dummy operating theatre

To test the ergonomics of the laser system before using it in vivo, we created a dummy operating theatre. The computer-assisted, robot-guided laser system was placed at the 3 o'clock position, at the level of the patient's shoulder. The instrument table was in its typical place, over the patient's chest. A tripod, which carried the infrared camera for the navigation system, was placed at different positions depending on the surgical site to ensure an unimpeded optical corridor. All procedures were recorded with photographs and video for subsequent analyses (Fig. 2).

In vivo operation

We used 6 fully grown female Göttingen minipigs (mean (SD) age 26 (5) months, mean (SD) weight 49 (3) kg).
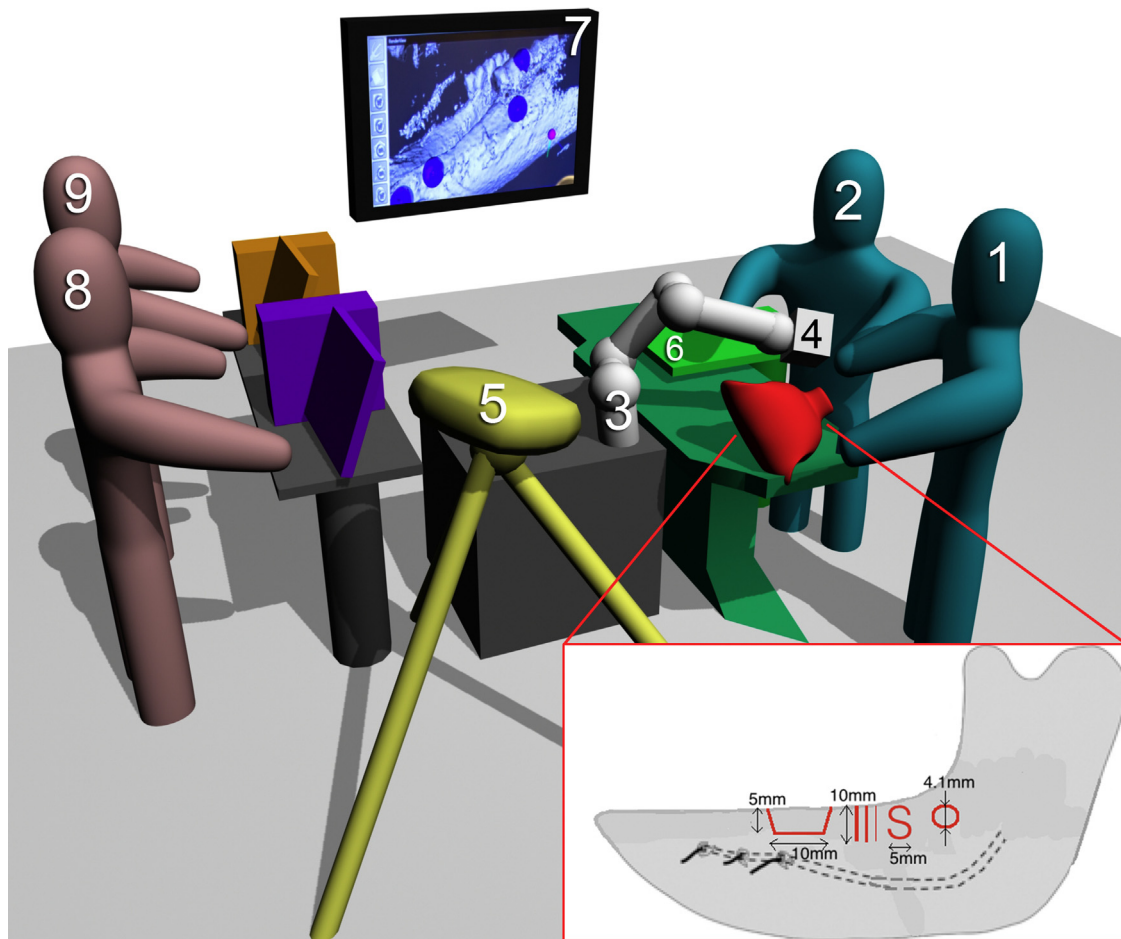
Fig. 1. Diagram of the robot-guided laser osteotome in the minipig experiment: 1=surgeon 1, 2=surgeon 2, 3=robot-guided laser osteotome, 4=laser head, 5=infrared camera, 6= instrument table, 7=main monitor, 8=technician 1, and 9=technician 2.

The operation was done in the Magneten animal facility of the Biomedical centre in Malmö-Lund University, Sweden, in accordance with the Swedish Animal Protection Law and under the ethics approval number M-204-11.3 (Malmö-Lunds djurförsöks etiska nämnd).

Fig. 2. Intraoral approach to the anterior maxilla in the dummy operating theatre.

To create an edentulous ridge, the lower 3 premolars and the first molar (P2, P3, P4, and M1) of each side mandible were removed under general anaesthesia with ketamine hydrochloride 500 mg (Ketalar® 50 mg/ml; Pfizer, New York, NY, USA) and midazolam 15 mg (Dormicum® 5 mg/ml; Roche, Basel, Switzerland) given intramuscularly. At this time 2 screws were placed in each side of the mandible to act as landmarks for intraoperative navigation.

The experimental operations were done 12 weeks later. Under general anesthesia, 3-dimensional C-arm (Siemens ARCADIS Orbic 3D, Siemens AG, Germany) data were acquired for preoperative planning. The minipigs were then moved to the operating table and the manual osteotomy was done (control side). The surgeons created different osteotomy patterns: a saddle defect, 3 straight lines 10 mm long and with differing widths (minimal, 0.5 mm, and 1 mm), an S-shaped line, and a cylindrical defect (4.2 mm diameter)—with a PZE osteotome (PIEZOSURGERY® 3, Mectron s.p.a., Carasco, Italy) and standard dental implant motor and drills (INTRAsurg® 300 plus, KaVo, USA and Straumann® implant drills, Institute Straumann AG, Switzerland) on the right of the mandible (Fig. 3). The time taken to create
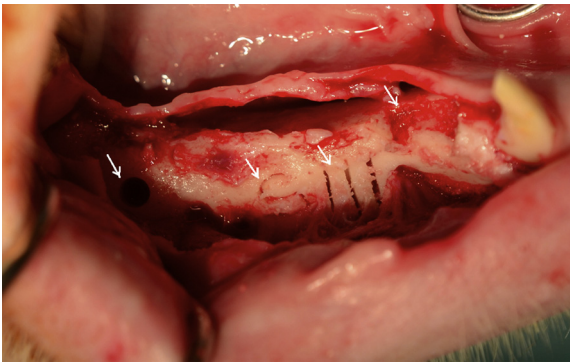
Fig. 3. Clinical photograph of piezoelectric osteotomy.
A cylindrical defect, one S-shaped line, 3 straight lines, and a saddle defect are marked with white arrows (from the posterior to the anterior mandible of minipig on the right). There is minimal bleeding from the bone.

each defect was recorded. Before the wounds were closed with absorbable sutures, a bone-chamber-implant (4.2 mm in diameter and 6 mm long, SLActive® surface, Institute Straumann AG, Switzerland) was inserted into the cylindrical defect. While the surgeons were manually operating on the right side of the mandible, the computer scientists executed the virtual planning for the laser osteotomy on the left side of the mandible.

To make the laser osteotomy, the head of the minipig was immobilised with a custom built device (experimental side). The minipig was then aseptically draped and the surgical access created. Based on the 3-dimensional reconstruction of the mandible, the surgeon did the referencing for the navigation. The time taken for the 3-dimensional registration and the mean back-projection error were measured. Using the navigation system, the surgical robotic arm guided the laser osteotome to create the osteotomy patterns on the left side of the mandible (Fig. 4). The time taken to create each defect was recorded. After insertion of the bone-chamber-implant into the cylindrical defect, the wound was closed. Postoperative images were taken before the animals woke up.
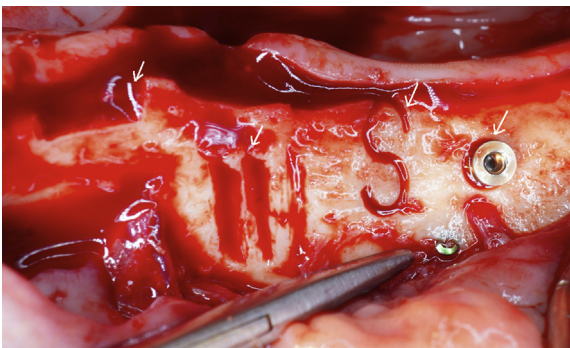

Fig. 4. Clinical photograph of laser osteotomy.
A saddle defect, 3 straight lines, one S-shaped line, and the bone chamber implant in a cylindrical defect are marked with white arrows (from the anterior to the posterior mandible of minipig on the left). There is fresh bleeding from the bone.

Results

Ergonomic tests under in vitro conditions

We tested the ease with which the anterior and posterior maxilla and mandible could be approached by the robot-guided laser osteotome through an intraoral approach in the dummy operating theatre. The surgeons' natural position could be guaranteed and enough space was provided (Fig. 2). Extraoral approaches to the mastoid area and the skull base were also successfully simulated. Several other functions of the robot were simulated and tested: manual guidance to a target point, saving of a starting position and automatic repositioning, and 3-dimensional registration of a target position by navigation. The actual workflow for the in vivo experiment was based on these experiences.

Workflow, ergonomics, and safety in vivo

The experiment followed the order: anaesthesia, preoperative 3-dimensional imaging, manual osteotomy, navigated laser osteotomy, postoperative 3-dimensional imaging, and waking. There was a steep learning curve for the whole procedure, as the accuracy of referencing increased and the overall duration of anaesthesia decreased during the 6 interventions. The improvement in the 3-dimensional registration accuracy can be confirmed by the reduction in back-projection error of the referencing points from 1.5 mm root mean square error (RMSE) for the first animal to 0.6 mm RMSE for the sixth animal.

There was no significant difference between the time for laser osteotomy (mean (SD) 766 (60) seconds) and for manual osteotomy (mean (SD) 734 (295) seconds), but the time taken for the laser osteotomy tended to decrease faster than that for the manual osteotomy. Considering that we created 2 cylindrical defects in the fifth animal and 3 in the sixth animal with laser, the actual decrease of the laser osteotomy time was more than it appears (Fig. 5).

With the second minipig, we could not make the laser osteotomy because the robot kept colliding with the body of the animal during its approach to the oral cavity. Once the robot detected the collision, it went back to its home position without enabling the laser system. The second operation was aborted and the laser head was modified to increase the distance to the target. This improved the optical pathway and the overall ergonomic plan, which resulted in a further reduction in operating time from the third animal on.

The ergonomic aspects and safety features of robot guidance were assessed and confirmed under optimal conditions. The computer-assisted, robot-guided laser osteotome was compact enough to allow 2 surgeons to operate comfortably. The previously suggested position of the laser system opposite the senior surgeon was confirmed as optimal (Fig. 6).
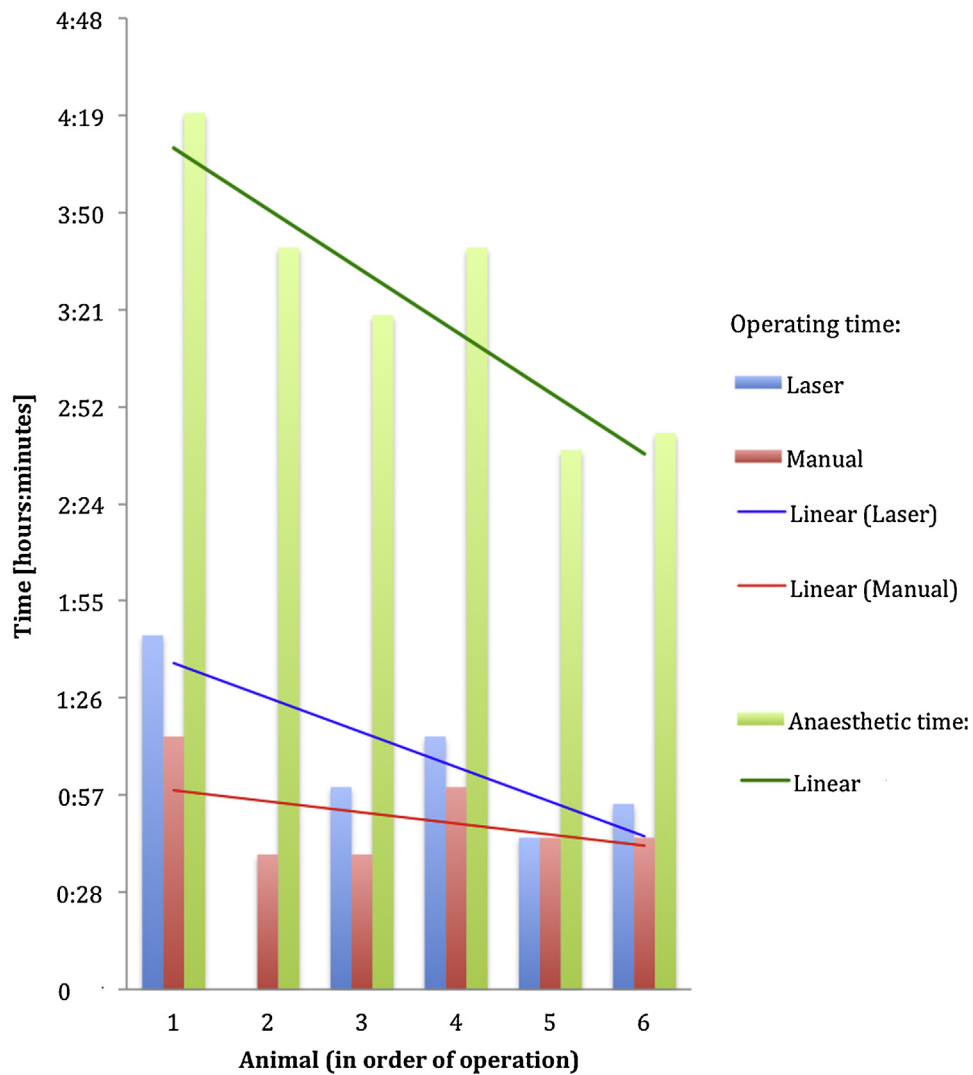
17

Fig. 5. Operating time in the comparative studies of the 6 minipigs.

Discussion

Any new technology becomes accepted only when the surgeon can use it comfortably. Lasers have been proved to

Fig. 6. Robot-guided laser osteotome functioning. Intraoral approach to the posterior mandible in the actual operating theatre during the minipig experiment.

be useful in medicine for a long time but their use in bone surgery have been investigated only recently. Robot-guided laser applications are common in industry, but medical lasers have usually been guided manually not only for preparation of teeth but also for cutting bone.[14–17] Even in studies in which robot guidance was used, the target of the laser photoablation was fixed and no dynamic adjustment of the beam position or focusing was made.[18,19] The most important questions that had to be answered before robot-guided laser systems could be brought into routine clinical use, therefore, are "How can a laser system be miniaturised to be integrated interactively into the operating theatre?" and "Where is the surgeon in this operation?".

Our computer-assisted, robot-guided laser osteotome tries to overcome these hurdles and intends to maximise the benefits of laser without hindering the surgeons. In this study we could see that there was seamless interaction between the surgeon and the laser system, which improved over time and experience. Our experiment also showed that the

robot-guided laser osteotome can be used under various circumstances in craniomaxillofacial surgery for the convenience of the surgeon. Should the surgeon need to take the laser osteotome out of the operative field during the procedure, the robot can memorise its current position, put away the laser, and guide it back to the same position, at any time. This ensures the actual cooperation of the surgeon and the robot-guided laser osteotome in the limited space around the operating table, unlike the previous robot-guided laser device described by Burgner et al.[13]

Safety is one of the most important issues, and the KUKA LWR4+ has several integrated safety features. One of them is the protection of the patient and the surgeon against a patient's unexpected movement. When the robot touches any object in the surgical field, it automatically stops moving, as it did during our second operation. As a consequence of the failure of the second laser operation, we modified our prototype system, which made the subsequent interventions shorter. The performance improved simultaneously, as we saw from the reduction in the mean back-projection error.

Future research should be focused on the improvement of real-time interaction between the laser system and the target tissue. This has been studied for manually-guided laser handpieces, and includes coupling the infrared camera to measure temperature, or using navigated control for automatically power-controlled laser handpiece.[16,17] Coupling of a visible laser such as a helium–neon laser, is also common for measurement of distance and visual targeting.[18,19] More investigations are also needed to measure the dynamic data of ablated bone tissue, and for real-time monitoring and control of the depth of the laser cut. This real-time interaction will add another important safety feature.

Conflict of Interest

We have no conflict of interest.

Ethics statement/confirmation of patients' permission

The operation was done in the Magneten animal facility of the Biomedical centre in Malmö-Lund University, Sweden, in accordance with the Swedish Animal Protection Law and under the ethics approval number M-204-11.3 (Malmö-Lunds djurförsöks etiska nämnd).

Acknowledgements

References

1. Zaret MM, Breinin GM, Schmidt H, et al. Ocular lesions produced by an optical maser (laser). *Science* 1961;**134**:1525–6.
2. Taylor R, Shklar G, Roeber F. The effects of laser radiation on teeth, dental pulp, and oral mucosa of experimental animals. *Oral Surg Oral Med Oral Pathol* 1965;**19**:786–95.
3. Lewis R. *Lasers in dentistry*. FDA Consumer Magazine Jan-Feb 1995.
4. Clayman L, Fuller T, Beckman H. Healing of continuous-wave and rapid superpulsed, carbon dioxide, laser-induced bone defects. *J Oral Surg* 1978;**36**:932–7.
5. Small IA, Osborn TP, Fuller T, et al. Observations of carbon dioxide laser and bone bur in the osteotomy of the rabbit tibia. *J Oral Surg* 1979;**37**:159–66.
6. Ivanenko MM, Fahimi-Weber S, Mitra T, et al. Bone tissue ablation with sub-microS pulses of a Q-switch CO_2 laser: histological examination of thermal side effects. *Lasers Med Sci* 2002;**17**:258–64.
7. Charlton A, Dickinson MR, King TA, et al. Erbium-YAG and holmium-YAG laser ablation of bone. *Lasers Med Sci* 1990;**5**:365–73.
8. Buchelt M, Kutschera HP, Katterschafka T, et al. Erb:YAG and Hol:YAG laser osteotomy: the effect of laser ablation on bone healing. *Lasers Surg Med* 1994;**15**:373–81.
9. Devlin H, Dickinson M, Freemont AJ, et al. Healing of bone defects prepared using the Erbium-YAG laser. *Lasers Med Sci* 1994;**9**: 239–42.
10. Stübinger S, Kober C, Zeilhofer HF, et al. Er-YAG Laser osteotomy based on refined computer-assisted presurgical planning: first clinical experience in oral surgery. *Photomed Laser Surg* 2007;**25**:3–7.
11. Stübinger S, Nuss K, Pongratz M, et al. Comparison of Er:YAG laser and piezoelectric osteotomy; An animal study in sheep. *Laser Surg Med* 2010;**42**:743–51.
12. Stübinger S, Biermeier K, Baechi B, et al. Comparison of Er:YAG laser, piezoelectric, and drill osteotomy for dental implant site preparation: a biomechanical and histological analysis in sheep. *Lasers Surg Med* 2010;**42**:652–61.
13. Burgner J, Muller M, Raczkowsky J, et al. Ex vivo accuracy evaluation for robot assisted laser bone ablation. *Int J Med Robot* 2010;**6**: 489–500.
14. Teng NC, Wang PDY, Chang WJ, et al. Er:YAG laser-roughened enamel promotes osteoblastic differentiation. *Photomed Laser Surg* 2012;**30**:516–22.
15. Lorenzo MC, Portillo M, Moreno P, et al. In vitro analysis of femtosecond laser as an alternative to acid etching for achieving suitable bond strength of brackets to human enamel. *Lasers Med Sci* 2015;**30**:891–900.
16. Wolff R, Weitz J, Poitzsch L, et al. Accuracy of navigated control concepts using an Er: Yag-laser for cavity preparation. *Conf Proc IEEE Eng Med Biol Soc* 2011;**2011**:2101–6.
17. Gabrić Panduric D, Bago I, Katanec D, et al. Comparison of Er:YAG laser and surgical drill for osteotomy in oral surgery: an experimental study. *J Oral Maxillofac Surg* 2012;**70**:2515–21.
18. Lo DD, Mackanos MA, Chung MT, et al. Femtosecond plasma mediated laser ablation has advantages over mechanical osteotomy of cranial bone. *Lasers Surg Med* 2012;**44**:805–14.
19. Sotsuka Y, Nishimoto S, Tsumano T, et al. The dawn of computer-assisted robotic osteotomy with ytterbium-doped fiber laser. *Lasers Med Sci* 2014;**29**:1125–9.

System Development

Inside a sealed housing, the Er:YAG laser beam was profiled by optical components for optimal cutting parameters. In addition to the robot, the profiled beam was directed by a steering mirror stepwise along the pre-programmed cutting shape for an enhanced precision and a faster beam positioning. The target tissue was permanently cooled and hydrated by a pulsed two twin-fluid nozzle array with external liquid mixture. Tables 4.1 and 4.2 show the laser and nozzle specifications, respectively.

Specification	Values
Wavelength	$2.94\,\mu m$
Pulse Energy	up to $150 - 500\,mJ$
Pulse Rate	up to $5 - 35\,Hz$

Table 4.1: System specifications of the flash lamp pumped Er:YAG laser

Specification	Values
Spray Angle (in respect to laser beam)	$18°$
Free Jet Spray Angle	$20 - 25°$
Water Volume Flow	$0.5 - 15\,ml/min$
Gas Volume Flow	$25\,l/min$ @ $2\,bar$

Table 4.2: Specifications for twin-fluid nozzle array

By incidence during the preclinical study, we verified the safety feature of the KUKA LWR4+. Detailed properties of the LWR4+ robot are provided in Table 4.3. Accurate navigation system was a key safety feature of our system. It monitored the position of the laser housing with respect to the target and converted the pre-op digital data into a real osteotomy line, by guiding the robot and the steering mirror to the target. The navigation system is entirely developed in house and the main hardware components are listed in Table 4.4. More detailed explanation can be found in the publication of Schneider, Pezold, Baek, Marinov, & Cattin [23].

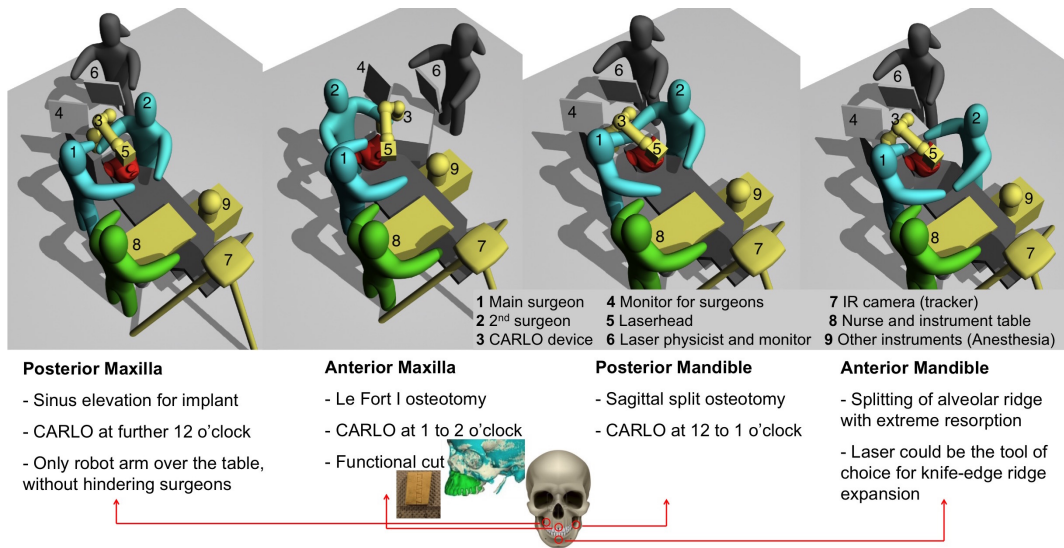| Mechanical Parameter	Values
Degrees of freedom	7 rotating joints
Weight	Approx. 16 kg
Payload	7 kg
Reach	1178 mm (stretched) to 790 mm (90° bent)
Joint ranges	± 170° or ± 120° (Joint dependent)
Repeatability	± 0.05 mm

Table 4.3: Mechanical properties of the KUKA LWR4+

| Specification	Main hardware components
Tracker	Axios CamBarB2 SN: B2-015
Pointer Tool	NDI
Laser head Marker	NDI
Target Marker	CAScination

Table 4.4: Summary of the navigation system

System Integration

The computer-robot-laser system was adapted to the ergonomic configuration. Figure 4.1 shows the graphical tests we ran for the intraoral approach to different jaw areas—for corresponding representative operations in CMF surgery. Test results were realized and amended in a dummy OR setting, until finalized as in Figure 1 of our first publication in the Section 4.1 (page 16). The final configuration was confirmed with the fresh pig cadaver head. CT images were acquired to plan the site, approach, and design of the osteotomy (Figure 4.2). Based on the pre-operative planning, the actual osteotomy was executed on the mandible of the cadaver head in a dummy OR environment (Figure 4.3). Testing the navigation system was the essential step before the preclinical study. Using anatomical landmarks as referencing points, the registration was performed by fitting two 3D point sets [24]. Through these preliminary studies, all aspects of the system were re-analyzed and prepared for the first *in vivo* study.

With the *in vivo* study we could confirm the successful system integration. By the operation time and anesthesia time, we proved that our laser osteotomy system was competitive and compatible with the conventional osteotomy. Figure

Posterior Maxilla

- Sinus elevation for implant

- CARLO at further 12 o'clock

- Only robot arm over the table, without hindering surgeons

Anterior Maxilla

- Le Fort I osteotomy

- CARLO at 1 to 2 o'clock

- Functional cut

Posterior Mandible

- Sagittal split osteotomy

- CARLO at 12 to 1 o'clock

Anterior Mandible

- Splitting of alveolar ridge with extreme resorption

- Laser could be the tool of choice for knife-edge ridge expansion

1 Main surgeon	**4** Monitor for surgeons	**7** IR camera (tracker)
2 2nd surgeon	**5** Laserhead	**8** Nurse and instrument table
3 CARLO device	**6** Laser physicist and monitor	**9** Other instruments (Anesthesia)

Figure 4.1: Graphic simulation of the robot-guided laser osteotome for the intraoral approach to different jaw bone regions.
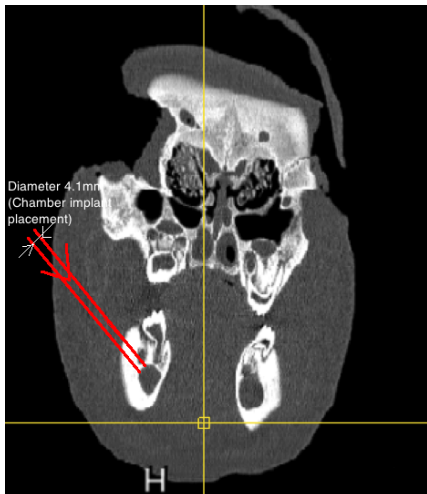
Figure 4.2: Frontal CT image of the pig cadaver head showing the planned intraoral approach to the posterior mandible.

Figure 4.3: Intraoral approach to the posterior mandible of the pig cadaver head.

5 of the publication (page 18) summarized our result, except that the actual decrease of the laser osteotomy time is bigger than shown in the graph. Figures 5.1 and 5.2 show the laser osteotomy side of the 5th and 6th animal, where we created

Figure 4.4: Surgeons performing 3-dimensional registration for the intra-operative navigation.

Figure 4.5: Robot-guided laser osteotome in function in CMF OR setup.

more cylindrical defects.

Figures 4.4 and 4.5 display the actual OR setup as a result of aforementioned preliminary studies. As shown in Figure 6 of the publication (page 18), the laser system worked together with the main surgeon and the assistant surgeon in the operation field. There was enough room around the operation table, whether the laser was at the home position (Figure 4.4) or in function (Figure 6 of the publication [page 18]). During the laser was operating, the surgeons could confirm the operation either by direct observation (Figure 6 of the publication [page 18]) or via the main monitor (Figures 4.5). The navigated robot system successfully finished its first preclinical study and now it was our turn to analyze the result.

Chapter 5

Interaction of Laser Light and Bone Tissue

We chose the minipig as an animal model. Their bone anatomy, metabolism, healing, and remodeling after reaching adulthood are known to be similar to those of humans. Pigs have been one of the major animals used in translational research and surgical models [25]. Especially in CMF surgery, strong similarity of the mandibular blood supply between Göttingen minipigs and humans was proven in 2002 by Saka, Wree, Anders, & Gundlach [26]. Our second publication reported the bone tissue reaction to Er:YAG laser light in the minipig mandible, which could be readily, if cautiously, applied to the human jaw bone.

A Comparative Investigation of Bone Surface after Cutting with Mechanical Tools and Er:YAG Laser

Key topics of this paper were post-op cut surface analysis and the smear layer on the bone surface. Our hypothesis was that the different surface characteristics, from laser osteotomy and mechanical osteotomy, yielded to different bleeding patterns and would subsequently result in different bone healing patterns. As a conclusion of comparative analyses of SEM images, we anticipated favorable bone healing after laser osteotomy and opened the question to upcoming paper with histologic analysis.

With the SEM results as the main findings, intermediate results of histology

was presented at the *10th Bernd-Spiessl Symposium (BSS)*, June 2014 in Basel, and awarded as the best presentation. The computer-robot-laser system was presented from the surgeon's point of view at the *28th International Congress and Exhibition for Computer Assisted Radiology and Surgery (CARS)*, June 2014 in Fukuoka. The development and integration of the whole system was introduced to Korean CMF surgeons at the *53rd Congress of Korean Association of Maxillofacial Plastic and Reconstructive Surgery (KAMPRS)*, October 2014 in Seoul. The paper was published in *Lasers in Surgery and Medicine*, in May 2015[1].

---

[1]The article is available online at http://onlinelibrary.wiley.com/doi/10.1002/lsm.22352/full (last accessed on November 19, 2017).

A Comparative Investigation of Bone Surface After Cutting with Mechanical Tools and Er:YAG Laser

Kyung-won Baek, DMD, MSD,[1,2] **Waldemar Deibel,**[3,4] **Dilyan Marinov, PhD,**[4] **Mathias Griessen,**[3,4]
Michel Dard, Prof DMD, PhD,[5] **Alfredo Bruno, PhD,**[4] **Hans-Florian Zeilhofer, Prof DMD, MD,**[1,2]
Philippe Cattin, Prof PhD,[3] **and Philipp Juergens, PD, DMD, MD**[1,2]*

[1]*Department of Cranio-Maxillofacial Surgery, University Hospital Basel, Spitalstrasse 21, Basel 4031, Switzerland*
[2]*Hightech Research Centre of Cranio-Maxillofacial Surgery, University of Basel, Schanzenstrasse 46, Basel 4031, Switzerland*
[3]*Medical Image Analysis Centre, University of Basel, Spitalstrasse 21, Basel 4031, Switzerland*
[4]*Advanced Osteotomy Tools AG, Spitalstrasse 21, Basel 4031, Switzerland*
[5]*Periodontology and Implant Dentistry, New York University College of Dentistry, 345E. 24th Street, New York City 10010*

Background and Objectives: Despite of the long history of medical application, laser ablation of bone tissue became successful only recently. Laser bone cutting is proven to have higher accuracy and to increase bone healing compared to conventional mechanical bone cutting. But the reason of subsequent better healing is not biologically explained yet. In this study we present our experience with an integrated miniaturized laser system mounted on a surgical lightweight robotic arm.
Study Design/Materials and Methods: An Erbium-doped Yttrium Aluminium Garnet (Er:YAG) laser and a piezoelectric (PZE) osteotome were used for comparison. In six grown up female Göttingen minipigs, comparative surgical interventions were done on the edentulous mandibular ridge. Our laser system was used to create different shapes of bone defects on the left side of the mandible. On the contralateral side, similar bone defects were created by PZE osteotome. Small bone samples were harvested to compare the immediate post-operative cut surface.
Results: The analysis of the cut surface of the laser osteotomy and conventional mechanical osteotomy revealed an essential difference. The scanning electron microscopy (SEM) analysis showed biologically open cut surfaces from the laser osteotomy. The samples from PZE osteotomy showed a flattened tissue structure over the cut surface, resembling the "smear layer" from tooth preparation.
Conclusions: We concluded that our new finding with the mechanical osteotomy suggests a biological explanation to the expected difference in subsequent bone healing. Our hypothesis is that the difference of surface characteristic yields to different bleeding pattern and subsequently results in different bone healing. The analyses of bone healing will support our hypothesis. Lasers Surg. Med. 47:426–432, 2015.
© 2015 Wiley Periodicals, Inc.

Key words: Bone surface analysis; Er:YAG laser; laser osteotomy; mechanical osteotomy; SEM

INTRODUCTION

Bone cutting is one of the oldest medical procedures performed to human. Owing to the high mineral contents of bone, we have archaeological evidence of skull trepanation, which dates back to 6,500 BC [1]. The oldest remaining instruments for bone surgery date back to the Roman era [2]. In the 18th century surgery became its own discipline in medicine, and surgical instruments developed rapidly with the advancement of technology and the invention of new materials. But the fundamental mechanism of bone cutting has not much changed from the instruments of the Roman age. Surgeons put mechanical stress onto the bone surface using various instruments—electric or pneumatic saw, drill, chisel and hammer—until it exceeds the surface hardness of bone so that the instrument breaks into the bone. The latest technology enables selective hard tissue cutting with new bone cutting instrument such as the piezoelectric (PZE) osteotome. Its biggest strength lies in the safety, as the adjacent soft tissue damage is reduced [3]. This is why the PZE osteotome has been extensively applied in the oral and cranio-maxillofacial (CMF) area, where important neurovascular structures are closely located to the facial bones [4,5]. But the PZE osteotome is another mechanical cutting tool with its cutting tip in direct contact with the bone. This means the PZE osteotome shares the same limitations of the aforementioned instruments: stuck

cutting tip into bone during the osteotomy, broken cutting tip, and limited cutting geometry. Recently, laser has been applied to osteotomy as it is expected to solve the aforementioned problems fundamentally by its non-contact feature. Erbium-doped Yttrium Aluminium Garnet (Er: YAG) laser has shown to be effective in bone cutting, and their application with robot guidance is actively studied in CMF surgery to maximize its advantages [6].

Bone healing has been a topic of great importance in medicine, especially in surgery. The oldest record of fracture and bone healing dates back to 2,500–3,000 BC [7]. Ever since then, the repositioning and fixating of the bone has been the base of many treatment concepts in bone surgery. CMF surgery specifically demands precise osteotomy and predictable bone healing, because of the complex three-dimensional anatomy and the close proximity of important neurovascular structures in the viscerocranium. Adequate bone healing without side effect is the goal of treatment and the barometer of prognosis. New treatment concepts and new devices are often evaluated based on the resultant bone healing of critical defects on the skull bone [5,8] or of long bones [9–11] in different animals. But few studies evaluate fresh bone cut surface after osteotomy, while the surface characteristic of enamel and dentine after teeth preparation has been a key topic in dentistry [12–15]. In this study we present the immediate post-operative result of our first experience with a new laser osteotome and analyze it in comparison to a PZE osteotome.

We performed osteotomies on the mandibles of mature female minipigs, with a new computer assisted and robot-guided laser osteotome and a PZE osteotome. An Er:YAG laser head was mounted on a medical lightweight robotic arm. The osteotomy was planned according to the pre-operative medical imaging and executed by the robotic guidance using the intra-operative navigation system. The computer assisted and robot-guided laser osteotome was used in an operation room (OR) environment to create different shapes of defects on the mandibles of six minipigs. Similar defects were created on the contralateral sides by a manually guided PZE osteotome and a conventional drill. The intra-operative findings were recorded and cut out bone pieces were evaluated post-operatively. With scanning electron microscope (SEM) we could observe characteristic surface changes of the bone after mechanical osteotomy. This article introduces new findings in *in-vivo* osteotomies. Through this we hope to better understand the bone healing process after laser osteotomy and possibly learn from dentistry how to accelerate it.

MATERIALS AND METHODS

Animals

Six grown up female Göttingen minipigs (mean age 25.5 months, mean weight 48.7 kg) were used in this study. The animals were housed in cots in groups of three, under controlled environmental conditions. Throughout the duration of the experiment, they were fed soft diet and water. The surgical procedure of this study was performed in the Magneten animal facility of the Biomedical centre in Malmö-Lund University, Sweden. All procedures were in accordance with the Swedish Animal Protection Law and under the ethical approval number M-204-11.3 (Malmö-Lunds djurförsöks etiska nämnd).

Study Design

The study was carried out in two surgical phases. In the first phase, the premolars and first molar on both sides of the mandible were extracted to create edentulous ridges. After 12 weeks of healing, planned osteotomy patterns were created on the edentulous mandibular ridges, one side with PZE osteotome and the other side with laser osteotome.

Surgical Procedure

All surgeries were performed under full narcosis starting with Ketamine hydrochloride 500 mg (Ketalar® 50 mg/ml; Pfizer, New York, NY, USA) mixed with Midazolam 15 mg (Dormicum® 5 mg/ml; Roche, Basel, Switzerland). After intramuscular injection of 10 ml Ketalar® and 3 ml Dormicum®, each surgical site received local anesthesia (Xylocain® Dental 20 mg/ml mixed with adrenalin 12.5 μg/ml, Dentsply Pharmaceutical, York, PA, USA) up to maximum 4 injections per animal. During the surgery, 10 ml of Ketalar® was injected additionally when needed, usually every 30 to 40 minutes. For all surgical procedures, no inhalation anesthesia was used.

In the first phase, the lower three premolars and the first molar (P2, P3, P4, and M1) on both sides of the mandible were removed under intramuscular full narcosis. Periapical radiographs taken from each site confirmed the absence of root tip remnants. Full closure of the wound area was achieved and sites were allowed to heal for 12 weeks.

After 12 weeks, comparative operations were performed in all six animals. Under the same procedure of intramuscular full narcosis, the minipig was put on the operation
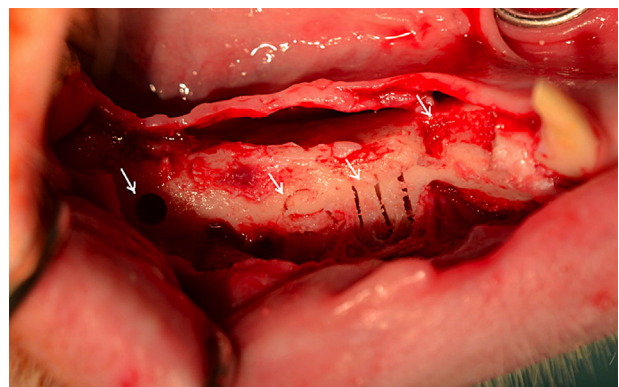

Fig. 1. Clinical photo of manual osteotomy. A cylindrical defect, one S-shaped line, three straight lines and a saddle defect are marked with white arrows (from the posterior to the anterior mandible of minipig, right side). Minimal bone bleeding can be observed.
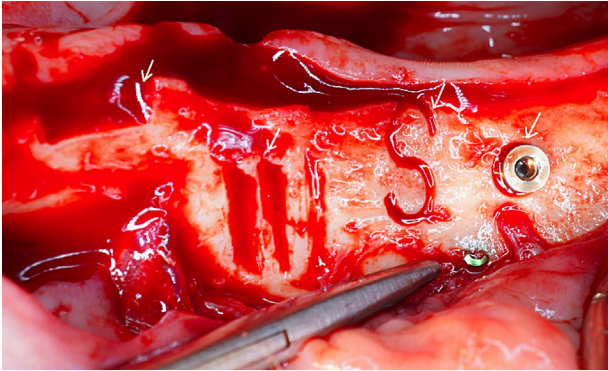
Fig. 2. Clinical photo of laser osteotomy. A saddle defect, three straight lines, one S-shaped line and the bone chamber implant in a cylindrical defect are marked with white arrows (from the anterior to the posterior mandible of minipig, left side). Fresh bone bleeding is notable.

table right side up and aseptic draping was done exposing only the mouth area. After local anesthesia, the surgeon incised into the mucosa, elevated the periosteal flap to expose the edentulous ridge of the mandible. Different osteotomy patterns—from anterior to posterior, one saddle defect, three straight lines with 10 mm lengths and different widths (minimal, 0.5 mm, 1 mm), one S-shaped curved line and one cylindrical defect (4.1 mm diameter)—were created manually by surgeon, on the right side of the mandible with a PZE osteotome and a standard implant drill (IntraSurg300 plus, KaVo, USA and Implant drills, Institute Straumann AG, Switzerland) (Fig. 1. Clinical photograph of manual osteotomy). For the laser operation the minipig was turned on the other side, and the head was fixed to the operation table using a customized device. Aseptic draping was applied once again and the surgeon exposed the edentulous ridge. Using the navigation system, the surgical robotic arm guided the laser

osteotome to create the same osteotomy patterns on the left side of the mandible (Fig. 2. Clinical photograph of laser osteotomy). At the end of all procedures, the minipig was moved to the monitoring room and the recovery from full narcosis was closely monitored until it woke up.

Laser Head

In this study, a prototype laser housing was used. The photoablation laser is a solid state Er:YAG laser lasing at a wavelength of 2,940 nm, integrated into a sealed housing, mounted on the last stage of the surgical robot. The pulsed Er:YAG laser is operated in the range of 150–500 mJ and a repetition rate ranging from 5–35 Hz to create a cut of 500 µm width. The laser beam is profiled by an optical system with a final focusing element rendering a working distance of 40 mm from the laser housing. The bone surface was permanently cooled and hydrated by a nozzle system to create a fine sterile aqueous vapor.

PZE Osteotome

The Piezo-surgery 3 (Mectron S.p.A., Carasco, Italy) was used as control. To make different size and shape of defects, OT6, OT7, OT7S-3, and OT7S-4 tips were used. During the osteotomy, the bone surface was permanently cooled and hydrated by a nozzle array with sterile sodium chloride with a flow rate of 80–90 ml/min.

Scanning Electron Microscopy (SEM)

The bone blocks from the saddle defects were analyzed with SEM. Bone blocks were fixed with 3.8% formaldehyde in phosphate buffered saline (PBS) for 24 hours and meticulously rinsed with PBS. The samples were gradually dehydrated in a series of graded ethanol/water mixtures (50%, 70%, 80%, 90%, and 100%; each step for 4 hours at room temperature). After the critical point drying, the samples were sputter-coated with a thin layer of platinum
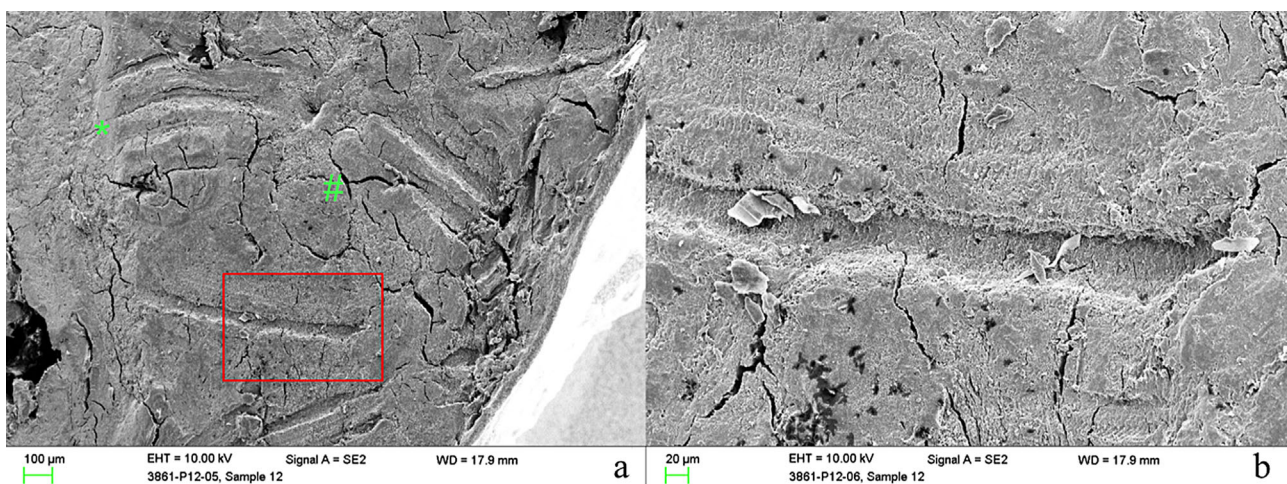

Fig. 3. SEM images of cut face created with PZE osteotome in different magnifications [a) x 50, b) x 200] showing the typical flattened down and closed surface. Scratches (*) caused by the instrument tip and tension cracks (#) as indicators for mechanical stress are clearly visible. Red boxes indicate cutout for the subsequent magnification.
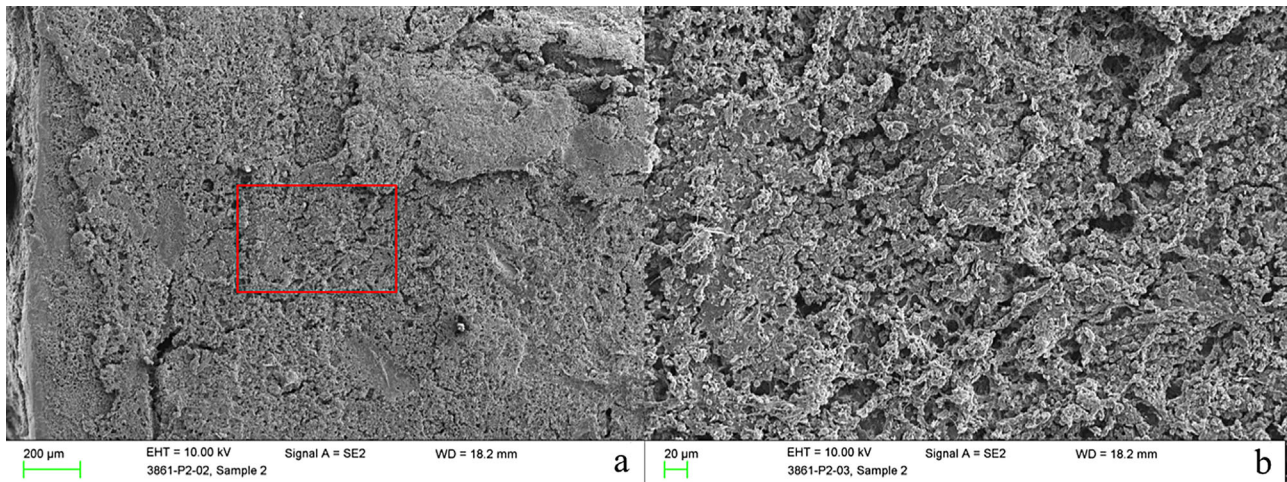
Fig. 4. SEM images of cut face created with laser osteotome in different magnifications [a) x 50, b) x 200] presenting an open surface and intact tissue structure. Red boxes indicate cutout for the subsequent magnification.

of 2 nm in thickness (Sputter coater, Cressington, Watford, England). Surface topography was qualitatively examined using SUPRA 55 (ZEISS, Oberkochen, Germany) scanning electron microscope.

RESULTS

Intra-Operative Observation

During the defect creation, fresh bleeding was clearly notable more on the laser osteotomy side as compared to the PZE osteotomy side (Fig. 1. and Fig. 2.). With all six minipigs, the bleeding on the PZE osteotomy side was minimal.

SEM–Closed Bone Surface and Open Bone Surface

The bone samples from PZE osteotomy showed a typical flattened down and closed surface with tension cracks and even scratches from the blade. This was clearly notable in higher magnifications (Fig. 3. SEM images of cut face created with PZE osteotome in different magnifications [a–b]). On the contrary, the bone samples from laser osteotomy showed an open surface with intact tissue structures (Fig. 4. SEM images of cut face created with laser osteotome in different magnifications [a–b]). We suspected that the fresh bleeding during laser osteotomy could be explained by the open surface structures documented in the SEM images, while the closed surface on the PZE osteotomy sides could explain the minimal bleeding from the osteotomy gaps. These observations were constant in all six animals.

Both experimentally created cut faces were compared to the natural bone surface from the alveolar crest of the mandible (Fig. 5. SEM images of natural bone surface in different magnifications [a–b]). The SEM images showed a
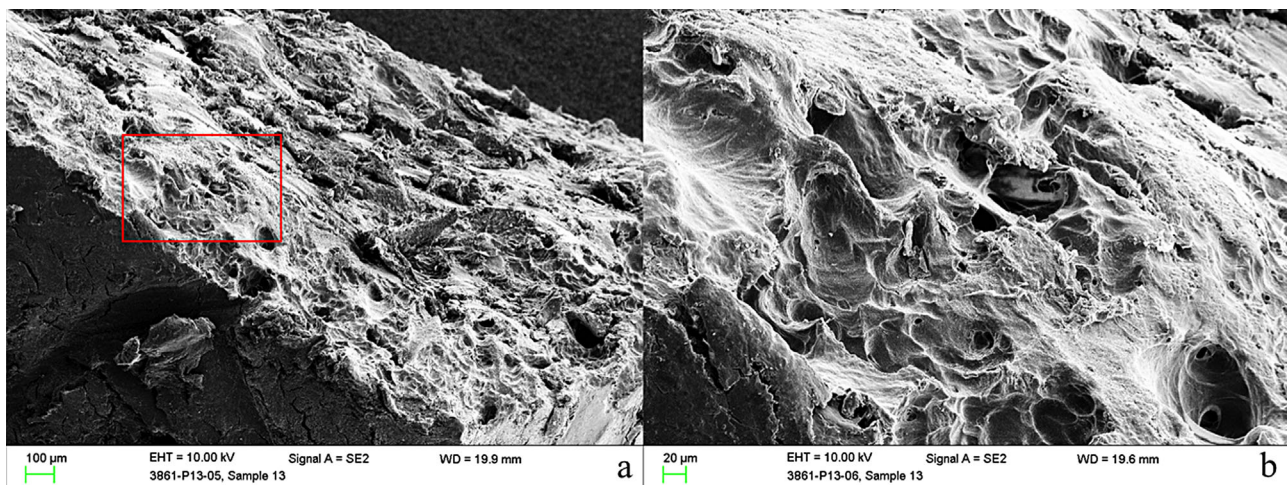

Fig. 5. SEM images of natural bone surface in different magnifications [a) x 50, b) x 200]. The sample was taken from the alveolar crest of the minipig's mandible. Red boxes indicate cutout for the subsequent magnification.
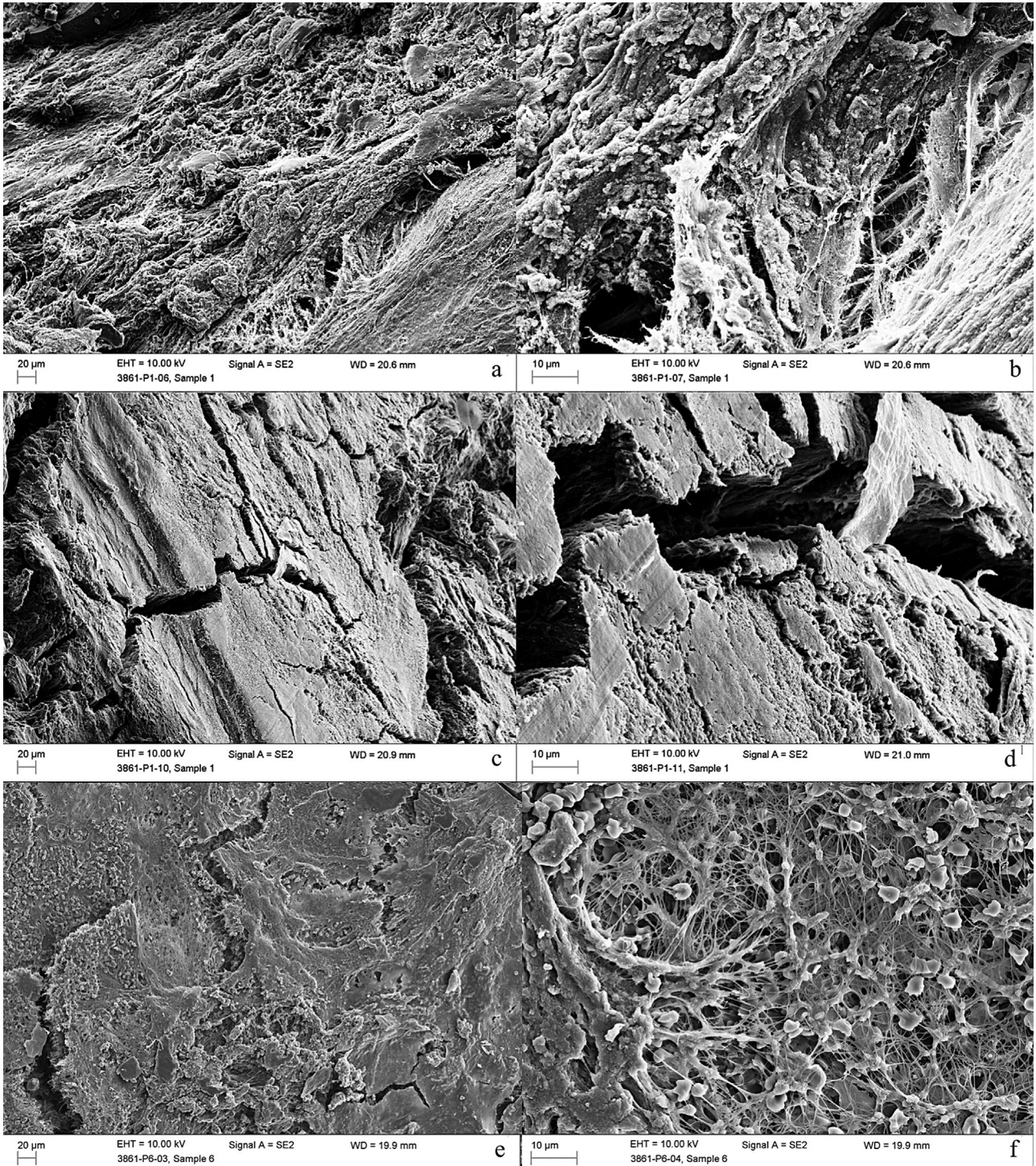
Fig. 6. Comparison of SEM images of natural bone surface [a) x 200, b) x 1000], cut face created with PZE osteotome [c) x 200, d) x 1000] and that created with laser osteotome [e) x 200, f) x 1000] at higher magnification. The cut face after PZE osteotomy appears to be covered and closed by a coating resembling the smear layer known in dentistry from tooth preparation. At the same time the cut face created by laser osteotomy is presenting a high structural analogy to the surfaces of natural bone.

high resemblance between the natural bone surface and the cut surface created with the laser osteotome (Fig. 6. Comparison of SEM images of natural bone surface [a, b], cut face created with PZE osteotome [c, d], and that created with laser osteotome [e, f] at higher magnification).

DISCUSSION

A typical smooth and regular surface is notable in the bone samples from the PZE osteotomy side. This closed surface was also observed in another study with PZE osteotome [16], and interpreted as a result of precise cutting. We concluded that this flattened down tissue structure resembles more the "smear layer" of the mechanically instrumented teeth surface. The smear layer is a two to five micrometer thick layer, which is left on the dentinal surface after mechanical teeth preparation, clogging the dentinal tubules [12]. In 1975 McComb and Smith observed an amorphous layer of debris with an irregular and granular surface, on instrumented dentinal walls and first described the smear layer [13]. Ever since, it has been debated whether the smear layer assists or prevents the penetration of bacteria into the dentinal tubules [17–20]. The smear layer became an important research topic in dentistry, in relation with the surface treatment after tooth preparation [14,15]. Nowadays the smear layer is routinely removed before the filling of the teeth, since it is proven to adversely affect the sealing ability of sealers [21]. While the removal of the smear layer and its effect on dental materials is actively studied in dentistry, its equivalent on the bone surface has not been reported yet. Does mechanical instrumentation not leave anything on the bone surface? If it does, will it not affect the subsequent bone healing?

Laser has been applied in medicine from the development stage, but bone tissue laser ablation became successful only recently. The problem of using laser in bone cutting was the cutting efficacy and carbonization. Especially carbonization was known to impair following bone healing, and became the focus of the surface evaluation after bone tissue laser ablation [22–24]. The improvement of laser technology and effective cooling system solved this problem, like Q-switched CO_2 lasers [23] and solid-state Er:YAG lasers [24]. Er:YAG lasers showed more efficient photoablation as compared to conventional lasers and proved to result in sufficient bone healing [24,25]. Contact-free bone cutting is one important feature of laser osteotomy. The absence of the cutting tip, in direct contact with the surface, must result in different surface characteristic after cutting. The preparation of the tooth with laser and its surface characteristics are already studied in dentistry [26,27]. The advantages of contact-free osteotomy are also well explained in many studies, especially when the osteotomy is guided by surgical robot to maximize the precision [10,28]. It is interesting that even in these studies, showing the advantages of laser osteotomy over mechanical osteotomy, the biological explanation of subsequent better healing is only briefly mentioned or omitted. We noted that very few studies reported the characteristics of bone surface after mechanical osteotomy [16], while the characteristics of enamel and dentine surface after mechanical tooth reduction have been widely studied [12–15].Consequently our assumption is that what we found on the bone surface after mechanical osteotomy is comparable to the smear layer on the tooth surface after tooth preparation, which resulted from mechanical ablation of enamel and dentine. We also think that this layer can explain reported better bone healing after laser osteotomy. We could confirm this layer's existence on the bone surface from the mandibles of six minipigs, which were cut by PZE osteotome. We furthermore concluded that this smear layer on the bone surface is responsible for the reduced bone bleeding observed after PZE osteotomy. On the contrary, fresh bone bleeding after laser osteotomy can be explained with the anatomically open and biologically active surface, which might even promote the healing process.

To prove that the smear layer is indeed responsible for the impaired bone healing after PZE osteotomy, we plan our next study on applying the techniques known from dentistry to bone, to remove the smear layer after PZE osteotomy. If this treatment improves bone healing, we could conclude that the smear layer is indeed responsible for the impaired healing characteristic after the mechanical bone cutting.

ACKNOWLEDGMENTS

analysis and interpretation of the collected data was executed by K.-W. Baek, M. Dard, and Ph. Juergens. K.-W. Baek, M. Dard, Ph. Cattin and Ph. Juergens were drafting and critically reviewing the manuscript. Ph. Cattin and Ph. Juergens finally approved the manuscript.

REFERENCES

1. Sigerist HE. A History of Medicine. Oxford: University Press; 1951.
2. Kirkup J. The evolution of surgical instruments: An illustrated history from ancient times to the twentieth century. Novato, Calif: Jeremy Norman Co 2006.
3. Vercellotti T. Piezoelectric surgery in implantology: a case report—A new piezoelectric ridge expansion technique. Int J Periodontics Restorative Dent 2000;20(4):358–365.
4. Stübinger S, Biermeier K, Baechi B, Ferguson SJ, Sader R, von Rechenberg B. Comparison of Er:YAG laser, piezoelectric, and drill osteotomy for dental implant site preparation: A biomechanical and histological analysis in sheep. Lasers Surg Med 2010;42(7):652–661.
5. Hollstein S, Hoffmann E, Vogel J, Heyroth F, Prochnow N, Maurer P. Micromorphometrical analyses of five different ultrasonic osteotomy devices at the rabbit skull. Clin Oral Implants Res 2012;23(6):713–718.
6. Stübinger S, Kober C, Zeilhofer HF, Sader R. Er-YAG Laser Osteotomy Based on Refined Computer-Assisted Presurgical Planning_First Clinical Experience in Oral Surgery. Photomed Laser Surg 2007;25(1):3–7.
7. Stiefel M, Shaner A, Schaefer SD. The Edwin Smith Papyrus: The birth of analytical thinking in medicine and otolaryngology. Laryngoscope 2006;116(2):182–188.
8. Lo DD, Mackanos MA, Chung MT, Hyun JS, Montoro DT, Grova M, Liu C, Wang J, Palanker D, Connolly AJ, Longaker MT, Contag CH, Wan DC. Femtosecond plasma mediated laser ablation has advantages over mechanical osteotomy of cranial bone. Lasers Surg Med 2012;44(10):805–814.
9. Gabrić Panđurić D, Bago I, Katanec D, Zabkar J, Miletić I, Anić I. Comparison of Er:YAG laser and surgical drill for osteotomy in oral surgery: an experimental study. J Oral Maxillofac Surg 2012;70(11):2515–2521.
10. Sotsuka Y, Nishimoto S, Tsumano T, Kawai K, Ishise H, Kakibuchi M, Shimokita R, Yamauchi T, Okihara S. The dawn of computer-assisted robotic osteotomy with ytterbium-doped fiber laser. Lasers Med Sci 2014;29(3):1125–1129.
11. Stübinger S, Nuss K, Pongratz M, Price J, Sader R, Zeilhofer HF, von Rechenberg B. Comparison of Er:YAG laser and piezoelectric osteotomy; An animal study in sheep. Laser Surg Med 2010;42(8):743–751.
12. Braennstroem M, Johnson G. Effects of various conditioners and cleaning agents on prepared dentin surfaces: A scanning electron microscopic investigation. J Prosthet Dent 1974;31-(4):422–430.
13. McComb D, Smith DC. A preliminary scanning electron microscopic study of root canals after endodontic procedures. J Endod 1975;1(7):238–242.
14. Korkmaz Y, Ozel E, Attar N, Bicer CO, Firatli E. Micro-leakage and scanning electron microscopy evaluation of all-in-one self-etch adhesives and their respective nanocomposites prepared by erbium:Yttrium-aluminum-garnet laser and bur. Lasers Med Sci 2010;25(4):493–502.
15. Kato C, Taira Y, Suzuki M, Shinkai K, Katoh Y. Conditioning effects of cavities prepared with an Er,Cr:YSGG laser and an air-turbine. Odontology 2012;100(2):164–171.
16. Simonetti M, Facco G, Barberis F, Signorini G, Capurro M, Rebaudi A, Sammartino G. Bone characteristics following osteotomy surgery: An in vitro SEM study comparing traditional Lindemann drill with sonic and ultrasonic instruments. POSEIDO 2013;1(3):187–194.
17. Tucker JW, Mizrahi S, Seltzer S. Scanning electron microscopic study of the efficacy of various irrigating solutions: Urea, Tublicid Red, and Tubulicid Blue. J Endod 1976; 2(3):71–78.
18. Williams S, Goldman M. Penetrability of the smeared layer by strain of proteus vulgaris. J Endod 1985;11(9): 385–388.
19. Orstavik D, Haapasalo M. Disinfection by endodontic irrigants and dressings or experimentally infected dentinal tubules. Endod Dent Traumatol 1990;6(4):142–149.
20. Love RM, Chandler NP, Jenkinson HF. Penetration of smeared or non smeared dentine by Streptococcus gordonii. Int Endod J 1996;29(1):2–12.
21. Kokkas AB, Boutsioukis ACh, Vassiliadis LP, Stavrianos CK. The influence of the smear layer on dentinal tubule penetration depth by three different root canal sealers. J Endod 2004;30(2):100–102.
22. Small IA, Osborn TP, Fuller T, Hussain M, Kobernick S. Observations of carbon dioxide laser and bone bur in the osteotomy of the rabbit tibia. J Oral Surg 1979;37-(3):159–166.
23. Ivanenko MM, Fahimi-Weber S, Mitra T, Wierich W, Hering P. Bone tissue ablation with sub-microsecond pulses of a Q-switch CO2 laser: Histological examination of thermal side effects. Lasers Med Sci 2002;17(4):258–264.
24. Buchelt M, Kutschera HP, Katterschafka T, Kiss H, Lang S, Beer R, Losert U. Erb:YAG and Hol:YAG laser osteotomy: The effect of laser ablation on bone healing. Lasers Surg Med 1994;15(4):373–381.
25. Devlin H, Dickinson M, Freemont AJ, King T, Lloyd R. Healing of bone defects prepared using the Erbium-YAG laser. Lasers Med Sci 1994;9(4):239–242.
26. Teng NC, Wang PD, Chang WJ, Feng SW, Fan KH, Lin CT, Hsieh SC, Huang HM. Er:YAG Laser-Roughened Enamel Promotes Osteoblastic Differentiation. Photomed Laser Surg 2012;30(9):516–522.
27. Lorenzo MC, Portillo M, Moreno P, Montero J, Castillo-Oyagüe R, García A, Albaladejo A. In vitro analysis of femtosecond laser as an alternative to acid etching for achieving suitable bond strength of brackets to human enamel. Lasers Med Sci 2014;29(3)):897–905.
28. Burgner J, Muller M, Raczkowsky J, W. Orn H. Ex vivo accuracy evaluation for robot assisted laser bone ablation. Int J Med Robot 2010;6(4):489–500.
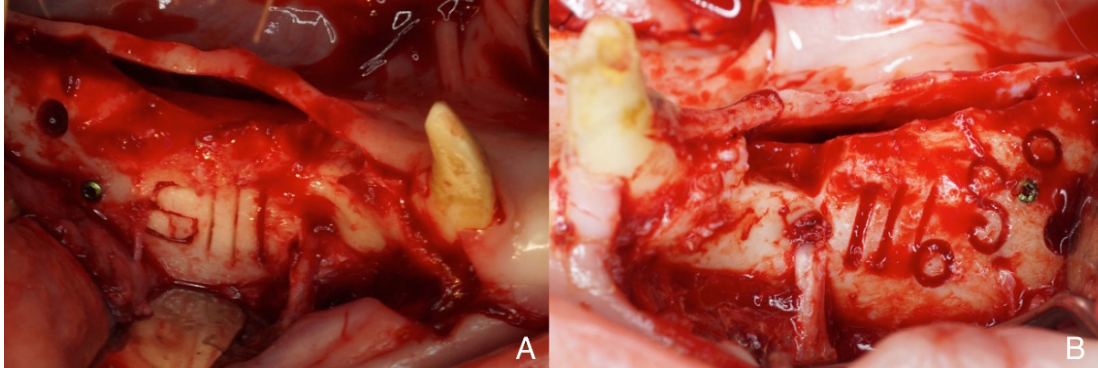
Intraoperative Findings of Laser Osteotomy

Manual osteotomy The first thing we could notice during the comparative operation was good visibility and exposure of the PZE osteotomy site. The tactile sense from the PZE osteotome cutting the minipig mandible was similar with that from cutting the (hard) human mandible. As the surgeons were already experienced with the instruments, changing of the tips following defect size and shape was smoothly done; however, it surely did take up some time. Even with the most slender tip, it was not so easy to make a planned curve of the S-shaped defect.
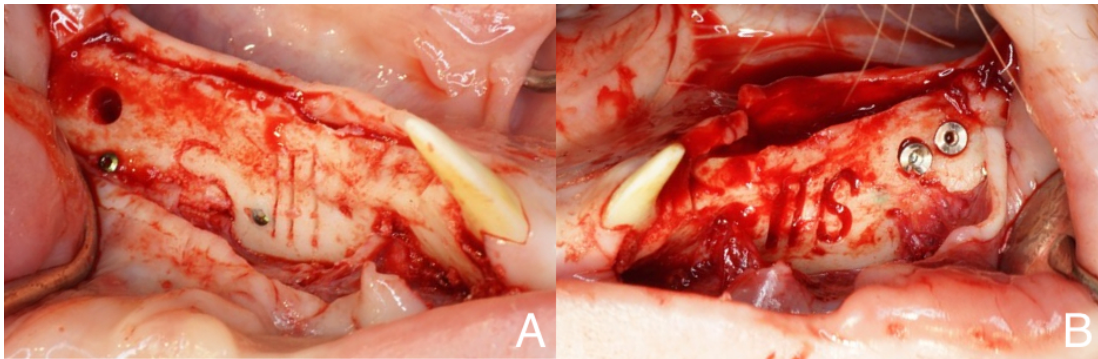
Figure 5.1: Intraoperative picture of (A) the mechanical osteotomy side and (B) the laser osteotomy side from the 5th minipig. We created 2 cylindrical defects with the laser osteotome.

Laser osteotomy Bleeding from the bone defect was prominent after laser osteotomy (Figure 5.1B and 5.2B). Good visibility of the PZE osteotomy site turned out to come from little bleeding from the bone, compared to the laser osteotomy site. It was also obvious that the laser osteotome was superior in creating complex defects, in terms of accuracy and speed. After we stopped laser osteotomy with the 2nd minipig and realigned the optical path, the overall performance of the laser osteotome improved. As can be seen in Figures 5.1B and 5.2B, we created multiple cylindrical defects by laser in the 5th and 6th minipigs. For the 6th minipig, one of the cylindrical defects was partially carbonized, because the cooling water ran out. The carbonized bone cylinder from the defect was subjected

Figure 5.2: Intraoperative picture of (A) the mechanical osteotomy side and (B) the laser osteotomy side from the 6th minipig. We created 3 cylindrical defects with the laser osteotome.

to the surface analysis with SEM.

Postoperative Surface Analysis of Bone Cut

From all saddle defects and some cylindrical defects from laser osteotomy, bone blocks were taken for the post-op cut surface analysis (Figure 5.3). The bone blocks were fixed in 3.8% formaldehyde in phosphate buffered saline (PBS) for 24 hours, meticulously rinsed with PBS afterwards, and shipped to Basel in 70% ethanol solution. The samples from the saddle defects were cut in two parts with a rotating disc bur, and each part was subjected to SEM and laser scanning microscope.
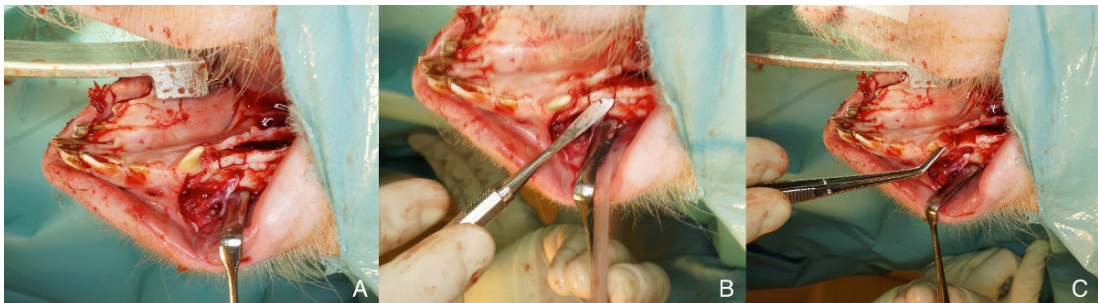

Figure 5.3: Taking the bone block from the saddle defect. These pictures are from the 5th minipig on the laser osteotomy side.

Scanning electron microscope Saddle defects from PZE osteotomy showed notably even and flat cut surfaces (Figure 5.4 and 5.5). When there were open pores on the cut surface, they seemed narrow as if crushed or pressed (Figure 5.4B). Also small and big cracks on the flattened surface were noticeable (Figure 5.5B and C). These findings agree with what Maurer et al. showed in 2008 [27]. With the same PZE osteotome used in our study, they compared *ex vivo* bone cutting with micro-saw, Lindemann bur, and 2 tips of PZE osteotome. On the bone block from the rabbit skull, the PZE osteotome yielded less debris and more intact bone structure compared to two conventional cutting tools, *i.e.* micro-saw and Lindemann bur. An "even surface" from the PZE osteotome was examined with environmental surface electron microscopy and with confocal laser scanning microscopy. The authors interpreted this even surface and low roughness of PZE cut as favorable results of the PZE osteotome. Later, Simonetti et al. got similar results with Lindemann bur, Sonosurgery, and PZE osteotome, to conclude this "smooth and regular surface" as "precise cutting" from the PZE osteotome [28].

On the other hand, the defects from laser osteotomy retained the clear shape of open pores on the surface (Figure 5.6). With varying degrees, their surfaces were irregular and rough compared to those from PZE osteotomy (Figure 5.6, 5.8, 5.9, and 5.10). This finding agrees with what Panduric et al. proved from Er:YAG laser osteotomy in comparison to conventional osteotomies. In 2012, they published in *JOMS* their *ex vivo* comparison between a surgical pilot drill and an Er:YAG laser in cutting bone blocks from porcine ribs [29]. Er:YAG
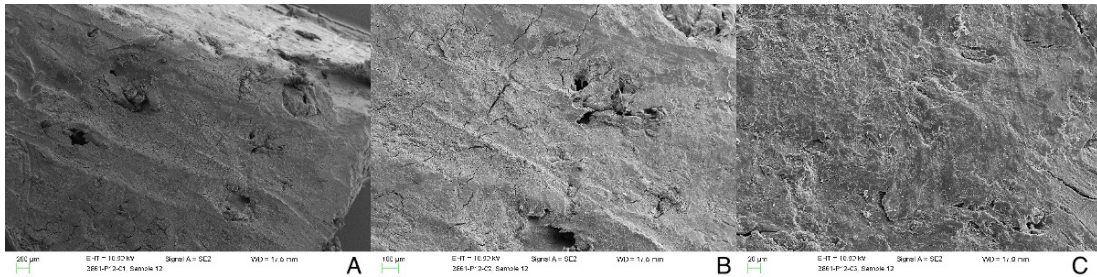
Figure 5.4: SEM images of the cut face from PZE osteotomy in different magnifications [A) x19, B) x50, C) x200]. Images are from the saddle defect of the 1st minipig.
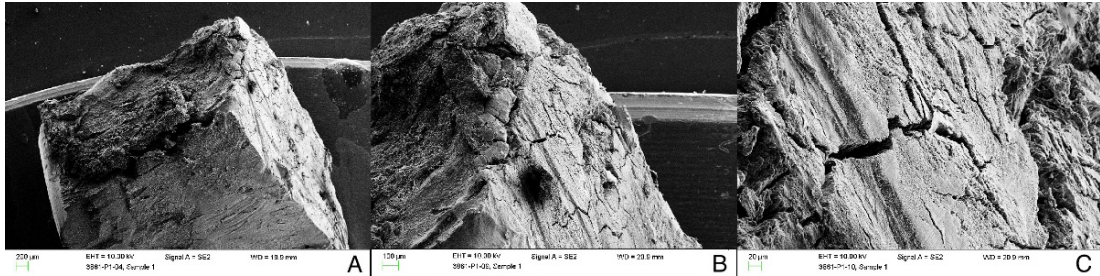
Figure 5.5: SEM images of the cut face from PZE osteotomy in different magnifications [A) x19, B) x50, C) x200]. Images are from the saddle defect of the 6th minipig.
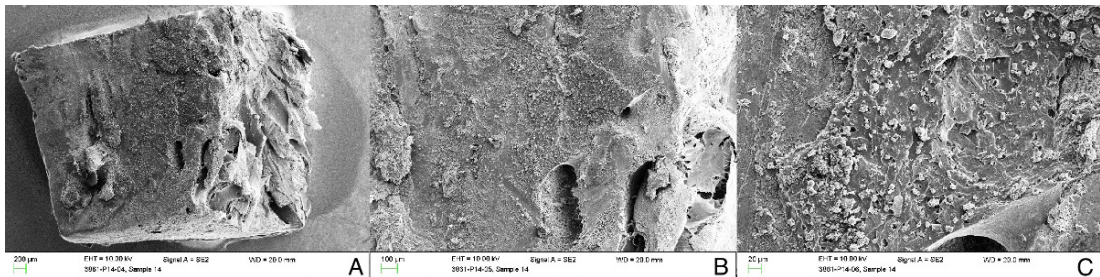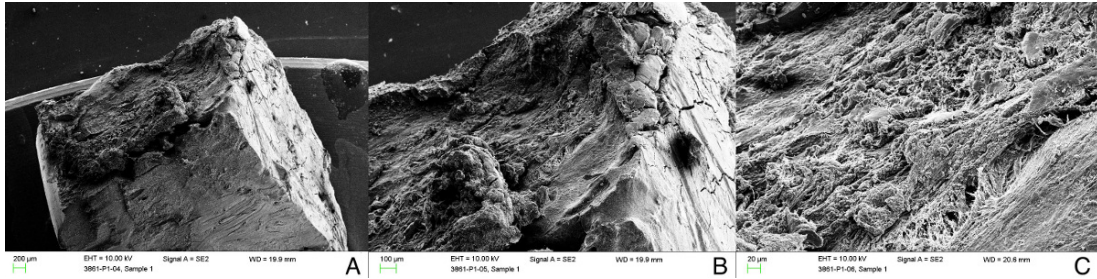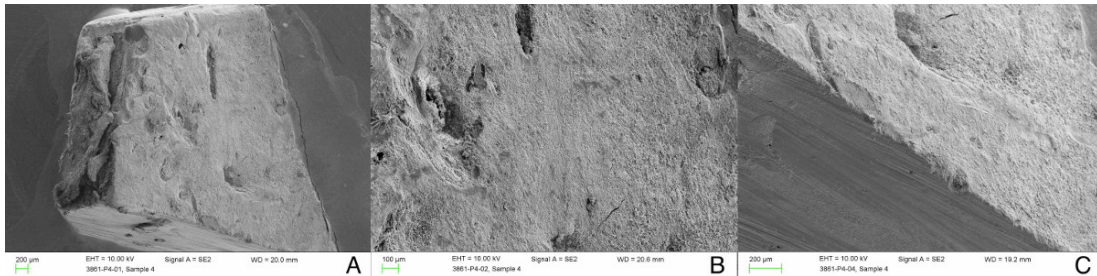

Figure 5.6: SEM images of the cut face from laser osteotomy in different magnifications [A) x19, B) x50, C) x200]. Images are from the saddle defect of the 3rd minipig.

laser removed more bone in a shorter time while retaining more of the original structure compared to surgical drills. Although the maximal temperature during laser ablation went up to 68.7 °C, overall average temperature was lower with laser osteotomy. They concluded this temporary temperature increase was necessary for bone ablation and, according to the histologic examination, did not cause thermal damage to the surrounding tissue. Indeed the histology confirmed smear layer formation only on the bone surface cut by surgical drills. In 2014, similar author group published another *ex vivo* comparative study analyzed with field emission SEM (FE-SEM), qualitative and semiquantitative energy dispersive x-ray analysis (SEM-EDX), and diffraction x-ray analysis (XRD) [30]. With FE-SEM, they showed a nice picture of the laser cut surface and described it as "rough, husky, and craggy, with micro-irregularities", compared to "smooth, completely covered with smear layer and visible microcracks" on drilled bone surfaces. From SEM-EDX and XRD, they confirmed that the laser ablated bone

Figure 5.7: SEM images of untreated alveolar bone surface in different magnifications [A) x19, B) x50, C) x200]. Images are from the saddle defect of the 6th minipig.
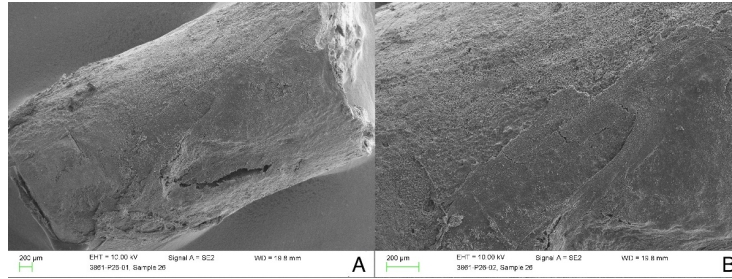

Figure 5.8: SEM images of the cut face from laser osteotomy in different magnifications [A) x19, B) x50]. The junction between disc bur (lower left) and laser osteotomy (upper right) [C) x50]. Images are from the saddle defect of the 5th minipig.

retained similar chemical and crystallographic characteristics with the untreated bone. Our evaluation with SEM also revealed high similarity between the laser ablated bone surface and the natural alveolar bone surface (Figure 5.6 and 5.7). Figures 5.5 and 5.7 are from the same bone block of the 6th minipig and depict a good contrast between the PZE cut surface and the untreated alveolar bone surface.

With some samples, we could capture other interesting contrasts in one picture. Figure 5.8 displays a saddle defect from laser osteotomy of the 5th minipig. In picture C, we could see the intact open pore on the laser cut surface, with which the cut surface from the disc bur meets (the disc bur was used to separate the bone block to two samples). The disc bur indeed rendered much more even and smooth cut surface compared to the PZE osteotome, as Maurer et al. [27] and Simonetti et al. [28] described (Figure 5.8C lower left). Figure 5.9 shows

Figure 5.9: SEM images of the cut face from laser osteotomy, partially carbonized (lower right), in different magnifications [A) x19, B) x50]. Images are from the cylindrical defect of the 6th minipig.
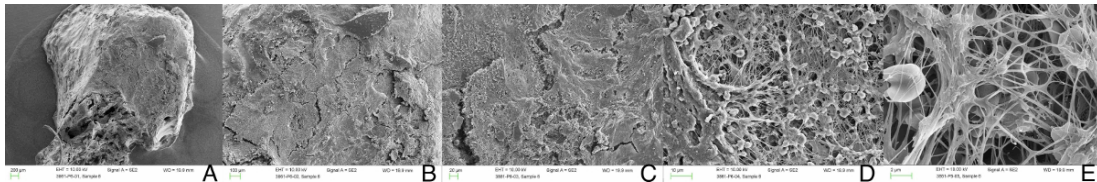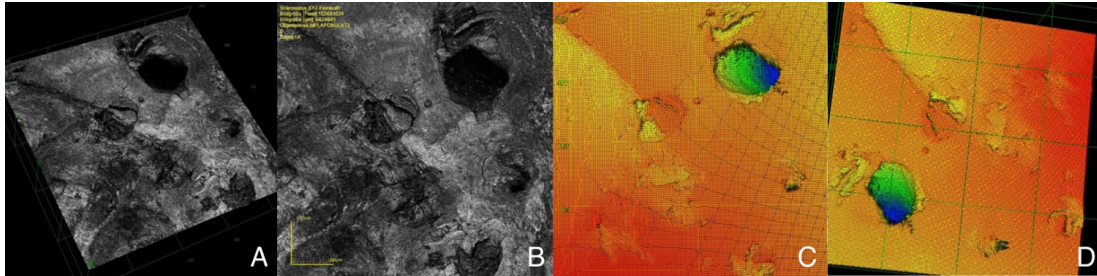

Figure 5.10: SEM images of the cut face from laser osteotomy in different magnifications [A) x19, B) x50, C) x200, D) x1000, E) x5000]. Images are from the saddle defect of the 4th minipig.

one of the cylindrical defects from laser osteotomy of the 6th minipig. During laser osteotomy, cooling water ran out and one cylindrical defect came out with partial carbonization. We can see the margin of the carbonized surface, where the charred layer covers micro-irregular laser cut surface (Figure 5.9B lower right). As shown by Kang et al. [15] and later studied by Zhang et al. [17], we could confirm that the water layer played an important role in successful laser ablation of bone tissue.

In Figure 5.10, we can see high magnification images of the laser cut surface, from the saddle defect of the 4th minipig. Together with typical micro-irregular, rough, craggy surface (B and C), higher magnification shows clear fibrin structure, mostly from blood clots (D and E).

Laser scanning microscope The cut surface was also evaluated by a laser scanning microscope (LEXT OLS4000, Olympus, Japan). For visualization, pictures of the surfaces were taken at original magnifications of x431 and at x1072 at a grayscale. The three-dimensional pictures were used to visualize the wire

Figure 5.11: Laser scanning microscope images of the cut surface from PZE osteotomy [A) 3D reconstruction, B) x1072]. Same images with A by the Image Slope Technique [C) from the top, D) from the bottom]; Red: Highest, lilac: deepest. Images are from the saddle defect of the 6th minipig.
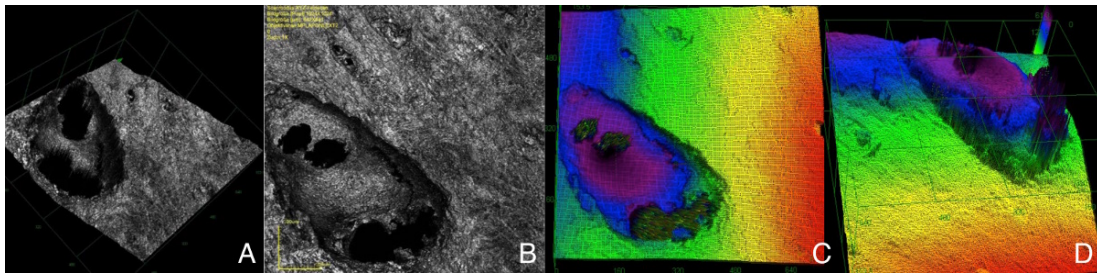
Figure 5.12: Laser scanning microscope images of the cut surface from laser osteotomy [A) 3D reconstruction, B) x1072]. Same images with A by the Image Slope Technique [C) from the top, D) from the bottom]; Red: Highest, lilac: deepest. Images are from the saddle defect of the 3rd minipig.

frame modus (X and Y directions were displayed, interval 16), and the primary area was enhanced with the image slope technique, for easy comparison of the pore depth. In Figures 5.11 and 5.12 we can compare the cut surface from PZE osteotomy with shallow pores and that from laser osteotomy with deep pores. With the image enhancement, deep pores are shown in dark colors.

By the pathology team in laboratory Anapath, laser scanning microscope images were quantitatively analyzed to compare the surface roughness from different osteotomies. The result is being prepared for publication, which will provide quantitative evidences to our observation.

# Surface Treatment of Conventional Bone Cut—at UniBasel and NYU

Analyzing the surface of the immediate bone cut and finding the smear layer was one of the most interesting parts of my PhD project. Reviewing related literature, I was convinced that further study in this part could expand the boundary of our research. Supposing the function of the smear layer on the bone surface is similar to that on the tooth surface, bone healing could have benefited from the surface conditioning—*i.e.* removing the smear layer from the cut surface. We had abundant references, from dentistry. I planned a single time point study with Dr. Kawasaki, using the mandible from the fresh pig cadaver (Figure 5.13). Mandibulectomy was performed with PZE osteotme, electric drill & bur, and chisel & mallet. As a control, one molar tooth was cut with electric drill & bur. Two small samples were taken from each surface with various shapes—to prevent the confusion when multiple samples were placed on a metal disk for the SEM analysis. One set of samples were treated by 38% Phosphoric acid for 15 seconds and rinsed with isotonic sodium chloride. After critical point drying, all samples were analyzed with SEM. Same study was repeated twice, but the visible change from the acid treatment was found only on the tooth surface (Figure 5.14). Including not enough time and workforce, there were many points to improve to overcome this failure. I concluded that finding a right surface conditioning protocol for the bone surface is what to be done first. Different etching time, different concentration of acid, or even different kind of acid could have been required. As I was soon leaving for NYU, the study was stopped as incomplete.

In NYU, I repeated the same study using the jaw bone from minipigs with Prof. Bromage. With 37% phosphoric acid, I tried several different amounts of etching time and found it worked the best with 5 to 10 seconds. In Figure 5.15 we can see acid etched surface (A [right half], C, and D) reveals repeated bumpy structures, compared to non-treated surface (B) which is covered by scaly layer. Environmental SEM made this study easier, as we could examine the surface immediately after the bone cutting, without the critical point drying and sputter coating. As the time in NYU was limited, this study also ended as a single trial.
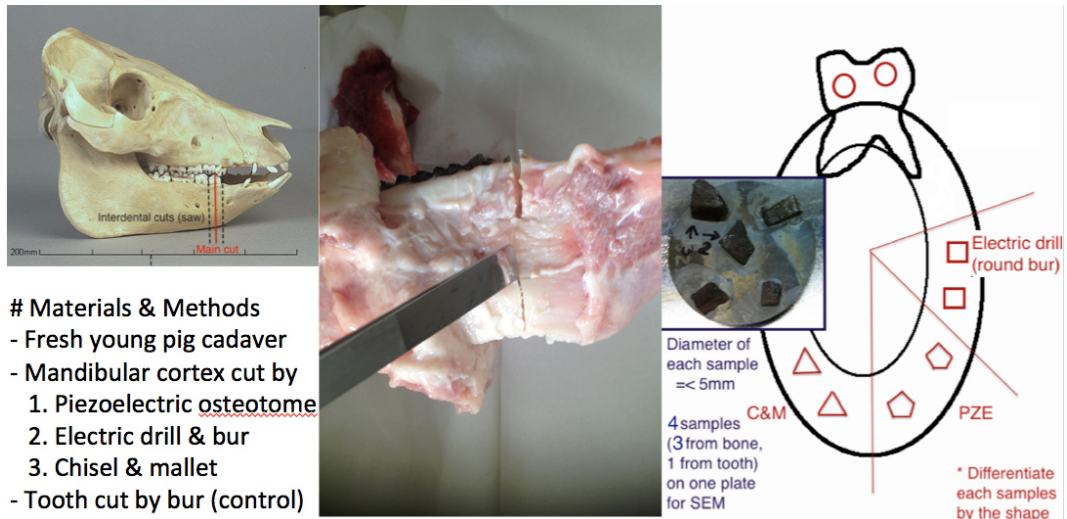
Figure 5.13: Summary of the study plan, [Surface analysis of immediate bone and teeth cut], performed at the University of Basel in 2014.
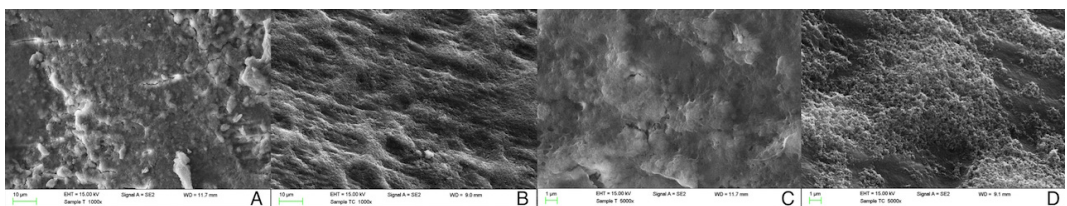
Figure 5.14: SEM images of the prepped tooth surface in high magnifications, taken at the NYU in 2015 [A) non-treated x1000, B) acid etched x1000, C) non-treated x5000, D) acid etched x5000].
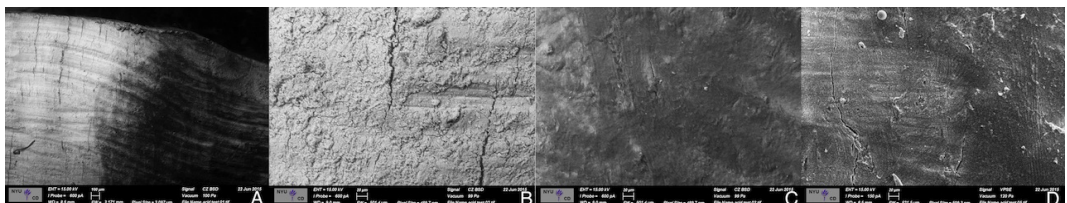
Figure 5.15: Environmental SEM images of the prepped bone surface in different magnifications, taken at the NYU in 2015 [A) juction of non-treated {left} and acid etched {right} x50, B) non-treated x200, C) acid etched x200, D) acid etched x200].

Chapter 6

Biologic Response to Er:YAG Laser—Bone Healing after Laser Osteotomy

The bone regeneration rate of the adult minipig mandible ($1.2 - 1.5\,\mu\text{m/day}$) is comparable to that of the young skeletally mature human mandible ($1.0 - 1.5\,\mu\text{m/day}$) [31]. Essential parameters related to the bone physiology of female Göttingen minipigs are well known to be similar in bone mineral density and bone mineral concentration compared to those of human [32]. Hence minipigs have been actively used as an experimental model for clinical CMF research, *e.g.* implant dentistry and graft materials for the bone regeneration [33].

In this final publication, we reported the histologic result of the preclinical study and compared the bone healing after laser osteotomy and mechanical osteotomy, in the mandible of the minipig.

Comparing the Bone Healing after Computer-assisted and Robot-guided Er:YAG Laser Osteotomy and Piezoelectric Osteotomy—a Pilot Study in Minipig Mandible

Summary of this paper was presented at the *66. Deutsche Geselschaft der Mund-, Kiefer- und Gesichtschirurgie (DGMKG)*, June 2016 in Hamburg. The paper was submitted to the *Lasers in Surgery and Medicine* in November 2017.

Title

Comparing the bone healing after computer-assisted and robot-guided Er:YAG laser osteotomy and piezoelectric osteotomy—a pilot study in minipig mandible

Author names and affiliations

Kyung-won Baek, DMD, MSD[1*], Michel Dard, DMD, MSD, PhD[2], Hans-Florian Zeilhofer, DMD, MD[3], Philippe C. Cattin, PhD[4†] and Philipp Juergens, DMD, MD[3†]

[1] PhD student, Department of Biomedical Engineering, Hightech Research Center of Cranio-Maxillofacial Surgery (HFZ), University of Basel, Gewerbestrasse 14-16, 4123 Allschwil, Switzerland

[2] Adjunct Assistant Professor, Department of Periodontology and Implant Dentistry, New York University College of Dentistry, 433 1st Ave, New York, NY10010, USA

[3] Professor, Department of Cranio-Maxillofacial Surgery, University Hospital of Basel, Spitalstrasse 21, 4031 Basel, Switzerland

[4] Professor, Department of Biomedical Engineering, Medical Image Analysis Center (MIAC), Department of Biomedical Engineering, University of Basel, Gewerbestrasse 14, 4123 Allschwil, Switzerland

[†] Both authors P. Cattin and P. Juergens contributed equally to this study.

* Corresponding author. Department of Biomedical Engineering, Hightech Research Center of Cranio-Maxillofacial Surgery (HFZ), University of Basel, Gewerbestrasse 14-16, 4123 Allschwil, Switzerland. Tel.: +41 61 265 96 41; Fax: +41 61 265 96 56; E-mail: kyung-won.baek@unibas.ch

Abstract

Purpose: To take major advantages of Erbium-doped Yttrium Aluminium Garnet (Er:YAG) lasers—like freedom of cutting geometries and high accuracy—in osteotomy, integration and miniaturization of robot, laser, and navigation technology is tried and applied to the minipigs. The investigators hypothesized laser osteotomy would render acceptable bone healing based on the intraoperative findings and postoperative cut surface analysis.

Methods: The investigators designed and implemented a comparative bone cutting surgery in the minipig mandible with the computer-assisted robot-guided Er:YAG laser osteotome and a piezoelectric (PZE) osteotome. The sample was composed of different patterns of defects in the mandibles of 6 grown-up female Goettingen minipigs. The predictor variable was Er:YAG osteotomy and PZE osteotomy. The outcome variable was the cut surface characteristics and the bone healing pattern 4 weeks and 8 weeks postoperatively. Descriptive and qualitative comparison was executed.

Results: The sample was composed of 4 kinds of bone defects in both sides of 6 minipigs. We observed more bleeding during the operation, open cut surfaces, and a faster healing pattern with the laser osteotomy. There was a possible association between the intraoperative findings, postoperative cut surface analysis and the bone healing pattern.

Conclusion: The results of this study suggest that characteristic open surfaces could explain favorable bone healing after laser osteotomy. Future studies will focus on the quantification of the early healing characteristics after laser osteotomy and the safety feature of laser osteotomy.

Ever since *Homo habilis* used stones as tools, human beings used hard tools to crack, open, and cut objects. "Harder tools for softer objects" has been a basic rule of instrumentation for a very long time. Medicine was no exception. Being probably the oldest surgical procedure, skull trepanation is still performed by opening the skull with mechanical instrument. Even with state-of-the-art devices, the basic mechanism is the same with the oldest existing bone cutting instruments from the Roman era[1]. With such instruments, cutting geometry is given by the shape of the cutting tip and affected by the surface characteristic of the bone. The latest technology of selective hard tissue cutting, with piezoelectric (PZE) osteotome, is not free from this limitation either[2]. On the other hand, there has been a development of totally different cutting method, neither with hard tool nor cutting tip. In 1960, Maiman[3] invented a ruby laser and realized Einstein's theory of stimulated emission of light[4]. Soon after its invention laser was applied in medicine. The first application was published in 1961 on retina coagulation[5] and two years later followed skin application[6]. The absence of cutting tip in direct contact with tissue surface made it ideal for the precise cut on delicate soft tissue. Laser was also applied in dentistry this time; on teeth, dental pulp, and oral mucosa[7]. But not until late 1900s it became commonly accepted by dentists[8]. Even then laser application was limited to oral mucosa and gingiva for another decade[9].

Laser cutting of bone was considered to be impossible for a long time, as the produced heat carbonized cut surface and denaturized surrounding tissue. The charred layer prevented favorable healing of the cut tissue[10]. Improvements in laser technology and development of effective cooling system were required to achieve char-free cutting of mineralized tissue. Recently Erbium-doped Yttrium Aluminium Garnet (Er:YAG) laser has shown to be effective in bone cutting and actively applied in oral surgery[11-13]. Besides the advantage of contact-free tissue ablation, laser osteotomy features a cutting width of 200-500 μm, which makes high precision and absolute freedom of cutting geometry achievable. However, to use these benefits to full capacity, a robotic guidance and a navigational control for the laser system is necessary. And in order to successfully introduce this technology into clinical routine, whole system needs to be miniaturized and adopted to the ergonomic needs in an operation room (OR) environment.

We developed a new computer-assisted and robot-guided laser osteotome and proved its applicability, efficacy and safety in oral and cranio-maxillofacial (CMF) surgery. [14,15] This paper focuses on the histological investigation of the bone healing after laser osteotomy. Uncomplicated bone healing is crucial for the routine application of the new laser osteotome. Proving adequate biologic response in CMF area will build a secure ground for further application of our laser system to other surgical fields.

Materials and Methods

Six fully-grown female Goettingen minipigs (mean age 25.5±5 months, mean weight 48.7±3 kg) were used in this study. The animals were housed in cots in groups of three, under controlled environmental conditions. Throughout the duration of the experiment, they were fed soft diet and water. All procedures were in accordance with the Swedish animal protection law and under the ethical approval number M-204-11.3 (Malmoe-Lunds djurfoersoeks etiska nämnd).

Study Design

The study was carried out in two surgical phases and analyses. In the first surgical phase, the premolars and the first molar on both sides of the mandible were extracted to create the edentulous ridges. After 12 weeks of healing, different osteotomy patterns—from anterior to posterior, one saddle defect (5 mm x 10 mm size and the thickness of the full alveolar bone), three straight lines (10 mm length, 2-3 mm depth, and different width [minimal, 0.5 mm, 1 mm]), one S-shaped curved line (5 x 10 mm size and 2-3mm depth) and one cylindrical defect (4.1mm diameter and 8-10 mm depth)—were created on the edentulous mandibular ridges; one side with the computer-assisted and robot-guided laser osteotome and the other side with manually guided mechanical osteotomes. Removed bone pieces form the saddle defects and cylindrical defects were subjected to the surface analyses. After 4 and 8 weeks the animals were sacrificed. The mandibles were harvested and histological examination was conducted to evaluate the bone healing.

Surgical Protocols

All surgeries were performed under full narcosis with intramuscular injection of Ketamine hydrochloride mixed with Midazolam, and local anesthesia with Lidocaine containing adrenalin. No inhalation anesthesia was used. Detailed information on anesthesia can be found in our previous paper.[15]

In the first phase, the lower three premolars and the first molar (P2, P3, P4, and M1) on both sides of the mandible were removed. At this time 2 screws were placed in each side of the mandible to act as landmarks for intraoperative navigation. After 12 weeks, the second and main phase was performed in all six animals. Under the intramuscular full narcosis, 3-dimensional C-arm (Siemens ARCADIS Orbic 3D, Siemens AG, Germany) data were acquired for preoperative planning. The animal was then moved to the operation table right side up and aseptic draping was done, exposing only the mouth area. After local anesthesia, the mucosa was incised and the mucoperiosteal flap was dissected to expose the edentulous ridge of the mandible. On the right side of the mandible, the planned osteotomy patterns were created by a skilled surgeon with a PZE osteotome (PIEZOSURGERY® 3, Mectron s.p.a., Italy) and a standard implant drill (INTRAsurg® 300 plus, KaVo, USA; Straumann® implant drills, Institute Straumann AG, Switzerland). While the surgeons were operating, computer scientists executed the virtual planning for laser osteotomy on the contralateral side. For the laser operation the animal was turned to the left side and the head was fixed to the operation table using a customized device. Aseptic draping was reapplied and the surgeon exposed the edentulous ridge in the same way. After referencing the navigation system and indicating the position of the cutting areas, the surgical robotic arm moved the laser osteotome to the surgical site to create similar osteotomy patterns in an automated way (Fig. 1). The wounds were closed using absorbable suture. After the intervention, the animal was moved to the monitoring room and the recovery was closely monitored until complete wake-up. All intraoperative findings were recorded by manual charting, video clips and clinical photos. Removed bone pieces form the saddle defects and cylindrical defects were shipped to the laboratory for scanning electron microscope (SEM) and laser scanning microscope.

Computer-assisted and robot-guided laser osteotome

In this study, a prototype laser system was used. A solid state Er:YAG laser, lasing at a wavelength of 2,940 nm, was integrated into a sealed housing and mounted on the surgical robot. The pulsed Er:YAG laser created a cutting width of 500μm with a working distance of 40 mm from the laser housing[16]. The bone surface was permanently cooled and hydrated by a nozzle system, which creates fine aqueous vapor of sterile sodium chloride. A KUKA light-weight-robot (LWR4+, KUKA Robotics, Germany) was used to position the laser head. Having 7 degrees of freedom, this robot was extremely sensitive and provides increased safety; because of its integrated sensors which make it ideal for force-controlled tasks.

The entire robot-guided laser system was integrated with a computer-assisted preoperative planning and intraoperative navigation system. A software package, developed in house, used preoperative imaging to define sites and designs of osteotomies. The navigation system was a key safety feature: it monitored the position of the laser housing with respect to the target, and converted the preoperative digital data into a real osteotomy by driving the robot[17]. Referencing was done through fixed screws and anatomical landmarks with a passive marker system.

PZE osteotome

A PZE osteotome was used as control. For the different sizes and shapes of defects, OT6, OT7, OT7S-3 and OT7S-4 tips of the PIEZOSURGERY® 3 system were used. During the osteotomy, the bone surface was permanently cooled and hydrated by a nozzle array with sterile sodium chloride with a flow rate of 80–90 ml/min.

Histology

4 and 8 weeks after surgery, necropsy was performed and the mandibles were fixed in 3.8% formaldehyde. The ventral half of the mandible underwent decalcification, processing, embedding in paraffin and cutting with an approximate thickness of 5 μm for the staining with hematoxylin and eosin (H&E). The dorsal half was non-decalcified, dehydrated, methylmetacrylate embedded, cut by a diamond saw, and grinded and polished to a final thickness of 30–50 μm (EXAKT System, EXAKT Advanced Technologies GmbH, Germany). These samples were stained by Paragon (toluidine blue and basic fuchsin). All cutting planes were defined based on intraoperative photographs as well as 3D C-arm data. The sections from all samples were examined under light microscopy.

SEM

The bone blocks harvested from the saddle defects were analyzed with SEM. The samples were fixed with 3.8% formaldehyde in phosphate buffered saline (PBS) for 24 hours and meticulously rinsed with PBS. Then they were gradually dehydrated in a series of graded ethanol/water mixtures (50%, 70%, 80%, 90%, and 100%). After the critical point drying, the samples were sputter-coated with a thin layer of platinum of 2 nm in thickness (Sputter coater, Cressington, England). Surface topography was qualitatively examined using SEM (SUPRA 55, ZEISS, Germany).

Laser scanning microscope

The cut surface was also evaluated by a laser scanning microscope (LEXT OLS4000, Olympus, Japan); including surfaces made by laser osteotomy, PZE osteotomy, and the surface produced arterially by post-biopsy mechanical trauma (break). The broken surface was made to compare the normal trabecular surface architecture to the cut surfaces made by laser or PZE osteotomy. For visualization, pictures of the surfaces were taken at original magnification of x431 and x1072 at a gray scale. The primary area was enhanced with the image slope technique, for easy comparison of the pore depth.

Results

Intraoperative findings

The tactile sense from the PZE osteotome cutting the minipig mandible was similar with that from cutting the (hard) human mandible. During the defect creation, fresh bleeding was clearly notable more on the laser osteotomy side than on the PZE osteotomy side (Fig. 1). In all six animals, bleeding on the PZE osteotomy side was recognizably less.
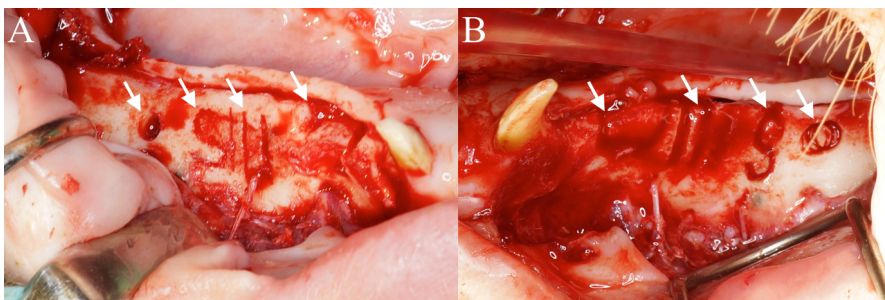
Figure 1. Clinical photograph of PZE osteotomy (A) and laser osteotomy (B).

(A) A cylindrical defect, one S-shaped line, three straight lines, and a saddle defect are marked with white arrows (from the posterior to the anterior mandible of the minipig on the right side). A minimal bleeding from the bone is noticeable. (B) A saddle defect, three straight lines, one S-shaped line, and a bone chamber implant in a cylindrical defect are marked with white arrows (from the anterior to the posterior mandible of the minipig on the left side). The saddle defect and cylindrical defect are not yet removed from the mandible. A fresh bleeding from the bone is observed.

Histology

After 4 weeks, straight and S-shaped defects in both groups were bridged mainly by mesenchymal tissue. Thin bony trabeculae were growing from the lateral aspects into the defect covering less than half of the previously existed bone tissue. Saddle defects in both groups were incompletely healed on the surface and covered by tissue containing a large amount of collagen fibers. No inflammatory cell reaction was noted in both osteotomies. In some samples cut by the laser osteotome, mainly in S-shaped defects, the healing was so advanced that only small residual dark stained bands indicated the margins of previously existing defects. No comparable healing was observed in samples cut by the PZE osteotome (Fig. 2).

After 8 weeks, all defects were almost covered by darker stained newly formed bone in both groups. The differences between the laser and PZE osteotomy sides were not very obvious, except that some defects made by the laser osteotome were no longer detectable in histology. In some cuts made by the laser osteotome, mainly in S-shaped defects, the healing was complete with only small residual dark stained bands. Again, no similar healing was observed

in those by the PZE osteotome. It was also notable that in some of the PZE osteotomy sides, subperiosteal bone resorption was observed; while in the laser osteotomy side, subperiosteal bone growth was observed (Fig. 3).
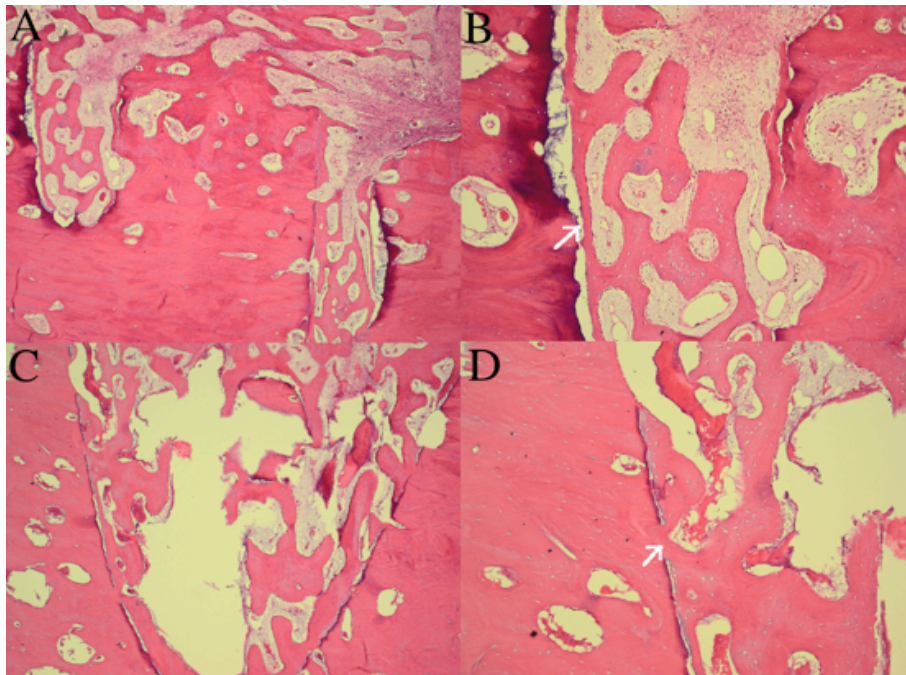
Figure 2. Histology of 4 weeks with H&E staining. S-shaped defect from PZE osteotomy [A) lens x4, B) lens x10], straight defect from laser osteotomy [C) lens x4, D) lens x10].

Both osteotomy sites are healed well. The healing of S-shaped defect is almost complete that only small residual dark stained bands indicated the previously existed cut line in laser osteotomy side (C, D). In the same defect made by the PZE osteotome, cut line is still notable with bony gap (A, B). Osteotomy lines are marked with white arrows.
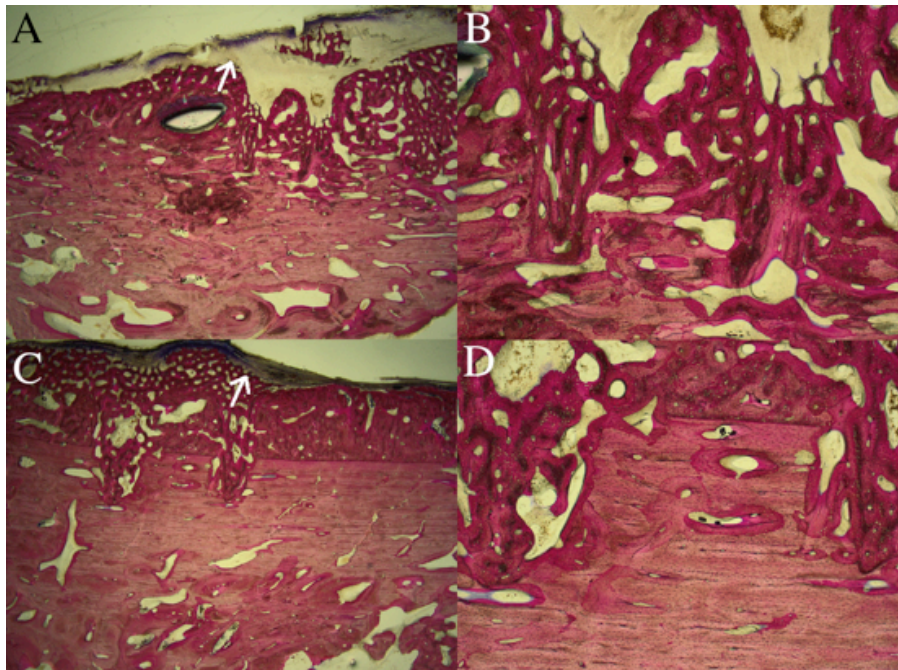

Figure 3. Histology of 8 weeks with Paragon staining. Straight lines from PZE osteotomy [A) lens x1.25, B) lens x4], those from laser osteotomy [C) lens x1.25, D) lens x4].

Both osteotomy sites are healed well. The differences between laser and PZE osteotomy sides are not very obvious except that the defects made with the laser osteotome were partially no longer detectable in higher magnification (D). In PZE osteotomy side, subperiosteal bone resorption is observed (A) while subperiosteal bone growth is observed in laser osteotomy side (C). Osteotomy lines are marked with white arrows.

SEM

The bone samples from PZE osteotomy showed a flattened down surface and closed pores with tension cracks and even scratches from the blade. On the contrary, the bone samples from laser osteotomy showed open pores with rough tissue structures. These observations were valid in all six animals. Both experimentally created cut surfaces were compared to the natural bone surface from the alveolar crest of the mandible. The SEM images showed a high resemblance between the natural bone surface and the cut surface from laser osteotomy (Fig. 4).
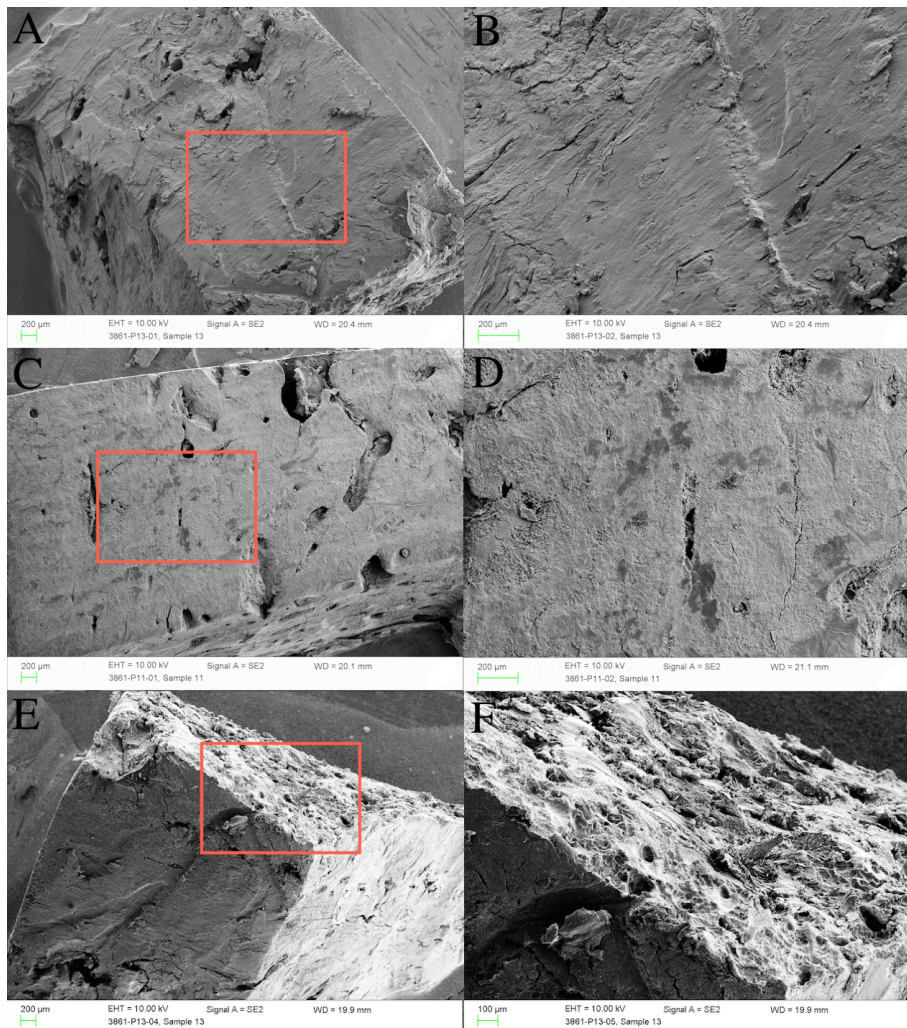
Figure 4. Comparison of SEM images of cut surface created with the PZE osteotome [A) x19, B) x50], those created with the laser osteotome [C) x19, D) x50] and natural bone surface [E) x19, F) x50].

The cut surface from PZE osteotomy appears to be smoothened and the pores closed by a coating resembling the smear layer known in dentistry from tooth preparation (A and B). The cut surface from laser osteotomy retains the pores opened (C and D). We can compare these to the natural bone surface (E and F).

Laser scanning microscope

The cut surface made by laser osteotomy revealed deep open pores. This surface architecture was comparable to the normal structural parameters retrieved from the mechanically broken bone surface. In contrast, the cut surface from PZE osteotomy was flat and often showed parallel cut lineation orthogonal to the surface. The pores were filled with

detritus, hence shallow compared to open pores on the surface from laser osteotomy. The color scale showed deep pores dark and manifested the rough surface from laser osteotomy. Mechanical sawing artifacts in form of striations were clearly visible on the surface from PZE osteotomy (Fig. 5).
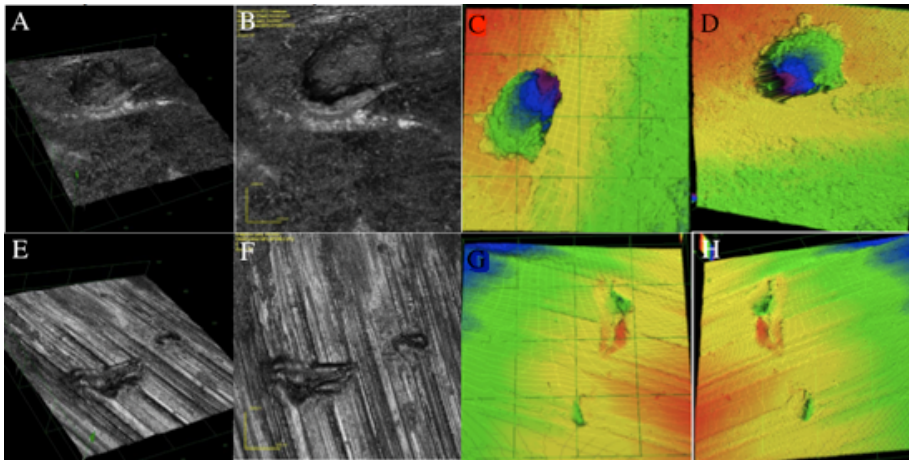
Figure 5. Comparison of laser scanning microscope images of cut surface created with the laser osteotome [A) 3D reconstruction, B) x1072] and those with the PZE osteotome [E) 3D reconstruction, F) x1072]. Same images with A by the Image Slope Technique [C) from the top, D) from the bottom] and those with E by the same technique [G) from the top, H) from the bottom].

Note the open pores on the cut surface created with the laser osteotome (A, B, C, and D). Also note the detritus over the pores and the mechanical striation artifacts on the cut surface created with the PZE osteotome (E, F, G, and H). In color images by Image Slope Technique, red color shows the highest and violet color shows the deepest point of the surface. The roughness of surfaces (including the size and depths of pores) revealed from both techniques can be estimated. Mechanical sawing artifacts in form of striations are visualized clearer by the latter technique (E–H).

Discussion

Efficient cutting and competitive bone healing with laser osteotomy has been reported in several studies. Panduric et al[18] showed that more bone tissue was cut in a shorter time with Er:YAG laser compared to conventional drill, in porcine rib bone block. Stübinger et al[19] used sheep tibia fracture model to compare the bone healing under functional load after PZE and Er:YAG laser osteotomy. The result was similarly acceptable, but they concluded that it indirectly confirmed the promising and profitable results of Er:YAG laser osteotomy. Similar author group[20] showed that bone preparation with Er:YAG laser lead to a highest osseointegration of dental implants in sheep pelvis, compared to conventional drill and PZE osteotome. But none of those studies explained yet how and why the bone heals different after laser osteotomy compared to conventional methods. Surface analysis is one way to understand the characteristics of bone cutting and explain subsequent bone healing. Sasaki et al[21] analyzed the ultrastructure of rat parietal bone treated by Er:YAG laser, CO_2 laser, and bur drilling. They showed formation of the smear layer after bur drilling and minimal microstructural changes after Er:YAG lasing. Zhang et al[22] studied on the cooling water layer thickness and consequent smear layer formation on fresh bovine shank bone with CO_2 laser. Using SEM they proved the critical thickness of water layer for a given radiant exposure, but left the mechanism of water mediated hard tissue ablation for further study. These studies well investigated immediate post-osteotomy conditions and some even anticipated better start of healing process with Er:YAG laser osteotomy, based on the absence of a smear layer[18,21]. But as in vitro study only, they could not follow how their immediate findings actually resulted in subsequent bone healing.

In this study we tried to verify preceding studies and complete them with resultant bone healing. We could confirm the proven efficiency of laser osteotomy along with the ergonomic setting and safety feature in our previous papers[14,15]. This paper focused on the biologic result of the translational study with minipig model. Our surface analysis of immediate post-laser-osteotomy showed the open cut face free of smear layer (Fig. 4), as was described by Panduric et al and Sasaki et al. The histologic analysis of post-osteotomy 4 and 8 weeks showed unimpeded bone healing after Er:YAG laser cutting. Some samples showed even more accelerated healing after laser cutting compared to PZE cutting (Fig. 2 and 3), which agrees with what Panduric et al and Sasaki et al anticipated, and Stübinger et al showed. But with small sample number and limited analysis methods, we could give only descriptive comparison, not the quantitative data. Also we found that the healing time for histologic analysis were too long for minipig mandible

model, while the osteotomy gaps were quite filled at both endpoints to see the early healing process. For further study, bigger sample number, quantitative analysis methods, and shorter endpoints—for example, 3 and 6 weeks—would give stronger evidence to support our interpretation.

Another novelty of our study is that we wrote a full story of our laser osteotome, from its development to pre-clinical application, using the jaw bone of the large animal model. Pigs are one of the major animal species used in translational research and surgical models[23]. Their bone is known to be representative of human bone[24]. Especially minipig jaw bone is investigated for CMF research due to its comprehensive similarity to human jaw bone[25,26]. This made our study different from preceding in vitro experiments or small animal in vivo applications. We built our laser system for CMF surgery and designed our study with intraoral approach from the laboratory stage[14]. Mouth is the most frequently used nevertheless not the easiest access to the bone in CMF surgery. Moreover its normal flora raises the risk of post-operative infection. But this gives particular significance to our result compared to that from long bone model with relatively easy accessibility.

We found an explanation for different healing speed and activity from the surface analysis. SEM images of an open surface after laser osteotomy (Fig. 4) corresponded to the laser scanning microscope images showing deeper pores on the cut surface (Fig. 5). Clinically, this explained the fresh bleeding we observed from the osteotomy gap after laser bone cutting (Fig. 1). On the contrary, closed cut surface and shallower pores can explain the minimal bleeding after the PZE bone cutting (Fig. 1, 4 and 5). Early studies with surface analysis also observed characteristic smooth surface of PZE cut and interpreted it as precise and delicate cut[27,28]. But later Sasaki et al[21] confirmed the smear layer on the cut surface after the mechanical osteotomy and compared to the irregular surface of laser osteotomy. On the tooth surface, smear layer after tooth reduction has been a key topic in dentistry[29–31]. Since it is proven to adversely affect the sealing ability of sealers, nowadays the smear layer on the tooth surface is routinely removed before filling[32]. Converging these studies in dentistry and osteology, we concluded that the characteristic open surfaces of laser cut bone explain accelerated bone healing after laser osteotomy. Laser osteotomy did not leave a layer of debris on the cut surface; therefore the healing process was accelerated, as no removal of devitalized tissue was necessary. On the other hand, the closed surfaces after conventional osteotomy and the smear layer could have impeded bone healing as their equivalent on tooth surface does in dentistry. Following studies should be designed for deeper investigation of the early healing characteristics after laser osteotomy, focused on the cut surfaces paralleled with bone healing. Another important direction of the system development and the follow-up study must be the enhancement of the safety feature. Depth control is the key prerequisite for any bone cutting tools in CMF surgery, but even more for robot-guided laser osteotomy, where surgeons have no direct control or information of the cutting process. Various auxiliary technologies like optical coherence tomography, multispectral optoacoustic tomography, and diffuse reflectance spectroscopy can be added to get more information of the cut tissue and ensure the controlled osteotomy.

References

1. Kirkup J: The evolution of surgical instruments: An illustrated history from ancient times to the twentieth century. Novato, CA, Jeremy Norman & Co., 2006, pp 21–30

2. Vercellotti T: Piezoelectric surgery in implantology: a case report—A new piezoelectric ridge expansion technique. Int J Periodontics Restorative Dent 20(4):358–365, 2000

3. Maiman TH: Stimulated optical radiation in ruby. Nature 187:493–494, 1960

4. Einstein A: Zur Quantentheorie der Strahlung. Physik Z 18:121–128, 1917 [Article in German]

5. Zaret MM, Breinin GM, Schmidt H, Ripps H, Siegel IM: Ocular lesions produced by an optical maser (laser). Science 134(3489):1525–1526, 1961

6. Goldman L, Blaney DJ, Kindel DJ, Richfield D, Frank EK: Pathology of the effect of the laser beam on the skin. Nature 197:912–914, 1963

7. Taylor R, Shklar G, Roeber F: The effects of laser radiation on teeth, dental pulp, and oral mucosa of experimental animals. Oral Surg Oral Med Oral Pathol 19:786–795, 1965

8. Joanne Spetz: Physicians and Physicists: The interdisciplinary introduction of the laser to medicine. In: Rosenberg N, Gelijns AC, Dawkins H, ed.: Sources of Medical Technology: Universities and Industry. Washington, DC, National Academies Press, 1995, p 58

9. Lewis R: Lasers in dentistry. FDA Consumer. Rockville, MD, U.S. Food and Drug Administration, Jan-Feb 1995 http://web.archive.org/web/20070713235109/http://www.fda.gov/bbs/topics/CONSUMER/CON00296d.html [Accessibility verified February 20, 2017]

10. Horch HH, Keiditsch E: Morphological findings on the tissue lesion and bone regeneration after laser osteotomy. Dtsch Zahnarztl Z 35(1):22–24, 1980 [Article in German]

11. Devlin H, Dickinson M, Freemont AJ, King T, Lloyd R: Healing of bone defects prepared using the Erbium-YAG laser. Lasers Med Sci 9(4):239–242, 1994.

12. Lee SC, Kim YG, Ryu DM, Lee BS, Yoon OB, Jee YJ, Kim HC: The effect of Erbium:YAG laser osteotomy on bone healing. J Korean Assoc Oral Maxillofac Surg 24(2):213–221, 1998 [Article in Korean]

13. Stübinger S, Kober C, Zeilhofer HF, Sader R: Er-YAG laser osteotomy based on refined computer-assisted presurgical planning: first clinical experience in oral surgery. Photomed Laser Surg 25(1):3–7, 2007

14. Baek KW, Deibel W, Marinov D, Griessen M, Bruno A, Zeilhofer HF, Cattin P, Juergens P: Clinical applicability of robot-guided contact-free laser osteotomy in cranio-maxillo-facial surgery: in-vitro simulation and in-vivo surgery in minipig mandibles. Br J Oral Maxillofac Surg 53(10):976–981, 2015

15. Baek KW, Deibel W, Marinov D, Griessen M, Michel D, Bruno A, Zeilhofer HF, Cattin P, Juergens P: A Comparative Investigation of Bone Surface after Cutting with Mechanical Tools and Er:YAG Laser. Lasers Surg Med 47(5):426–432, 2015

16. Deibel W, Schneider A, Augello M, Bruno AE, Juergens P, Cattin P. A compact, efficient, and lightweight laser head for CARLO: integration, performance, and benefits. Proc SPIE 9579: Novel Optical Systems Design and Optimization XVIII, 957905 2015. doi: 10.1117/12.2187992

17. Schneider A, Pezold S, Baek KW, Marinov D, Cattin PC. Direct calibration of a laser ablation system in the projective voltage space. Med Image Comput Comput Assist Interv–MICCAI 2015 9349:274–281, 2015. doi: 10.1007/978-3-319-24553-9_34

18. Gabrić Pandurić D, Bago I, Katanec D, Zabkar J, Miletić I, Anić I: Comparison of Er:YAG laser and surgical drill for osteotomy in oral surgery: an experimental study. J Oral Maxillofac Surg 70(11):2515–2521, 2012

19. Stübinger S, Biermeier K, Bächi B, Ferguson SJ, Sader R, von Rechenberg B: Comparison of Er:YAG Laser, Piezoelectric, and Drill Osteotomy for Dental Implant Site Preparation: A Biomechanical and Histological Analysis in Sheep. Lasers Surg Med 42(7):652–661, 2010

20. Stübinger S, Nuss K, Pongratz M, Price J, Sader R, Zeilhofer HF, von Rechenberg B: Comparison of Er:YAG laser and piezoelectric osteotomy; An animal study in sheep. Laser Surg Med 42(8):743–751, 2010

21. Sasaki KM, Aoki A, Ichinose S, Ishikawa I: Ultrastructural analysis of bone tissue irradiated by Er:YAG laser.

Lasers Surg Med 31:322–332, 2002

22. Zhang X, Zhan Z, Liu H, Zhao H, Xie S, Ye Q: The infulence of water layer thickness on microstructure changes of bone tissue ablated with pulse CO2 laser: an SEM evaluation. J Biomed Opt 17(3):038003, 2012. doi: 10.1117/1.JBO.17.3.038003

23. Bode G, Clausing P, Gervais F, Loegsted J, Luft J, Nogues V, Sims J; Steering Group of the RETHINK Project: The utility of the minipig as an animal model in regulatory toxicology. J Tharmacol Toxicol Methods 62:196–220, 2010

24. Behrends DA, Khendek L, Gao C, Zayed N, Henderson JE, Martineau PA: Characterization of a Pre-Clinical Mini-Pig Model of Scaphoid Non-Union. J Funct Biomater 6(2):407–421, 2015

25. Saka B, Wree A, Alnders L, Gundlach KKH: Experimental and comparative study of the blood supply to the mandibular cortex in Gottingen minipigs and in man. J Cranio Maxillo Surg 30:219–225, 2002

26. J Stembirek, M Kyllar, I Putnova , L Stehliik, M Buchtova: The pig as an experimental model for clinical craniofacial research. Lab Anim 46:269–279, 2012

27. Hollstein S, Hoffmann E, Vogel J, Heyroth F, Prochnow N, Maurer P: Micromorphometrical analyses of five different ultrasonic osteotomy devices at the rabbit skull. Clin Oral Implants Res 23(6):713–718, 2012

28. Simonetti M, Facco G, Barberis F, Signorini G, Capurro M, Rebaudi A, Sammartino G: Bone characteristics following osteotomy surgery: An in vitro SEM study comparing traditional Lindemann drill with sonic and ultrasonic instruments. POSEIDO 1(3):187–194, 2013

29. Braennstroem M, Johnson G: Effects of various conditioners and cleaning agents on prepared dentin surfaces: A scanning electron microscopic investigation. J Prosthet Dent 31(4):422–430, 1974

30. Williams S, Goldman M: Penetrability of the smeared layer by strain of proteus vulgaris. J Endod 11(9):385–388, 1985

31. Love RM, Chandler NP, Jenkinson HF: Penetration of smeared or nonsmeared dentine by Streptococcus gordonii. Int Endod J 29(1):2–12, 1996

32. Kokkas AB, Boutsioukis ACh, Vassiliadis LP, Stavrianos CK: The influence of the smear layer on dentinal tubule penetration depth by three different root canal sealers. J Endod 30(2):100–102, 2004

Analysis of Bone Healing—post-op 4 weeks

Six animals were randomly allocated in two groups and serial-numbered for blinded analysis. (However, because of the 2nd animal, where we could not perform laser osteotomy, complete blinding was impossible.) One group of three animals were sacrificed at post-op 4 weeks and the other group of three animals were sacrificed at post-op 8 weeks. The minipigs were induced cardiac arrest by an intracardiac injection of 20% pentobarbital solution. The block resection of the mandible was performed using an oscillating autopsy saw, including the soft tissue intact to the bone. The mandible blocks were fixed by immersion in 3.8% formaldehyde solution until shipped to Basel in 70% ethanol solution.

When the mandible blocks arrived in Basel, nanoCT images were acquired first (phoenix nanotom®, GE, USA). Based on the intra-operative photographs and nanoCT images, small bone blocks were created of each defect for the histologic analysis. Each bone block was cut in half and processed for non-decalcified (stained with Paragon) and decalified (stained with H&E) samples. In the appendix, the illustrations of the small bone blocks and cutting planes can be found. (Appendix A)
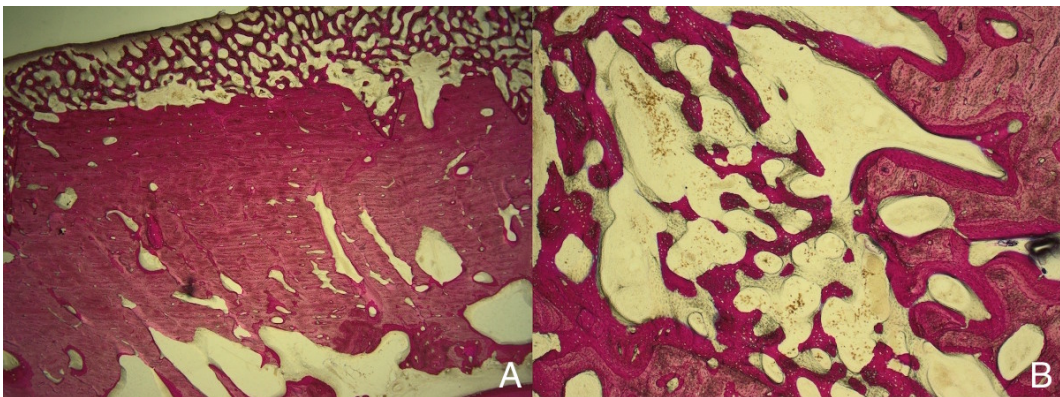
Histology   Figure 6.1 depicts the saddle defect from PZE osteotomy of the 1st minipig. Figure 6.2 displays the same defect from laser osteotomy of the 4th minipig. Both defects were incompletely healed on the surface and covered by collagen tissue. In Figure 6.1A, we can see the level of the grown bone is lower than the previous bone level. In both defects, no inflammatory lesions were observed.

Figure 6.3 illustrates the straight defects from PZE osteotomy of the 1st minipig. Figure 6.4 demonstrates the same defects from laser osteotomy of the 1st minipig. Both defects were incompletely healed. In both cases the wider the defect was, the less the new bone had grown. In Figures 6.3A and B, we can see the widest defects (1 mm width) are filled less than half, while narrower defects (0.5 mm and minimal width) are almost filled up. This could be explained by the fact that two narrower defects were made with one stroke of the corresponding piezosurgery tips (OT7, OT7S-4), but the widest defect needed more
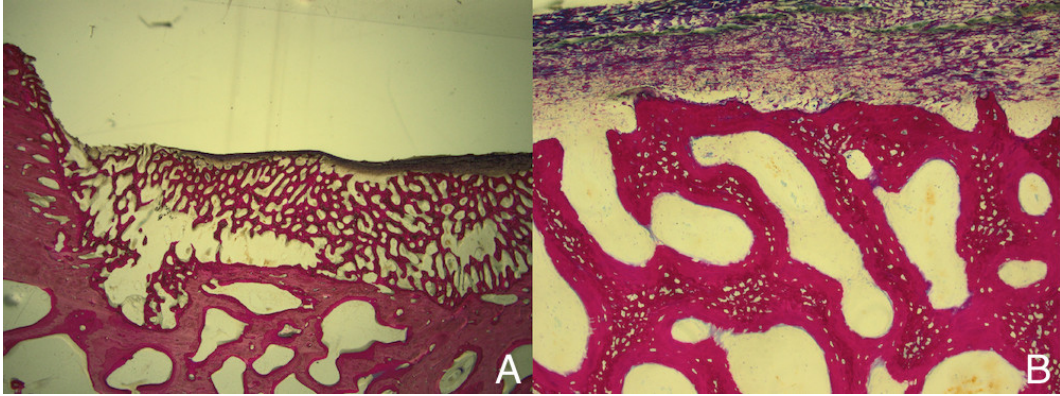
Figure 6.1: Histology of the saddle defect from PZE osteotomy, post-op 4 weeks, Paragon stain [A) lens x1.25, B) lens x4].


Figure 6.2: Histology of the saddle defect from laser osteotomy, post-op 4 weeks, Paragon stain [A) lens x1.25, B) lens x4].

strokes—*i.e.* more trauma. In Figure 6.4, from the bone growth pattern and the surrounding bone level, supraperiosteal bone growth can be suspected. Again no inflammatory lesion was found in either case.

Figure 6.5 depicts the S-shaped defect from PZE osteotomy of the 1st minipig. Figure 6.6 shows the same defect from laser osteotomy of the 1st minipig. There was no inflammatory lesion in both sides. In Figure 6.6B, we can see the healing from the defect wall is very advanced that only small residue of dark bands indicates the margin of original defect. Also in Figure 6.5, the growing bone fills almost the whole defect but we can clearly notice the defect margin by the wide gap with dark lining—which indicates residual thermal damage, accord-
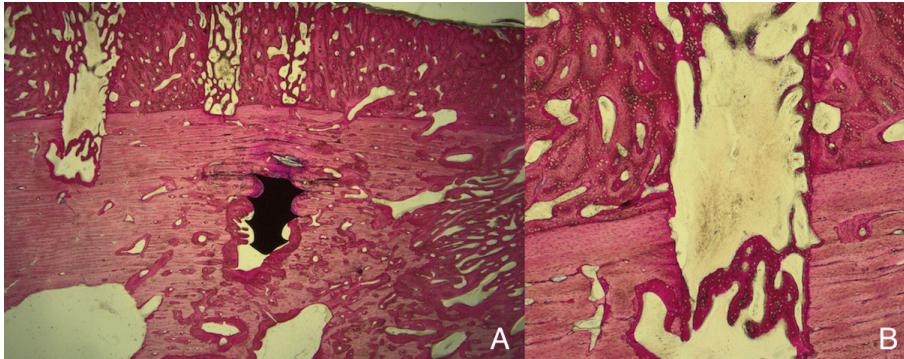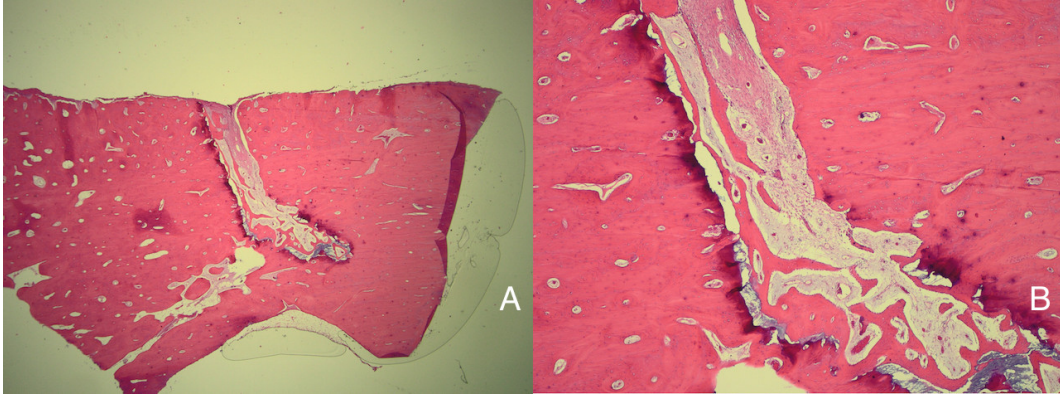
Figure 6.3: Histology of the straight defects from PZE osteotomy, post-op 4 weeks, Paragon stain [A) lens x1.25, B) lens x4].
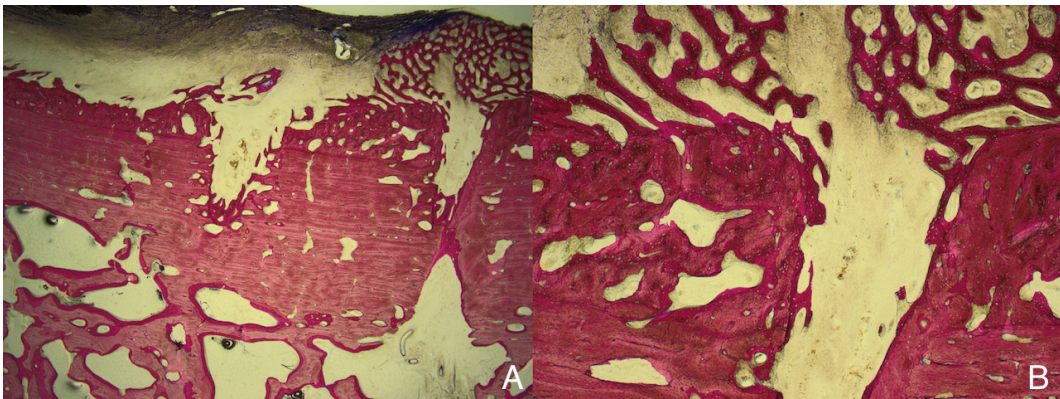

Figure 6.4: Histology of the straight defects from laser osteotomy, post-op 4 weeks, Paragon stain [A) lens x1.25, B) lens x4].

ing to Martins, Puricelli, Baraldi, & Ponzoni [34]. Martins et al. compared *in vivo* bone healing in dentoalveolar surgery with bur drilling and Er:YAG laser. They performed in 20 Wistar rats comparative mandibulotomy—one side with bur drilling and the other side with Er:YAG laser—which they fixed with titanium plate and analyzed at post-op 7, 14, 45, 60, and 90 days. Without giving detailed laser parameters, their laser osteotomies resulted in a thin layer of thermal damage. They concluded that the bone healing was faster when surgical burs were used. Had the unfavorable healing of laser cut attributed to unclarified laser parameters and cooling environment, this paper is important in that it observed *in vivo* bone healing pattern after laser osteotomy in the mandibles. They concluded that the bone healing after Er:YAG laser osteotomy started on the surface

Figure 6.5: Histology of the S-shaped defect from PZE osteotomy, post-op 4 weeks, H&E stain [A) lens x1.25, B) lens x4].
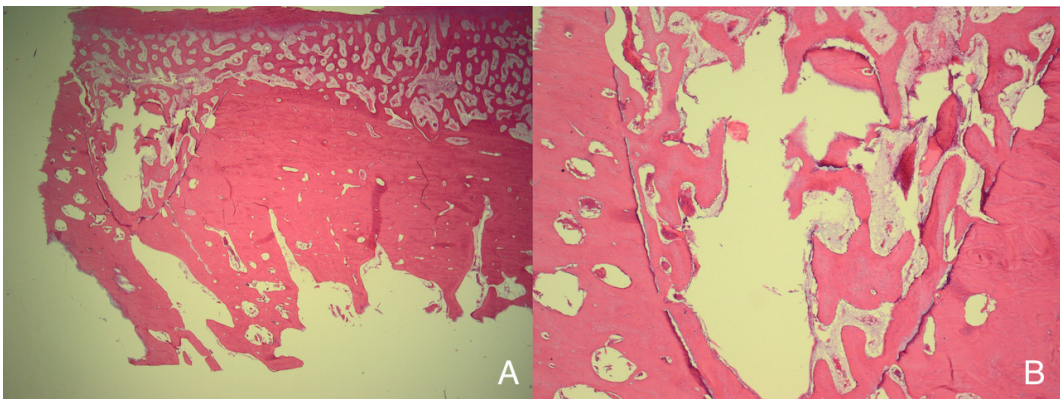
Figure 6.6: Histology of the S-shaped defect from laser osteotomy, post-op 4 weeks, H&E stain [A) lens x1.25, B) lens x4].

margins of the bone defect, similar to the process observed in a bone callus formation, after a fracture. Their description of bone healing after laser ablation seems to agree with our result. In Figures 6.2, 6.4, and 6.6, we can suspect the new bone growth from the osteotomy margin into the defect. In addtion, it actually explains SEM images from the laser cut surfaces, *e.g.* Figures 5.6, 5.8, and 5.10. Together with open pores, micro-irregularity, and roughness, the cut face made by the laser osteotome resembles the (purposedly and nicely) fractured bone surface. We could also observe this with the laser scanning microscope. On the contrary, new bone formation from conventional osteotomy is described by Martins et al. as from the inner lesion towards the surface margin. Figure 6.7
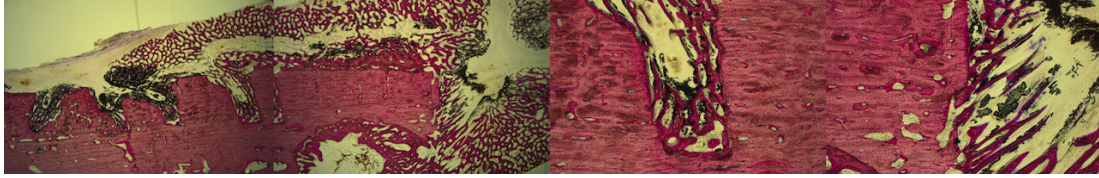
Figure 6.7: Histology of the straight defects from PZE osteotomy, post-op 4 weeks, Paragon stain [A and B) lens x1.25, C and D) lens x4].

shows straight defects from PZE osteotomy in the 2nd minipig. Like shown in Figures 6.3 and 6.4, straight defects are partially filled with the newly forming bone. With paragon stain, we can see the pattern of new bone formation, from the defect margin growing upwards.

In 2002 Sasaki et al. analyzed the ultrastructure of rat parietal bone tissue irradiated by Er:YAG laser [12]. From the result of their *in vitro* study, they anticipated favorable start of the healing process. In the same year, the same author group used Fourier Transformed Infrared (FTIR) Spectrometry to compare the bone removal by Er:YAG laser, CO_2 laser, and bur drilling [35]. In this paper they presented SEM images of various magnifications, among which the high magnification of Er:YAG laser cut showed fibrin structures similar to our Figure 5.10. With FTIR spectroscopy, they found that the chemical composition of the Er:YAG laser irradiated bone surface was similar to that from bur drilled bone surface. (On the other hand, CO_2 laser irradiation produced toxic substances.) Following this author group's publications gives a brief picture of how the research of Er:YAG laser osteotomy has evolved in CMF surgery. Although their serial works broadened and deepened the understandings of Er:YAG laser, their works had been limited to *in vitro* applications until mid 2000. In 2004 Pourzarandian et al. (from Sasaki group) published the early stages of bone healing after Er:YAG laser irradiation [36]. Basically, this study confirmed their anticipation from previous studies, about favorable healing after Er:YAG laser ablation . They irradiated the calvarial bones of rats with Er:YAG laser, cw CO_2 laser, and mechanically cut by bur drilling. The time points of termination were post-op 10 minutes, 6 and 24 hours and 3, 7, and 14 days. They could prove that the initial healing was faster following Er:YAG laser irradiation. We could ask at this point whether our time point of 4 weeks was appropriate to compare the
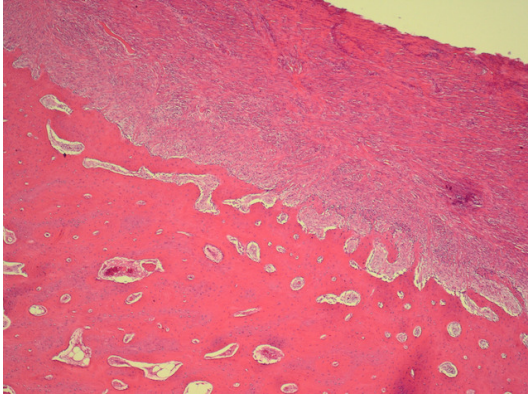
**Figure 6.8:** Histology of the saddle defect from PZE osteotomy, post-op 8 weeks, H&E stain (x1.25).
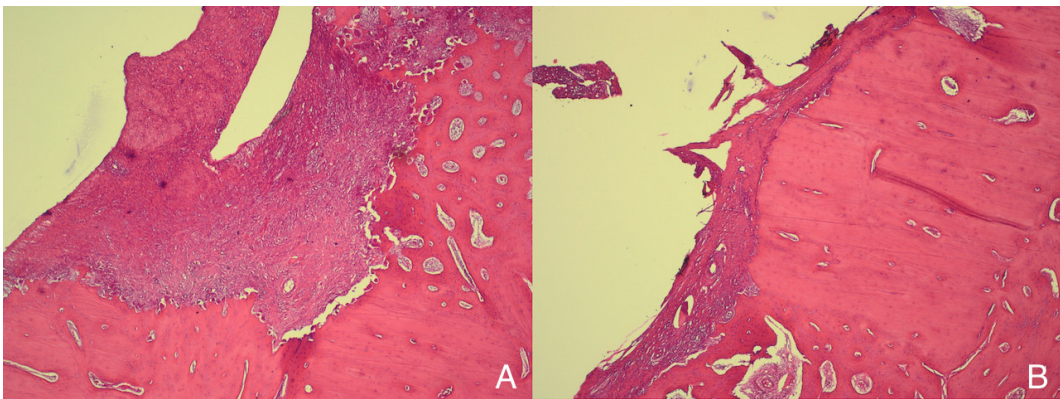
Figure 6.9: Histology of the saddle defect from laser osteotomy, post-op 8 weeks, H&E stain [A) lens x1.25, B) lens x4].

early healing. This question will be carried on and discussed again.

Analysis of Bone Healing—post-op 8 weeks

Histology   After 8 weeks of healing, all saddle defects were almost filled by the newly formed bone. Figure 6.8 depicts the saddle defect from PZE osteotomy of the 6th minipig. Figure 6.9 displays the same defect of the same animal, from laser osteotomy. Both defects showed no inflammatory lesions, and the difference was not very obvious throughout 3 animals.

Figure 6.10 illustrates the straight defects from PZE osteotomy of the 5th
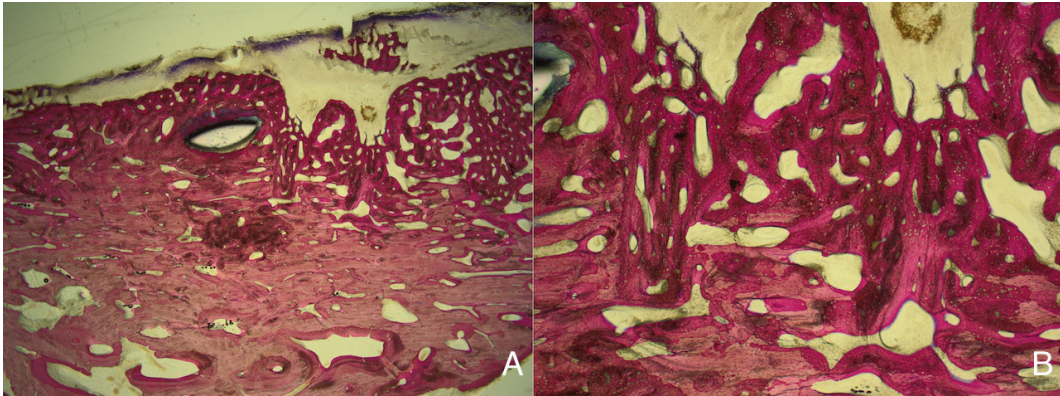
Figure 6.10: Histology of the straight defects from PZE osteotomy, post-op 8 weeks, Paragon stain [A) lens x1.25, B) lens x4].
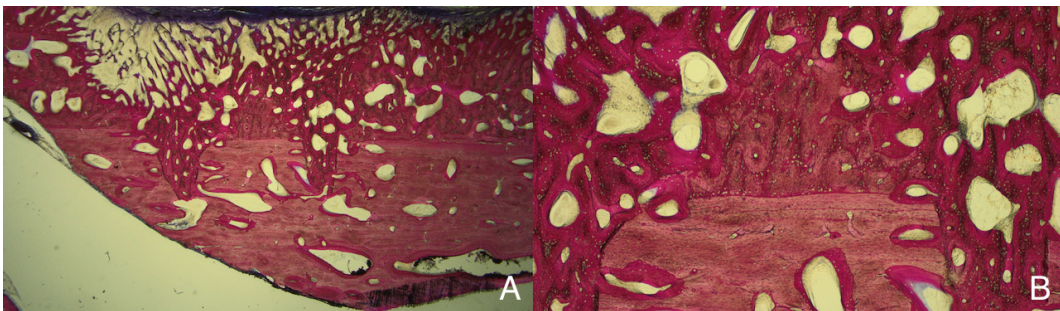
Figure 6.11: Histology of the straight defects from laser osteotomy, post-op 8 weeks, Paragon stain [A) lens x1.25, B) lens x4].

minipig. Figure 6.11 demonstrates the same defects from laser osteotomy of the 3rd minipig. Both defects are completely filled with the new bone and the boundary of defect is noticeable only by different staining depth and bone structure. In Figure 6.10A, we can observe subperiosteal bone resorption over the newly formed bone. Figure 6.11A shows lower density of new bone close to the periosteum, compared to near the defect margin, but subperiosteal resoprtion is not so obvious. However, if we see the contralateral side of Figure 6.10 animal (the 5th minipig), the straight defects from laser osteotomy show subperiosteal bone growth. The histology with paragon stain is shown in Figure 3 of the third paper in the Section 6.1 (page 47). Here the description by Martins et al. about different healing patterns after laser and bur osteotomy is worth reflection:

In ostetomies performed with a surgical bur, bone repair was initi-

ated in the inner regions of the bone defect, progressing toward the periosteum. No bone callus was formed over the external surface of the original cortical layer. When the laser system was used, however, bone repair was initiated on the periosteum and endosteum of the surface cortical margins of the lesion and progressed toward the central regions. The process resulted in modifications of the external cortical outline, with a convex morphology similar to that observed when a bone callus is formed after a bone fracture [34].

Similarity of bone healing after laser osteotomy and fracture healing has coincides with the result of the 5th minipig, especially for the convex cortical margin resembling callus formation. In 1997, El Montaser, Devlin, Sloan, & Dickinson studied the healing pattern of calvarial bone following Er:YAG laser application with environmental scanning microscope and histology [37]. Given that many study conditions were different, one of the most important being the absence of cooling water, overall healing pattern agreed with what was reproduced later by Martins et al. [34], and also with our result. Noteworthy is that the lased margin defect remained till post-op 15 weeks, even though they used the rat calvarial defect with the guided bone regeneration technique (using polytetrafluoroethylene membranes). Persistent defect margin must be a remnant of layer of amorphous material which deposited on the ostectomy site. In the study of Martins et al. this layer disappeared up to post-op 8–9 weeks. In our study the amorphous layer *i.e.* defect margin was the most prominent in the S-shaped defects.

Figure 6.12 displays the S-shaped defect from PZE osteotomy of the 3rd minipig. Figure 6.13 shows the same defect of the same minipig, from laser osteotomy. Both defects were completely filled. In Figure 6.13, new bone is as mature as surrounding old bone that without small remnants of aforementioned margin defect it's difficult to distinguish the two.

We can bring the time point of analysis again and discuss about it here. Several studies imply that 4 and 8 weeks can be a long time to compare the bone healing, if not too long. Lo et al. compared the bone healing of mouse calvariotomy by trephine drill bit and Ti:Sapphire femtosecond pulsed laser [38]. Using critical-size circular calvarial defects on wild-type CD1 mice, they followed *in vivo* healing by microCT scans for 8 weeks. They also harvested the calvaria at various
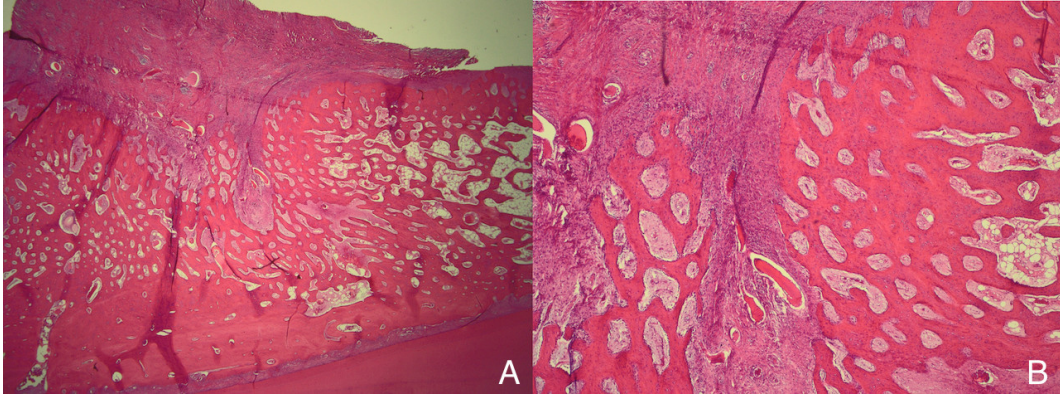
Figure 6.12: Histology of the S-shaped defect from PZE osteotomy, post-op 8 weeks, H&E stain [A) lens x1.25, B) lens x4].
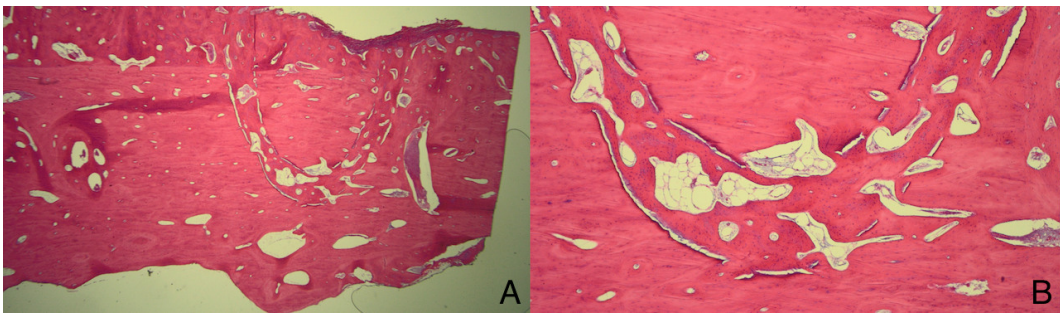
Figure 6.13: Histology of the S-shaped defect from laser osteotomy, post-op 8 weeks, H&E stain [A) lens x1.25, B) lens x4].

time points and histologically analyzed thermal damage, microstructure, and the speed of bone healing. Femtosecond laser showed less thermal damage, faster and better ossification compared to trephine drill throughout all time points. However, they could not see the significant difference between two groups anymore by post-op 8 weeks. They used small animal models and immobilized their defects, like Martins et al. [34] or El Montaser et al [37]. Our study design was essentially reproduced actual jaw bone defect of human, so the results of those studies could not be applied to our case. However, we could still infer that with shorter time point we could have found more to compare, especially for the early healing patterns.

In 2009, Yoshino et al. from Sasaki's author group published a long term histologic analysis of Er:YAG laser irradiation [39]. The study condition was to

compare contact and non-contact dry (without water cooling) irradiation and electrosurgery. Long term in this study was 12 months in rat calvarial bones. They concluded that the thermal damage from Er:YAG irradiation was much less than that from electrosurgery—even without water cooling—and did not interfere with the ensuing bone healing. Nevertheless, it was remarkable that the affected layer on the lased surface remained in the cortical bone 1 year after irradiation. This shows the grave impact of the thermal damage. Granted that the main issue of bone healing has been the thermal damage during the cutting, we can imagine that the realization of cold ablation would ensure the favorable aspects of laser osteotomy, in early and long term bone healing.

Chapter 7

Conclusion and Outlook

In this thesis, we introduced our robot-guided laser osteotomy system and tried to prove its clinical applicability. In light of the history of laser hard tissue cutting, Er:YAG laser was chosen as irradiation source. The computer-robot system was simultaneously developed to guide the laser. The whole system was designed to maximize the benefits of contact-free laser cutting while ensuring the usability for surgeons and the safety for surgeons and patients.

With the first preclinical study, we could confirm the operation of our laser system with the ergonomic setup and safety features. Intraoperatively a high precision of the cut and more bleeding was noticeable for osteotomies performed with the laser. Post-op surface analysis revealed a cut surface made by the laser osteotome analogous to the natural bone surface. In contrast, the cut surface from PZE osteotomy looked similar to the smear layer, which is well known from dentistry. At post-op 4 and 8 weeks, both mandibulotomies showed comparable bone healing without complication, with a faster healing tendency for laser osteotomy. Our study proved that an Er:YAG laser guided by the robotic system is applicable in a clinical environment and has potential for fast bone healing compared to state-of-the-art mechanical osteotomy tools.

Certainly there were limitations given that this was our first preclinical application. The animal number was minimal and we didn't have enough samples to make quantitative comparisons. Interesting findings from the surface analysis were merely descriptive. However, the pathology team conducted a further analysis of the same cut surfaces, so their publication will supplement shortcomings of this thesis. Many questions will be soon answered by follow-up studies.

Contribution of this Thesis

Biologic evidence of new laser osteotome   Uncompromised and adequate bone healing is a prerequisite of any medical device. Better bone healing after laser osteotomy was anticipated and already shown in several studies. This thesis proved the accelerated bone healing tendency after Er:YAG osteotomy. Using the mandible of the minipig model, our study condition had high similarity with the human jaw bone. With the result from this first preclinical study, following preclinical and clinical applications could be planned on a secure ground.

Preclinical application of new laser osteotome   Throughout this thesis, we focused on applying our miniaturized computer-assisted robot-guided laser osteotome in a clinical environment. Trying to figure out ergonomic configurations in an actual CMF OR setup, mixed team of surgeons, computer scientists, robot scientists, and engineers worked together to solve encountered problems from each field. As a result, we could confirm the clinical applicability, necessary learning curve, optimal ergonomic setup, and the safety features of our system clinical environment.

Cut surface analysis   From the SEM images, a typical flattened down surface was observed from the bone cut by the PZE osteotome. As CMF surgeons, we hypothesized it to be equivalent of the smear layer. Originally found on treated teeth surface, the smear layer on the bone surface was already described in a few preceding papers. This hypothesis worked as Ockham's razor and explained several observations from our study. But our verification was limited by the qualitative characteristics of the data from SEM and histology. In several ways I tried to reproduce the smear layer formed by mechanical osteotomy and employ surface treatment concept of dentistry. This is the part where further study can be planned to improve the healing in diverse bone surgeries.
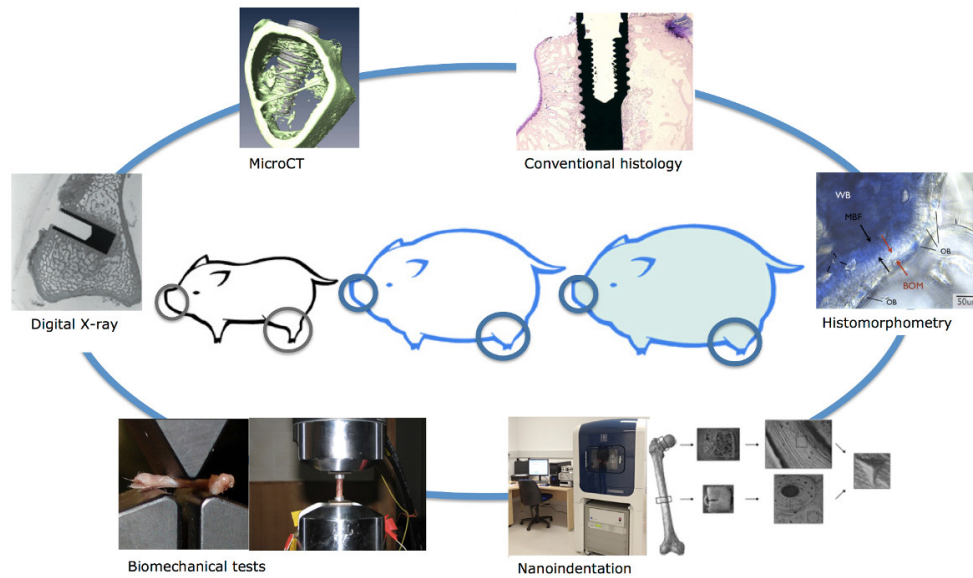
Figure 7.1: Diagram of the methods of the project CMBDM. Diagram of Nanoindentation is reprinted from Zysset PK in 1999.

Understanding Bone Metabolism—SNF Doc. Mobility Fellowship

The original project title was [Convergent Morphological analysis of Bone in induced type II Diabetes in Minipigs (CMBDM, Figure 7.1)]. Awarded by the Swiss National Science Foundation (P1BSP3_155203), this fellowship program was a part of my PhD for the enhancement of the scientific profile by working at a research institution abroad. I worked for 8 months in the department of Biomaterials and Biomimetics of New York University College of Dentistry (NYUCD) as a visiting scholar. For the project CMBDM (later renamed as [Characterization of compromised minipig bone {NYU-110514}]), the whole procedure of the bone sample preparation and various analyses was performed by myself. Figure 7.1 shows the summary of the project CMBDM, aimed to evaluate bony changes in the progress of induced type II diabetes. High similarity of the minipig model with humans gave a significance in this project. Following the natural disease progress of obesity and diabetes in humans, we tried to understand how they affect the general skeletal condition in minipigs. We found significant bony changes

with diabetes and obesity in minipig long bones. Using minipigs as translational animal model, like the main *in vivo* experiment for this thesis, I gained deeper understandings about bone metabolism and healing, which were readily applied to this thesis.

Future work

Immediate post-op cut surface analysis is worth further study. Even though it is not the exact equivalent to the smear layer on the teeth surface from mechanical cutting, analyzing the bone surface after mechanical osteotomy will give an understanding of both contact and non-contact osteotomy. If further studies can prove benefits from conditioning of bone surface, its contribution will not be confined to CMF surgery only.

Depth control is the key prerequisite for any bone cutting tool in CMF surgery, but even more for robot-guided laser osteotomy, where surgeons have no direct control or information of the cutting process. Optical coherence tomography is already part of our system for this. Various auxiliary technologies like multispectral optoacoustic tomography and diffuse reflectance spectroscopy can be added to get more information of the cut tissue and enhance safety.

A follow-up preclinical study with our laser system is already ongoing. Based on our 4 and 8 weeks result and preceding publications, the animal number, time point of analysis, and methodology of analysis will be rectified to deepen the understanding of early bone healing after laser osteotomy.

Conclusion

Robot-guided laser osteotomy is applicable in a clinical environment, particularly when an individual cut design, high precision, minimal trauma, or faster healing is required. Contact-free Er:YAG laser ablation renders cut surfaces similar to the natural bone surface, which is believed to result in favorable bone healing.

Appendix A

Bone Blocks and Cutting Planes

Based on the intra-operative photographs and nanotom images, small bone blocks were created for each defect and cutting planes were defined for different histologic analysis.
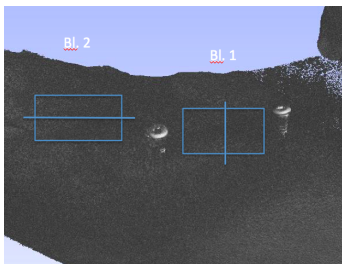
Pig1 210227L Laser side
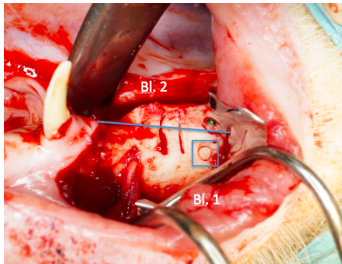
Figure A.1: Lower part of the defects for the plastic embedding (2 blocks). Upper part for the paraffin embedding (1 block).

Pig1 210227R Piezo side
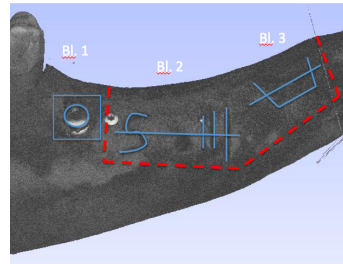
Figure A.2: Lower part of the defects for the plastic embedding (3 blocks). Upper part for the paraffin embedding (2 blocks).

Pig2 210217L Laser side

Figure A.3: Lower part of the defects for the plastic embedding (2 blocks). Upper part for the paraffin embedding (2 blocks).

Pig2 210217R Piezo side

Figure A.4: Lower part of the defects for the plastic embedding (2 blocks). Upper part for the paraffin embedding (1 block).

Pig3 209990L Laser side

Figure A.5: Lower part of the defects for the plastic embedding (3 blocks). Upper part for the paraffin embedding (2 blocks).
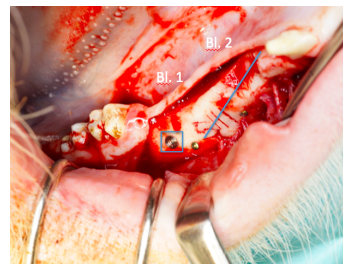
Pig3 209990R Piezo side

Figure A.6: Lower part of the defects for the plastic embedding (3 blocks). Upper part for the paraffin embedding (2 blocks).

Pig4 307551L Laser side

Figure A.7: Lower part of the defects for the plastic embedding (2 blocks). Upper part for the paraffin embedding (1 block).

Pig4 307551R Piezo side

Figure A.8: Lower part of the defects for the plastic embedding (2 blocks). Upper part for the paraffin embedding (1 block).
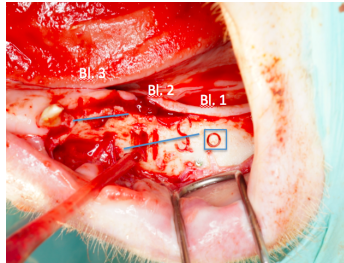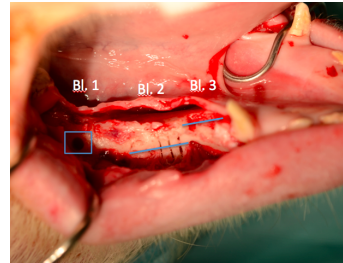
Pig5 210349L Laser side

Figure A.9: Lower part of the defects for the plastic embedding (4 blocks). Upper part for the paraffin embedding (2 blocks).

Pig5 210349R Piezo side

Figure A.10: Lower part of the defects for the plastic embedding (3 blocks). Upper part for the paraffin embedding (2 blocks).
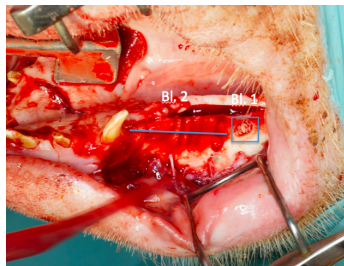
Pig6 310412L Laser side

Figure A.11: Lower part of the defects for the plastic embedding (2 blocks). Upper part for the paraffin embedding (5 blocks).
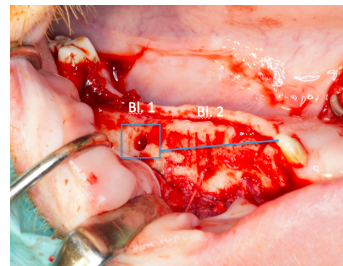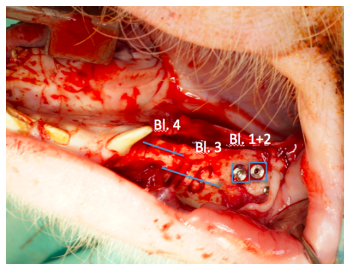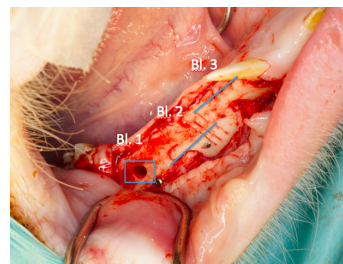
Pig6 301412R Piezo side
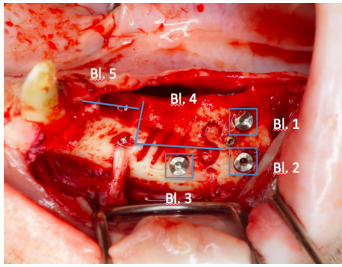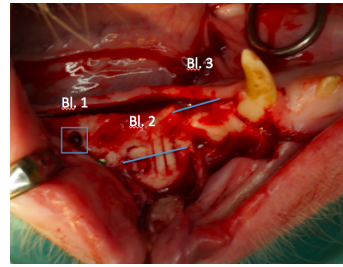

Figure A.12: Lower part of the defects for the plastic embedding (3 blocks). Upper part for the paraffin embedding (2 blocks).

References

[1] A. Einstein, "Zur quantentheorie der strahlung," *Physikalische Zeitschrift*, vol. 18, pp. 121–128, 1917. 3

[2] T. H. Maiman, "Stimulated optical radiation in ruby," *Nature*, vol. 187, pp. 493–494, 1960. 3

[3] M. M. Zaret, G. M. Breinin, H. Schmidt, H. Ripps, I. M. Siegel, and L. R. Solon, "Ocular lesions produced by an optical maser (laser)," *Science*, vol. 134, no. 3489, pp. 1525–1526, 1961. 3

[4] L. Goldman, D. J. Blaney, D. J. Kindel, D. Richfield, and E. K. Franke, "Pathology of the effect of the laser beam on the skin," *Nature*, vol. 197, pp. 912–914, 1963. 3

[5] R. Taylor, G. Shklar, and F. Roeber, "The effects of laser radiation on teeth, dental pulp, and oral mucosa of experimental animals," *Oral Surgery, Oral Medicine, Oral Pathology*, vol. 19, no. 6, pp. 786–795, 1965. 3, 4

[6] J. Spetz, "Physicians and physicists: the interdisciplinary introduction of the laser to medicine," *Sources of medical technology: universities and industry*, pp. 41–66, 1995. 4

[7] R. Lewis, "Lasers in dentistry," *FDA Consumer Magazine Jan-Feb*, 1995. 4

[8] H. Horch and E. Keiditsch, "Morphological findings on the tissue lesion and bone regeneration after laser osteotomy," *Deutsche Zahnarztliche Zeitschrift*, vol. 35, no. 1, p. 22, 1980. 4

[9] H. Horch, "Current status of laser osteotomy," *Der Orthopade*, vol. 13, no. 2, pp. 125–132, 1984. 4

[10] R. C. Nuss, R. L. Fabian, R. Sarkar, and C. A. Puliafito, "Infrared laser bone ablation," *Lasers in Surgery and Medicine*, vol. 8, no. 4, pp. 381–391, 1988. 5

[11] U. Keller and R. Hibst, "Experimental studies of the application of the Er:YAG laser on dental hard substances: II. Light microscopic and SEM investigations," *Lasers in Surgery and Medicine*, vol. 9, no. 4, pp. 345–351, 1989. 5, 6

[12] K. M. Sasaki, A. Aoki, S. Ichinose, and I. Ishikawa, "Ultrastructural analysis of bone tissue irradiated by Er:YAG laser," *Lasers in Surgery and Medicine*, vol. 31, no. 5, pp. 322–332, 2002. 6, 57

[13] L. R. Friesen, C. M. Cobb, J. W. Rapley, L. Forgas-Brockman, and P. Spencer, "Laser irradiation of bone: II. Healing response following treatment by CO_2 and Nd:YAG lasers," *Journal of periodontology*, vol. 70, no. 1, pp. 75–83, 1999. 6

[14] F. Schwarz, A. Sculean, M. Berakdar, T. Georg, E. Reich, and J. Becker, "Periodontal treatment with an Er:YAG laser or scaling and root planing. A 2-year follow-up split-mouth study," *Journal of periodontology*, vol. 74, no. 5, pp. 590–596, 2003. 7

[15] H. Kang, J. Oh, and A. Welch, "Investigations on laser hard tissue ablation under various environments," *Physics in medicine and biology*, vol. 53, no. 12, pp. 3381–3390, 2008. 7, 38

[16] J. Diaci and B. Gaspirc, "Comparison of Er:YAG and Er, Cr:YSGG lasers used in dentistry," *Journal of the Laser and Health Academy*, vol. 2012, no. 6, 2012. 8

[17] X. Zhang, Z. Zhan, N. Liu, S. Xie, and Q. Ye, "The infulence of water layer thickness on microstructure changes of bone tissue ablated with pulse CO_2 laser: An SEM evaluation," in *Photonics and Optoelectronics (SOPO), 2012 Symposium on*, pp. 1–4, IEEE, 2012. 8, 38

[18] R. Wolff, J. Weitz, L. Poitzsch, B. Hohlweg-Majert, H. Deppe, and T. C. Lueth, "Accuracy of navigated control concepts using an Er:Yag-laser for cavity preparation," in *2011 Annual International Conference of the IEEE Engineering in Medicine and Biology Society*, pp. 2101–2106, IEEE, 2011. 8

[19] J. J. Kuttenberger, S. Stübinger, A. Waibel, M. Werner, M. Klasing, M. Ivanenko, P. Hering, B. Von Rechenberg, R. Sader, and H.-F. Zeilhofer, "Computer-guided

CO_2-laser osteotomy of the sheep tibia: technical prerequisites and first results," *Photomedicine and laser surgery*, vol. 26, no. 2, pp. 129–136, 2008. 9

[20] J. Burgner, M. Müller, J. Raczkowsky, and H. Wörn, "Ex vivo accuracy evaluation for robot assisted laser bone ablation," *The International Journal of Medical Robotics and Computer Assisted Surgery*, vol. 6, no. 4, pp. 489–500, 2010. 9

[21] K. Henn, G. G. Gubaidullin, J. Bongartz, J. Wahrburg, H. Roth, and M. Kunkel, "A spectroscopic approach to monitor the cut processing in pulsed laser osteotomy," *Lasers in medical science*, vol. 28, no. 1, pp. 87–92, 2013. 9, 10

[22] Y. Sotsuka, S. Nishimoto, T. Tsumano, K. Kawai, H. Ishise, M. Kakibuchi, R. Shimokita, T. Yamauchi, and S.-i. Okihara, "The dawn of computer-assisted robotic osteotomy with ytterbium-doped fiber laser," *Lasers in medical science*, vol. 29, no. 3, pp. 1125–1129, 2014. 10, 11

[23] A. Schneider, S. Pezold, K.-w. Baek, D. Marinov, and P. C. Cattin, "Direct calibration of a laser ablation system in the projective voltage space," in *International Conference on Medical Image Computing and Computer-Assisted Intervention*, pp. 274–281, Springer, 2015. 20

[24] K. S. Arun, T. S. Huang, and S. D. Blostein, "Least-squares fitting of two 3-D point sets," *IEEE Transactions on pattern analysis and machine intelligence*, no. 5, pp. 698–700, 1987. 21

[25] P. A. McAnulty, A. D. Dayan, N.-C. Ganderup, and K. L. Hastings, *The minipig in biomedical research*. CRC press, 2011. 24

[26] B. Saka, A. Wree, L. Anders, and K. K. Gundlach, "Experimental and comparative study of the blood supply to the mandibular cortex in Göttingen minipigs and in man," *Journal of Cranio-Maxillofacial Surgery*, vol. 30, no. 4, pp. 219–225, 2002. 24

[27] P. Maurer, M. S. Kriwalsky, R. Block Veras, J. Vogel, F. Syrowatka, and C. Heiss, "Micromorphometrical analysis of conventional osteotomy techniques and ultrasonic osteotomy at the rabbit skull," *Clinical oral implants research*, vol. 19, no. 6, pp. 570–575, 2008. 35, 37

[28] M. Simonetti, G. Facco, F. Barberis, G. Signorini, M. Capurro, A. Rebaudi, and G. Sammartino, "Bone characteristics following osteotomy surgery: an in vitro SEM study comparing traditional lindemann drill with sonic and ultrasonic instruments," *Poseido*, vol. 1, no. 3, pp. 187–194, 2013. 35, 37

[29] D. G. Pandurić, I. Bago, D. Katanec, J. Žabkar, I. Miletić, and I. Anić, "Comparison of Er:YAG laser and surgical drill for osteotomy in oral surgery: an experimental study," *Journal of oral and maxillofacial surgery*, vol. 70, no. 11, pp. 2515–2521, 2012. 35

[30] D. G. Panduric, I. B. Juric, S. Music, K. Molčanov, M. Sušic, and I. Anic, "Morphological and ultrastructural comparative analysis of bone tissue after Er:YAG laser and surgical drill osteotomy," *Photomedicine and laser surgery*, vol. 32, no. 7, pp. 401–408, 2014. 36

[31] J.-L. Ma, J.-L. Pan, B.-S. Tan, and F.-Z. Cui, "Determination of critical size defect of minipig mandible," *Journal of tissue engineering and regenerative medicine*, vol. 3, no. 8, pp. 615–622, 2009. 42

[32] H. Tsutsumi, K. Katagiri, S. Takeda, T. Nasu, S. Igarashi, M. Tanigawa, and K. Mamba, "Standardized data and relationship between bone growth and bone metabolism in female Göttingen minipigs," *Experimental animals*, vol. 53, no. 4, pp. 331–337, 2004. 42

[33] J. Štembírek, M. Kyllar, I. Putnová, L. Stehlik, and M. Buchtová, "The pig as an experimental model for clinical craniofacial research," *Laboratory animals*, vol. 46, no. 4, pp. 269–279, 2012. 42

[34] G. L. Martins, E. Puricelli, C. E. Baraldi, and D. Ponzoni, "Bone healing after bur and Er:YAG laser ostectomies," *Journal of Oral and Maxillofacial Surgery*, vol. 69, no. 4, pp. 1214–1220, 2011. 55, 60, 61

[35] K. M. Sasaki, A. Aoki, S. Ichinose, T. Yoshino, S. Yamada, and I. Ishikawa, "Scanning electron microscopy and fourier transformed infrared spectroscopy analysis of bone removal using Er:YAG and CO_2 lasers," *Journal of periodontology*, vol. 73, no. 6, pp. 643–652, 2002. 57

[36] A. Pourzarandian, H. Watanabe, A. Aoki, S. Ichinose, K. M. Sasaki, H. Nitta, and I. Ishikawa, "Histological and tem examination of early stages of bone healing

after Er:YAG laser irradiation," *Photomedicine and Laser Therapy*, vol. 22, no. 4, pp. 342–350, 2004. 57

[37] M. A. El Montaser, H. Devlin, P. Sloan, and M. R. Dickinson, "Pattern of healing of calvarial bone in the rat following application of the Erbium-YAG laser," *Lasers in surgery and medicine*, vol. 21, no. 3, pp. 255–261, 1997. 60, 61

[38] D. D. Lo, M. A. Mackanos, M. T. Chung, J. S. Hyun, D. T. Montoro, M. Grova, C. Liu, J. Wang, D. Palanker, A. J. Connolly, *et al.*, "Femtosecond plasma mediated laser ablation has advantages over mechanical osteotomy of cranial bone," *Lasers in surgery and medicine*, vol. 44, no. 10, pp. 805–814, 2012. 60

[39] T. Yoshino, A. Aoki, S. Oda, A. A. Takasaki, K. Mizutani, K. M. Sasaki, A. Kinoshita, H. Watanabe, I. Ishikawa, and Y. Izumi, "Long-term histologic analysis of bone tissue alteration and healing following Er:YAG laser irradiation compared to electrosurgery," *Journal of periodontology*, vol. 80, no. 1, pp. 82–92, 2009. 61

Curriculum Vitae

Particulars

Name   Kyung-won Baek
Date of Birth   25th April 1978
Place of Birth Seoul, Korea (Republic of)

For a family portrait, refer to the Figure 2 on page 16.

Skills

Oral and Maxillofacial Surgeon (board certified Maxillofacial Plastic and Reconstructive Surgeon)
Advanced clinical experiences in oral and maxillofacial surgery, dental anesthesia and dental implant
Leading the preclinical and clinical studies for new diagnostic and treatment tools
Experiences in various animal surgeries for the preclinical study
Experiences in the volunteer work and team leading with limited facility

Education

When	What	Where
Mar 2012–May 2017	PhD in biomedical engineering	University of Basel Faculty of medicine, Switzerland
Nov 2014–Jun 2015	Swiss National Science Foundation (SNF) Doc. Mobility scholar	New York University College of Dentistry, U.S.A.
Jan 2009–Dec 2009	International Team for Implantology (ITI) scholar	Tsurumi University School of Dentistry, Japan
Mar 2007	Acquired diplomate Korean Board of Maxillofacial Plastic and Reconstructive Surgery	Korea
Mar 2004–Feb 2007	Master of Science in Dentistry (M.S.D.)	Seoul National University Graduate School, Korea
Mar 2003	Acquired Korean license of dentist Korean Ministry of Health and Welfare	Korea
Mar 1999–Feb 2003	Bachelor study, Doctor of Dental Medicine (D.M.D.)	Seoul National University College of Dentistry, Korea
Mar 1997–Feb 2003	Pre-dentistry bachelor course	Seoul National University College of Natural Science, Korea
Mar 1994–Feb 1997	High school (secondary school)	Myungduk Foreign Language High School, Korea

Professional Experiences

When	What	Where
Nov 2016–Jan 2017	Assistentin (Doktorandin)	University of Basel, Department of Biomedical Engineering
May 2012–Oct 2016	Wissenschaftliche Mitarbeiterin	University Hospital of Basel, Department of Oral and Maxillofacial Surgery, Switzerland
Feb 2010–Dec 2011	Assistant professor	Department of Dentistry, Jeju National University School of Medicine, Korea
Mar 2008–Jan 2010	Clinical instructor Head of dental clinic	Jeju National University Hospital, Korea
Mar 2007–Feb 2008	Clinical fellow in Dental anesthesiology	Seoul National University Dental Hospital, Korea
Jan 2004–Feb 2007	Resident in Oral and Maxillofacial Surgery	Seoul National University Dental Hospital, Korea
Jan 2003–Dec 2003	Internship	Seoul National University Hospital, Korea

Research

When	What	Where
2015	Convergent morphological analyses of bone in induced type II Diabetes in minipigs	New York University College of Dentistry, Department of Biomaterials and Biomimetics, U.S.A.
2013	A comparative study to assess the safety, accuracy and healing characteristics of contact-free laser osteotomy guided by a surgical robot versus manually-performed conventional methods. A radiological and histomorphometric evaluation in mini pigs at 4 and 8 weeks	Surgical Research Service Facility Magneten at BMSD Lund University, Malmö, Sweden Straumann facility, Basel, Switzerland Advanced Osteotomy Tools (AOT), Hightech Forschungs Zentrum (HFZ), University of Basel, Switzerland
2013	In-vitro ergonomic study to determine intraoral approachability of CARLO in pig cadaver heads	AOT, HFZ, University of Basel, Switzerland
2011	Skeletal PET for diagnosis of temporomandibular joint disorder - clinical usefulness of 18F-fluoride bone PET in patients with TMD	Jeju National University Hospital, Korea
2009	Retrospective application of SAC classification to Implant patients of Tsurumi University	Tsurumi University, Japan
2007	Clinical study of velopharyngeal closure using nasoendoscopy	Seoul National University, Korea
2006-2007	Clinical test of new dental implant coated nanoscale Ca-P on the anodizing surface using IBAD (ion beam assisted deposition) for the early osteointegration	Seoul National University, supported by Korean ministry of health and welfare, Korea

Volunteer Works

When	What	Where
2011.8.	Charity operation–Dental surgery	Iloilo, Philippines
2010-2011	Charity clinic and home visit care for disabled people–Dental surgery	Pusan, Korea
2010.8.	Charity operation–Dental surgery	Shaoshuitang, China
2010.8.	Charity operation–Dental surgery	Cavite, Philippines
2009.9.	Workhouse Shinjuku Park–Volunteer	Tokyo, Japan
2009.4.	Charity operation–Cleft	Phnom phen, Cambodia
2007.11	Charity operation–Cleft	Bihn Duong, Vietnam
2005	Special clinic for HIV patients–Dental surgery	Seoul, Korea
2003-2004	Charity clinic and legal consulting office for sex workers [House of Magdalena]–Dental Surgery	Seoul, Korea

Awards

When	What
2014	Doc. Mobility grant from Swiss National Science Foundation (SNF) Project [Convergent morphological analyses of bone in induced type II diabetes in minipigs] in NYU, USA, starting from September 2014 for 8 months
2014	Award of the best oral presentation at Bernd-Spiessl-Symposium 2014 Oral Presentation [The Computer-assisted and Robot-guided Laser Osteotome for Mandibular Osteotomies–The Biological Responses]
2009	International Team for Implantology (ITI) International Scholar Visiting scholar at Tsurumi University, in Yokohama, Japan, for 1 year

Languages

Korean as mother tongue
English, fluent
Japanese, fluent (JLPT N1)
German, fair (telc C1)
French, fair (B1-B2)
Mandarin, basic (A2)

Peer-reviewed Publications

Accepted Peer-reviewed Publications, on PhD topic (2012-2016)

2016	Schneider A, Pezold S, **Baek KW**, Marinov D, Cattin PC. Simultaneous intrinsic and extrinsic calibration of a laser deflecting tilting mirror in the projective voltage space. *Int J Comput Assist Radiol Surg* 2016 Jun 13. [Epub ahead of print]
2015	**Baek KW**, Deibel W, Marinov D, Griessen M, Bruno A, Zeilhofer HF, et al. Clinical applicability of robot-guided contact-free laser osteotomy in cranio-maxillo-facial surgery: in-vitro simulation and in-vivo surgery in minipig mandibles. *Br J Oral Maxillofac Surg* 2015;53:976-81.
2015	**Baek KW**, Deibel W, Marinov D, Griessen M, Michel D, Bruno A, et al. A Comparative Investigation of Bone Surface after Cutting with Mechanical Tools and Er:YAG Laser. *Lasers Surg Med* 2015;47:426-32.
2015	Schneider A, Pezold S, **Baek KW**, Marinov D, Cattin PC. Direct calibration of a laser ablation system in the projective voltage space. *Med Image Comput Comput Assist Interv– MICCAI 2015* 2015;9349:274-81.

Presentations, on PhD topic (2012-2016)

2016	Oral presentation at 66. Deutsche Geselschaft der Mund-, Kiefer- und Gesichtschirurgie (DGMKG), June 01, 2016, Hamburg, Germany
2014	Oral and poster presentation at 53. Congress of Korean Association of Maxillofacial Plastic and Reconstructive Surgery (KAMPRS), October 30, 2014, Seoul, Korea
2014	Oral presentation at 28. Computer Assisted Radiology and Surgery (CARS) conference, June 26, 2014, Fukuoka, Japan
2014	Oral presentation at 10. Bernd-Spiessl Symposium (BSS), June 20, 2014, Basel, Switzerland *Awarded as the best presentation*
2013	Oral presentation at 28. Annual Reunion of Swiss Society of Oral and Maxillo-Facial Surgery (SGMKG), November 23, 2013, Basel, Switzerland
2013	Oral presentation at 21. International Conference on Oral and Maxillofacial Surgery (ICOMS), October 23, 2013, Barcelona, Spain
2013	Poster presentation at 9. Bernd-Spiessl Symposium (BSS), June 14, 2013, Basel, Switzerland